THERMAL DECOMPOSITION AND GASIFICATION OF CELLULOSE AND WOOD WASTES

BY

© PETER FONG

A THESIS SUBMITTED TO THE DEPARTMENT OF CHEMISTRY

IN PARTIAL FULFILLMENT OF THE REQUIREMENTS FOR

THE DEGREE OF MASTER OF SCIENCE

LAKEHEAD UNIVERSITY

THUNDER BAY, ONTARIO, CANADA.

MAY, 1980.

THERMAL DECOMPOSITION AND GASIFICATION OF CELLULOSE AND WOOD WASTES

BY: PETER FONG

LAKEHEAD UNIVERSITY

THUNDER BAY, ONTARIO

Acknowledgements

The work in preperation for this thesis was carried out at Lakehead University from September, 1976, to May, 1980. The author wishes to thank his supervisor Dr. R. A. Ross, DSc, PhD, BSc, ARCST, CEng, FInstE, FCIC, CChem, FRIC, for his continual encouragement and direction.

In addition, the author would like to acknowledge the expert assistance provided by the technical staff of the Faculty of Science.

Table of contents

Abstract

The thermal decomposition of jack pine bark, white birch sawdust and cellulose has been studied by both isothermal weight-change determinations and dynamic thermogravimetry mostly in inert atmospheres up to 900°C. Gaseous products formed in helium and helium/water vapour atmospheres from 350 to 650°C and 101 to 2533 kPa were analysed by gas chromatography. The effects of a number of additives, alkali metal and transition metal compounds, on the kinetics of the reaction and on the gas yields have been examined. The effect of pressure on the chemical balance and distribution of the gaseous products was also studied. Residues were analysed for CHN contents and any structural changes on heating were detected by scanning electron microscopy.

Both kinetic data and gaseous product analysis showed that cellulose was more susceptible to the influence of additives than the wood samples. Isothermal decomposition data for bark and sawdust were similar to results expected for diffusion-controlled processes. The addition of potassium carbonate shifted the kinetics of decomposition of cellulose from a description consistent with a phase-boundary controlled model to that for a diffusion-controlled process. The apparent activation energy for cellulose pyrolysis was lowered by the addition of both potassium carbonate and iron (III) oxide.

Gaseous products analysis suggested that the addition of iron (III) oxide catalyzed the water-gas reaction in the overall gasification while zinc (II) chromite behaved as an inhibitor in this regard. Potassium carbonate appeared to catalyze the carbon-steam reaction and there was some indication that more gases and tar could be formed from the secondary reactions of tars when the pressure of the system was raised to 2533 kPa.

In the gasification of cellulose and jack pine char, the addition of water vapour, potassium carbonate, iron (III) oxide and zinc (II) chromite was found to increase the total gas yields which in turn increased the heat content of the mixtures.

1. Introduction

1.1 General

In recent years, the crisis resulting from the scarcity and increased cost of traditional fossil fuels has accelerated the search for alternative sources of energy. Thus, increasing attention has been placed on other sources of energy such as geo-thermal, wind, tidal and solar as well as biomass, in its various forms, which has effectively collected and stored low-intensity solar energy through photo-chemical synthesis.

It has been estimated that the total energy potential of the world's biomass ranges from 2427 to 4431 x 10^{15} kJ/yr [1,2]. In 1970, world consumption of energy from petroleum, natural gas and solid fuel was estimated to be 208 x 10^{15} kJ [3]. These figures indicate that biomass could provide about 10 to 20 times the planet's energy needs.

The total biomass production of the United States is estimated to be 75 x 10^{15} kJ/yr [4]. Statistics for Canada indicate a comparable figure of 27 x 10^{15} kJ/yr [5] and a total Canadian energy consumption in 1973 of 6.1 x 10^{15} kJ/yr [5]. Though not all the biomass would be used for energy production, it still has substantial potential for this purpose.

The complete utilization of a single tree is emphasized in today's forest industry, but there still remains a lot of wood waste in the form of bark and slash. Canada produces about 3.0 x 10^{10} kg/yr of bark [6] of which over half is merely incinerated. If this wood waste were used effectively as a fuel, then it would make a small but not insignificant contribution towards our energy requirements, especially in regard to townships and cities close to forest-based industries.

Active development of the interconversion of coal to other fuels continues to progress [7, 8] but studies with biomass feedstocks are less

well-established even though such materials have some advantages over coal as an initial source. All biomass has a chemical composition similiar to that of cellulose. It has a greater volatile component and a higher reactivity than coal. It contains almost no sulphur and about 1% ash whereas coal typically contains 2% sulphur and 10% ash. Thus as a gasification feedstock, biomass will result in less sulphur emission and fewer problems with ash disposal. However, there are some drawbacks. Biomass generally has a high moisture content and significant quantities of heat are consumed in vapourising the moisture in biomass gasification processes. Furthermore, biomass has a lower bulk density than coal and also the reactor size has to be increased for a given amount of product relative to that for coal.

Biomass can be converted to solid, gaseous and liquid fuels. The various routes are shown in Figure 1.

Anaerobic digestion [9,10,11] to methane, enzymatic hydrolysis and fermentation to alcohol [12,13] represent biological methods of conversion of biomass to fuel. Generally in these processes, a micro-organism is used at closely-controlled temperatures. Bioconversion efficiencies are usually below 60% and the rate of digestion is slow. The effects of ball-milling [14], heating [15], radioactivity [16], acid and base pretreatments [17] on the digestibility of such feedstocks have been reported.

Literature reports of thermochemical liquefaction are limited but there appears to be two direct liquefaction processes under development. Both flash pyrolysis (Occidental Research Corp.) and the PERC (Pittsburg Energy Research Centre) processes [18] yield heavy fuel oils. Carbon monoxide is reacted with the biomass in an aqueous carbonate solution in the PERC process and it has been reported that alkali-catalyzed Adol-type condensations may be involved in the liquefaction mechanism. These liquid fuels are expensive to make. The energy efficiencies are low and rarely exceed 33%.

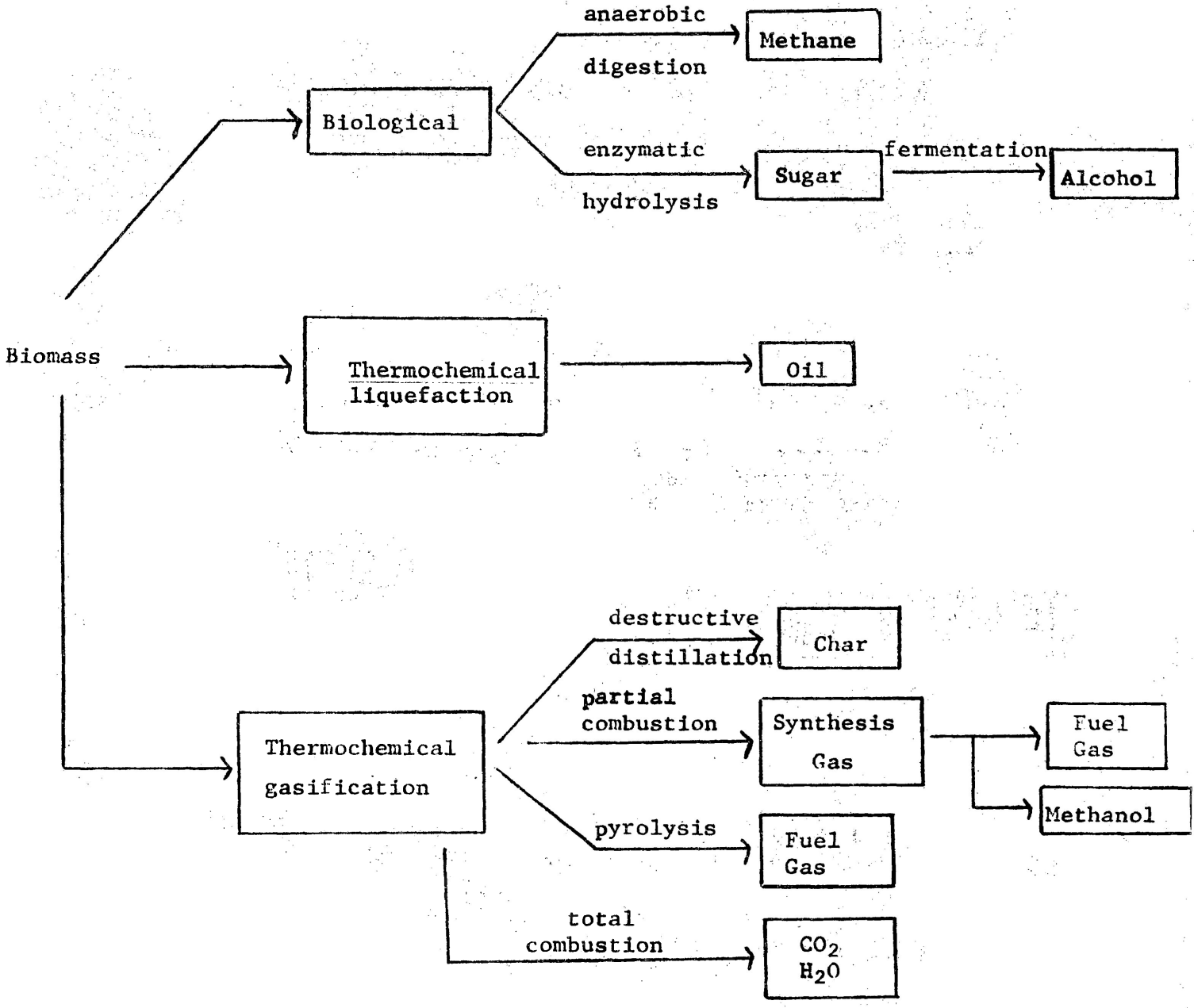

Figure 1 The various biomass to fuel conversion routes.

Moreover, the liquors can be corrosive and present difficulties in materials handling.

Thermochemical gasification processes have been extensively researched. They generally result in higher conversion efficiencies and production rates than the two biological routes.

Combustion of wood for heating and cooking has been used since the dawn of civilization. Partial combustion and destructive distillation of wood have also been used for making charcoal, wood alcohol, tar and other chemicals for many decades. Today, developments in gasification technology are often keyed to catalytic processes or to steam gasification in contrast to the earlier emphasis on air-blast generation. Recently, alkali metal carbonates, calcium oxide [19] and wood ash [19] have been reported to be useful catalysts for gasification of biomass.

The first step in biomass gasification can be regarded as the conversion of cellulose to carbon and water. Then the following reactions may be considered [20]:

	ΔH°_{298} (kJ)	
$C(s) + O_2(g) \longrightarrow CO_2(g)$	-393	(1)
$C(s) + CO_2(g) \longrightarrow 2CO(g)$	+170	(2)
$C(s) + H_2O(g) \longrightarrow CO(g) + H_2(g)$	+130	(3)
$C(s) + 2H_2(g) \longrightarrow CH_4(g)$	-75	(4)
$C_nH_m \longrightarrow (m/4)CH_4(g) + (n-m/4)C(s)$		(5)
$CO(g) + H_2O(g) \longrightarrow CO_2(g) + H_2(g)$	-40	(6)
$CO(g) + \frac{1}{2}O_2(g) \longrightarrow CO_2(g)$	-282	(7)
$H_2(g) + \frac{1}{2}O_2(g) \longrightarrow H_2O(g)$	-286	(8)
$CH_4(g) + H_2O(g) \longrightarrow CO(g) + 3H_2(g)$	+209	(9)

Reactions (1) to (4) involve the gasification of the fixed carbon in tne biomass. Volatile matter in the biomass decomposes to yield methane and higher hydrocarbons as in reaction (5). Reactions (6) to (9) involve the gaseous products. Pressure, temperature and the ratios steam/biomass and air or oxygen/biomass are the major variables in the gasification processes [21]. Generally, increasing temperature and pressure would be expected to increase reaction rates. Increasing the oxygen/biomass ratio tends to increase the amount of carbon gasified while hydrogen production is proportional to the steam/biomass ratio.

The 'Purox' gasification system [22] which has been developed commercially operates with a fixed-bed reaction base-fed with oxygen. Other systems in development include the Battelle process [23], the Wright-Malta process [24], and the Moore-Canada process [21]. The Wright-Malta process combines pyrolysis and steam gasification reactions with a sodium carbonate catalyst in a pressurized fixed-bed gasifier. The Battelle system involves a multi-solid fluid-bed reactor with calcium oxide as a catalyst and the Moore-Canada process uses a moving-bed reactor with an air/steam mixture as the oxidizing medium. Most of the gasification processes are aimed at maximizing the yield of synthesis gas (a mixture of 2 volumes of hydrogen to one of carbon monoxide) with the minimum oxygen and steam requirement. The main differences in the various methods rest with variations in pressure, catalyst, the oxygen or steam to biomass ratio, and the type of reactor. No one method seems to have a clear technical superiority over any other at the present time.

1.2 Kinetics

1.2.1 Thermogravimetry

Thermogravimetry has been used extensively to study the kinetics of the thermal decomposition of cellulosic materials. Thermal gravimetric analysis

may be carried out in a 'dynamic' mode when the sample weight is continously recorded as a function of temperature attained or in a 'static' mode in which the sample weight is recorded as a function of time at constant temperature.

Cameron and Kerr [25] found that good agreement for apparent activation energies determined by the two techniques occurred only when the mechanism of decomposition was invariant with the extent of decomposition on polymer degradation. Fairbridge [26] noted that the apparent activation energy values determined by dynamic techniques were consistently greater than those found by isothermal techniques. Furthermore, there were indications that the final weight loss of samples was dependent on the heating rate. Thus it was thought that data obtained from isothermal techniques were the more reliable when results obtained by the two methods differed [26].

1.2.2 Dynamic thermogravimetry (TG)

Several kinetic models have been developed and applied to derive standard kinetic parameters from thermogravimetric data obtained at different heating rates. In the method of Freeman and Carroll [27], the following relation was used:

$$\frac{\log d\alpha/dt}{\log(1-\alpha)} = n - \frac{E_a}{2.303R} T^{-1}/\log(1-\alpha) \qquad (10)$$

where n is the order of the reaction and α is the degree of conversion. Coats and Redfern [28] used equations (11) and (12) for (1) $n = 1$:

$$\log\left\{-\frac{\ell n(1-\alpha)}{T^2}\right\} = \log\frac{\Delta R}{a\Delta E_a} - \frac{\Delta E_a}{2.303RT} \qquad (11)$$

where a is the heating rate, and when (ii) $n \neq 1$:

$$\log\left\{\frac{1-(1-\alpha)^{1-n}}{T^2(1-n)}\right\} = \log\frac{\Delta R}{a\Delta E_a} - \frac{\Delta E_a}{2.303RT} \qquad (12)$$

Sharp and Wentworth [29] estimated the reaction rate constant from the expression $(d\alpha/dt)/(1-\alpha)^n$, and if the assumed order of reaction n was correct, a linear Arrhenius plot would be obtained. Ozawa [30] used the following

approximate relation, for a given value of α:

$$\log a + 0.4567\ E_a/RT = \text{constant} \qquad (13)$$

The apparent activation energy could be derived from the plot of log a against T^{-1}.

The above models would give reasonable results for single first or second order reactions. However, the pyrolysis step consists of many concurrent and consecutive reactions, where the sample changes physically and chemically. Thus the apparent activation energy may be dependent on the extent of the reaction. Tran and Rai [31] proposed that the apparent activation energy is a direct function of conversion and equation (14) was used:

$$E_a = E_o + b\alpha \qquad (14)$$

where E_o is the apparent activation energy at $\alpha = 0$ and b is a constant. The kinetic equation (15) was used in this model:

$$\frac{1}{w_o}\frac{dw}{dt} = ke^{-E_a/RT}\ \alpha^n \qquad (15)$$

where w is the weight of sample at a given time, t.

While kinetic parameters obtained from TG may not be so accurate as those from isothermal techniques, TG has been used extensively to study the effects of inorganic salts on wood decomposition [25,32,33,34,35]. TG curves from samples treated with various inorganic salts were basically similar in shape but revealed marked differences in the temperature of the onset of rapid pyrolysis and the amount of residue remaining.

1.2.3 Isothermal techniques

The accuracy of the result depends largely on the rapidity by which the sample reaches the reaction temperature, since a significant weight loss may occur before the sample has attained thermal equilibrium with the furnace.

Several models have been proposed to explain the kinetics. Stamm [36] gave the following equation (16) based on the weight of residue:

$$-\frac{dw}{dt} = kw^n = -Ae^{E_a/RT}w^n \qquad (16)$$

and Martin [37] expressed the kinetics of decomposition for cellulosic materials as a composite of two reactions:

$$-\frac{dw}{dt} = (k_1 + k_2)w^n \qquad (17)$$

A slow pyrolysis reaction, k_1, was thought to predominate at low temperatures, and a fast pyrolysis reaction, k_2, was predominant at temperatures >673K. Shafizadeh, Cochran and Sakai [38] employed equation (17) to describe the degradation of cellulose. One first-order reaction producing char and the other producing tars and volatile products were the two processes believed to be involved.

The above equations imply an equilibrium state of complete weight loss, and thus are unlikely to be valid at high values of conversion. Later, van Krevelen [39] proposed a model (18) based on the weight loss after infinite time.

$$\frac{dw}{dt} = k\left(1 - \frac{w}{w_\infty}\right)^n \qquad (18)$$

where w_∞ = weight loss at infinite time. Equation (18) has been used with $n = 1$ by Roberts and Clough [40] and Akita and Kase [41]. Barooah and Long [42] investigated the decomposition of carbonaceous materials in a fluidized bed and found two stages. They reported that about 85% of the total weight change took place in the first stage and the residual 15% in the second stage. They used Stamm's equation (16) with $n = 1$ to describe the first stage and van Krevelen's equation with $n = 2$ to describe the second stage.

Broido [43] suggested a kinetic model comprising an initial "incubation period" with no weight loss, followed by (a) depolymerization leading to volatile products and (b) a series of steps leading to char formation. He concluded that the last step in the char-forming sequence involved a weight

loss corresponding to the formation of $C_8H_6O_2$ per repeating cellubiose unit in the original cellulose. For longer times at higher temperatures or for cellulose contaminated with inorganic catalysts, an additional step led to $(C_7H_4O)_n$.

Shafizadeh and Bradbury [44] investigated the thermal degradation of cellulose in air and nitrogen at low temperatures. They concluded that above 300°C, the pyrolysis rate was essentially the same in air and nitrogen, indicating that thermal degradation was independent of oxidative reactions.

From these laboratories, Fairbridge and Ross [45,46,47] have reported that the maximum rate of pyrolysis for the sawdust and bark of jack pine was most likely related to the rapid decomposition of the cellulose, and the principal kinetic parameters obtained from the decomposition of a range of wood products were found to fit a reaction rate compensation curve.

Values of apparent activation energy and frequency factors obtained from the two thermogravimetric techniques vary considerably and kinetic parameters obtained under the different experimental conditions reported in the literature are summarized in Table 1.

1.3 Pyrolysis products

Hemicellulose, cellulose and lignin are the main constituents of wood. Their relative proportions vary from species to species although the elemental composition of wood is almost constant (49.5% C, 6.3% H, 44.2% O) [48].

Cellulose is a condensation polymer of repeated β-D-glucose containing the 1,4-glycosidic linkage. Hemicellulose polymers contain a number of sugars, including D-glucopyranose, D-xylopranose and D-mannopyranose as the structural units. Lignin is a complex polymer with the phenylpropane groups as the structural units, but the exact structure is not known. The basic

Table 1 Kinetic parameters for pyrolysis of various wood and wood components as obtained by various workers.

Workers	Feedstock	Apparent activation energy ($kJmol^{-1}$)	Frequency factor (min^{-1})
Stamm [36]	Douglas fir stock	123.5	3.1×10^{13}
	Douglas fir sawdust	104.7	1.1×10^{11}
	Cellulose from Douglas fir	108.8	2.0×10^{11}
	Hemicellulose from Douglas fir	107.0	2.2×10^{12}
	Lignin from Douglas fir	96.3	8.4×10^{11}
Browne and Tang [32]	Ponderosa pine	149.9	
Akita and Kase [41]	α-cellulose	222.4	1.0×10^{19}
	Modified cellulose	134.0	1.0×10^{12}
Brown [33]	White pine	207	1.7×10^{16}
	Oak	238	2.3×10^{19}
Barooah and Long [42]	Wood	18.0 (< 330°C) 84.1 (> 330°C)	3.2 (< 330°C) 1.4×10^{6} (> 330°C)
	Cellulose	71.2	2.4×10^{5}
Tran and Rai [31]	Douglas fir	101.7 (0% conversion) 201.7 (70% conversion)	1.28×10^{10}
	K_2CO_3 Catalyzed Douglas fir	102.5 (0% conversion) 162.8 (70% conversion)	1.37×10^{10}

structural units of these polymers are shown in Figure 2.

The pyrolytic products of cellulosic materials can be collected in three fractions: a carbonaceous residue (char), a viscous condensate at room temperature (tar) and a mixture of volatile gases. Bolton et. al. [49] indicated that the primary gaseous products were methane, hydrogen and the two oxides of carbon. Goos et. al. [50] reported that 213 compounds have been identified in the tar from the destructive distillation of wood. Levoglucosan is the major tarry product obtained from cellulose alone while much of the acetic acid formed in wood pyrolysis can be attributed to hemicellulose decomposition. Aromatic products such as phenols and xylenols are formed from the aromatic nuclei of lignin.

It has been suggested that the pyrolysis of cellulose proceeds as shown in Figure 3 [51]. This general mechanism can be divided into primary and secondary reactions. Reaction 1 takes place below 250°C and consists of reactions such as depolymerization, hydrolysis, oxidation, dehydration and decarboxylation. Reaction 2 is the formation of levoglucosan which takes place above 250°C and reaction 3 involves fragmentation and formation of combustible products.

The relative proportions of gas, tar and char produced depend greatly on the heating rate [52]. Slow heating rates tend to produce more chars, little tar and less inflammable gas. In slow heating, decomposition proceeds in an orderly manner. Thus more stable molecules, which are rich in carbon tend to form with the hexagonal structure of graphitic carbon. Rapid heating, on the other hand, tends to produce little chars, much tar and highly inflammable gases that are rich in hydrogen, carbon monoxide and hydrocarbon. Shafizadeh [38] reported that the pyrolysis of cellulose in 1 atmosphere of nitrogen yielded more char and less tar than the corresponding

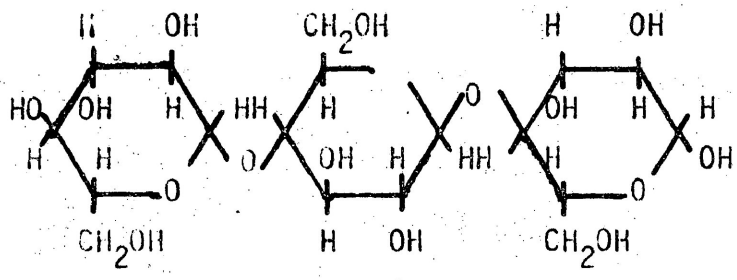

cellulose polymer

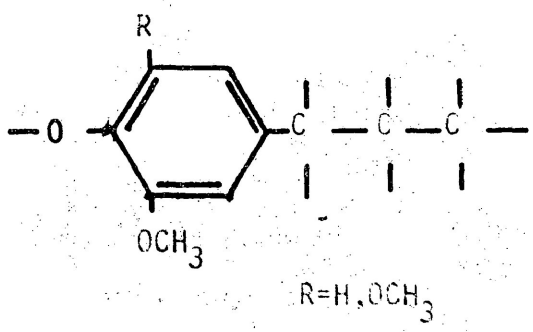

phenylpropane group

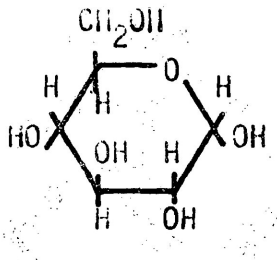

D-glucopyranose

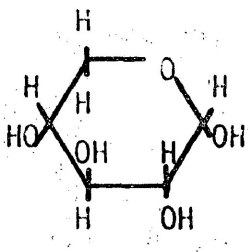

D-xylopyranose

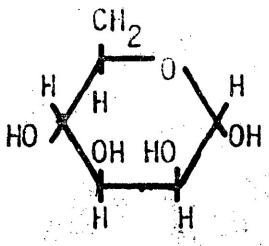

D-mannopyranose

Figure 2 Structural units of wood constituents.

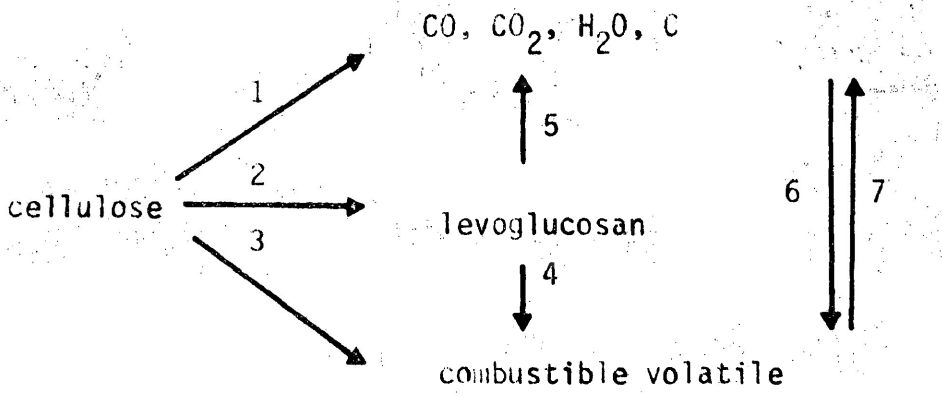

Figure 3 Pyrolysis reactions of cellulose.

pyrolysis under vacuum. At atmospheric pressure, the volatization and removal of the tar is limited, resulting in further decomposition and char formation as opposed to any secondary reactions. Thus the yield of pyrolytic products is highly influenced by the physical and chemical conditions under which pyrolysis occurs. Physical parameters such as temperature, pressure and time may affect the yields of the products. Chemical conditions such as the presence of catalysts may alter the nature and the extent of the pyrolysis reaction.

1.4 The effect of catalysts

The effect of inorganic impurities on the gasification of carbon and graphite has been investigated for many years. The subject has recently received increased attention because of the revival of interest in coal gasification. However, not much work on the catalytic gasification of wood has been undertaken. Although wood and cellulosic materials have a greater hydrogen component than coal, when they are pyrolyzed above 600^{o}C, the carbonaceous residue assumes a hexagonal graphite network which closely resembles that of coal [13]. Thus, any inorganic impurities might be expected to exert similiar general effects on the gasification of wood and related materials as in carbon and coal. Metals, metal oxides, metal halides, metal carbonyls, several alkali metal and transition metal compounds have all been tested as possible catalysts for gasification reactions.

Rewick et. al. [53] studied the effect of Pt, Ni and Fe in the gasification of activated carbon at atmospheric pressure and found that Pt was the most active catalyst. Otto and Shelef [54] reported that the effect of impregnated nickel nitrate on the gasification of graphite was to increase the rate of gasification without a change in the activation energy with respect to the uncatalyzed reaction. Haynes et. al. [55] investigated the effects of 40 different catalysts and concluded that Raney nickel was the most active

catalyst in the production of methane. Appell and Pantages [56] studied the effectiveness of a number of metals for the direct decomposition of cellulose by impregnating sawdust with compounds that were converted to the metal at the operating condition of the experiment. They found that cobalt was the most active and the most selective catalyst.

The use of alkali metal compounds as promoters for the steam gasification of coal has been studied for many years. Haynes et. al. [55] reported that K_2CO_3, KCl and Li_2CO_3 were effective catalysts. Veraa and Bell [57] reported that K_2CO_3 and KOH were active catalysts in the gasification of sub-bituminous coal at atmospheric pressure. However, they did not find any catalytic effect of KCl and NaCl, in disagreement with other studies [55]. High catalytic activity has also been reported for Na_2CO_3 [58]. The Kellogg steam gasification process [59], which employs a recirculating Na_2CO_3 melt, also yields high coal reaction rates.

The role of alkali metal carbonates as catalysts during pyrolysis of wood bark has been investigated by Rai and Tran [60], while Appell and Pantages [56] studied the effect of the concentration of potassium carbonate on the overall gas yields and compositions in the gasification of glucose. They indicated that the result of increasing potassium carbonate concentration was to cause an increase in the water-gas shift reaction (6). Lewis et. al. [61] reported that at low pressure, K_2CO_3 enhanced H_2 and CO_2 production and as the pressure was increased, significant amounts of methane were produced.

Alkali earth metal compounds have also been reported to catalyze the carbon-steam reaction. Otto and Shelef [62] reported that the catalytic effect on the gasification of graphite increased in the order of Ca < Sr < Ba. Feldmann [63] reported that CaO chemically incorporated into coal and wood from an elevated-temperature ($\sim 250^{\circ}C$) slurry, catalyzed the gasification

reaction. It was also observed that wood ash was itself an effective catalyst when simply sprayed on to wood in the form of an aqueous solution and the suggestion was made, from an analysis of H_2/CO ratios, that these catalysts caused an increase in the contribution of the water-gas shift reaction (6).

1.5 Objective of the present work

From the above survey, it is apparent that most previous work with additives has been concerned with their effects on coal and carbon gasification although in recent reports from these laboratories, emphasis has been placed on studies of the effects of selected additives on the pyrolysis of wood wastes and wood components [26,41,46,47]. The present contribution extends this work to include gasification experiments with wood waste materials in the presence of transition, alkali and alkaline-earth metal compounds in various atmospheres at pressure up to 2533 kPa.

The bark of jack pine, Pinus banksiana, Lamb, and sawdust of white birch, Betula papyrifera, were used as the wood wastes. In addition, parallel experiments were carried out on cellulose in an attempt to obtain more explicit and fundamental data regarding the kinetics and mechanisms of the reactions.

2. Experimental

2.1 Materials

2.1.1 Gases

Industrial grade helium (> 99.9%) and hydrogen (> 99.9%); K grade nitrogen (> 99.9%); dry grade carbon dioxide (> 99.7%); C. P. grade carbon monoxide (> 99.4%) and methane (> 99.4%) and a calibrated gas mixture containing carbon monoxide (0.105%), carbon dioxide (0.104%), hydrogen (0.10%) and methane (0.105%) in helium were used as supplied by Canadian Liquid Air Ltd.

2.1.2 Additives

Reagent grade (> 99.5%) $BaCO_3$, K_2CO_3, Li_2SO_4, K_2SO_4, ZnO and Cr_2O_3 were used as supplied by BDH Chemicals Ltd. Fe_2O_3 (99.9%) was obtained from

Ventron, Inc.

Zinc (II) chromite was prepared by heating a mixture of 1 mole of zinc (II) oxide and 1 mole of chromium (III) oxide at 1000°C in a nitrogen atmosphere for 8 h [64] and subsequently characterized by x-ray powder diffraction photography.

2.1.3 Cellulose

Whatman column chromedia CF1 fibrous cellulose powder (maximum 0.015% ash) was obtained from W. and R. Balston Ltd.

2.1.4 Jack pine bark

Jack pine bark samples (Pinus banksiana, Lamb.) were obtained from the Lakehead University Woodlot in Flower and Jacques Townships, Thunder Bay District. The trees were 80 to 150 years old. The bark was hand screened to remove wood traces and shredded in a high-speed blender. Samples were sieved to <212 μm.

2.1.5 White birch sawdust

The sawdust was obtained by repeated cuts through a white birch (Betula papyrifera) log, which had been cut in Raith, Ontario. The tree was about 70 years old. The sawdust was shredded in a high-speed blender and sieved to <212 μm.

2.1.6 Cellulose and white birch sawdust containing additives

Cellulose, white birch sawdust and each of the solid additives were sieved to <212 μm. Each additive was mixed with cellulose or white birch sawdust and ball-milled for 25 min. for the dry-mixed samples. Cellulose samples impregnated with K_2CO_3 were prepared by mixing cellulose into a saturated K_2CO_3 solution at room temperature. The slurry was stirred for 24 h, filtered, washed with distilled water, dried and then heated in a thermobalance to 1000°C in nitrogen. The amount of carbonate in the final cellulose samples was obtained from the mass of ash left after heating.

2.1.7 Jack pine chars containing additives

Each of the additives was mixed with jack pine bark and ball-milled for 25 min. Char samples were obtained by pyrolysing the corresponding bark and additive mixture in nitrogen at 350°C for 3 h.

2.2 Apparatus and method

2.2.1 Thermobalance

A Stanton-Redcroft Thermobalance, model HT-5F, was used. The automatic weight-loading assembly allowed a wide weight range (20 to 200 mg) for study. A schematic of the thermobalance assembly is shown in Figure 4. The sample support was connected to the back pan of the balance. Weights were added to the front pan to bring the recorder pen on scale. A servo-driven capacity-follower device was used to transmit beam movement to the recording mechanism.

A platinum/rhodium-wound furnace was mounted around the sample support. Furnace temperature was controlled by a platinum/platinum-rhodium (13%) thermocouple positioned between the furnace wall and a silica sheath. The silica sheath allowed a flowing gas to surround the sample continuously. The gas was dried over calcium sulphate before entering the furnace. In isothermal experiments, the temperature was controlled by a proportional controller. In dynamic experiments, the furnace temperature was programmed to increase linearly at a rate of 7K min^{-1}.

Sample temperatures were monitored on a Leeds and Northup recorder from a platinum/platinum-rhodium (13%) thermocouple located within the sample support. The recorder was calibrated using a Honeywell portable potentiometer over the range 0-10 mv. The accuracy of the measurement was within $\pm$ 1°C over the temperature range studied.

2.2.2 Isothermal technique

About 40 mg of sample was weighed into a platinum crucible. It was

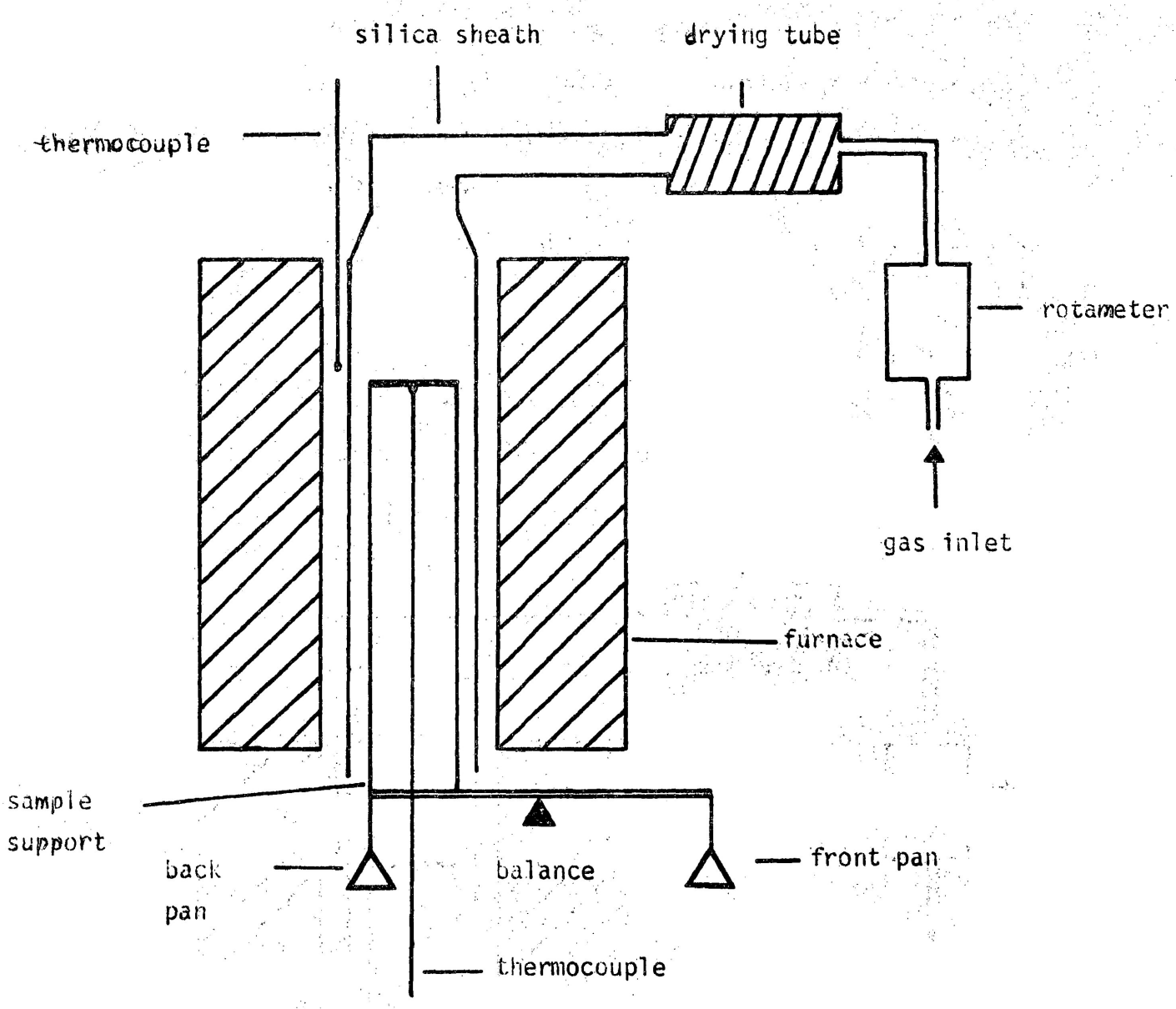

Figure 4 Thermobalance assembly.

then balanced on the back pan of the thermobalance. Meanwhile, the sample support and the furnace were heated to a preselected temperature with gas flowing. The specimen was transferred to the sample support quickly (about 30 s). The sample temperature was within 3°C of the preselected temperature in 2 min and attained thermal equilibrium with the furnace in 4 min. In all of the experiments, the nitrogen flow rate was kept at 230 ml min^{-1} (NTP).

2.2.3 Dynamic thermogravimetric technique

Some samples appeared to cause platinum crucibles to pit at high temperatures. Thus a conical alumina crucible was used to contain the 40 mg samples. The specimen was balanced on the sample support at room temperature with nitrogen gas flowing at 230 ml min^{-1} (NTP). When a straight base line was obtained, the furnace was turned on, which increased the temperature linearly to 1000°C in approximately 2.5 h.

2.2.4 Gaseous products analysis in the high-pressure 'static system'

A stainless-steel high-pressure apparatus was used as reactor to pyrolyse the samples for gas analysis, Figure 5. The reactor was constructed from 5 cm o.d. stainless steel tubing, total length of 60 cm, in two sections mated with a copper gasket. It was heated by a moveable resistance-wound furnace. The temperature was controlled by a chromel/alumel thermocouple which was positioned directly below the sample container and connected to a 'Thermoelectric 400' proportional controller.

The gaseous products were analysed using a Beckman GC-5 gas chromatograph with thermal conductivity detectors. The separation columns were packed with "Carbosieve B" and the chromatograms recorded on a Beckman 10" recorder.

About 100 mg of sample was weighed into the stainless steel sample container and placed in the reactor. Pure helium or water-saturated helium could be fed into the reactor, depending on experimental requirements, as

shown in Figure 5. The reactor was flushed with helium before the start of the experiment and gas samples were analysed to ensure that air had been removed. Then the pressure of the system was set to a preselected value, 101.3 to 2,532.5 kPa. The temperature was raised to a preselected value in 5 min and kept constant for a further 30 min. Then the product gases were analysed by the gas chromatograph.

2.2.5 Gaseous products analysis in 'flow system'

The reactor was constructed from 20 mm i.d. quartz tubing, total length 47 cm. About 0.4 g of sample was sandwiched between quartz wool plugs supported on three dimples in the reactor wall. The reactor was resistance-heated by 'Chromel A' resistance wire. The temperature was controlled by a chromel/alumel thermocouple positioned directly above the couples and connected to a 'Thermoelectric 400' controller.

A Beckman GC-5 gas chromatograph with thermal conductivity detectors was used to analyse the gases. The columns were packed with "Carbosieve B" and the chromatogram recorded on a Linear Instruments 10" strip chart recorder. A typical chromatogram of the gaseous products is shown in Figure 6.

Flow rates were maintained using 'Matheson Rotameters' fitted with fine-control needle valves. In line (a), helium passed through a water saturator as shown in Figure 7. The saturator was maintained at $81 \pm 0.5^{o}C$ by means of a water bath equipped with a circulatory heater. The water-saturated helium was channelled into a common manifold where it was allowed to mix with other reactants or helium carrier gas. The gas mixture entered the preheater which raised the temperature of the gas close to that of the reactor and prevented any water condensation. The reaction products were conducted from the reactor through heated lines to the gas chromatograph for analysis.

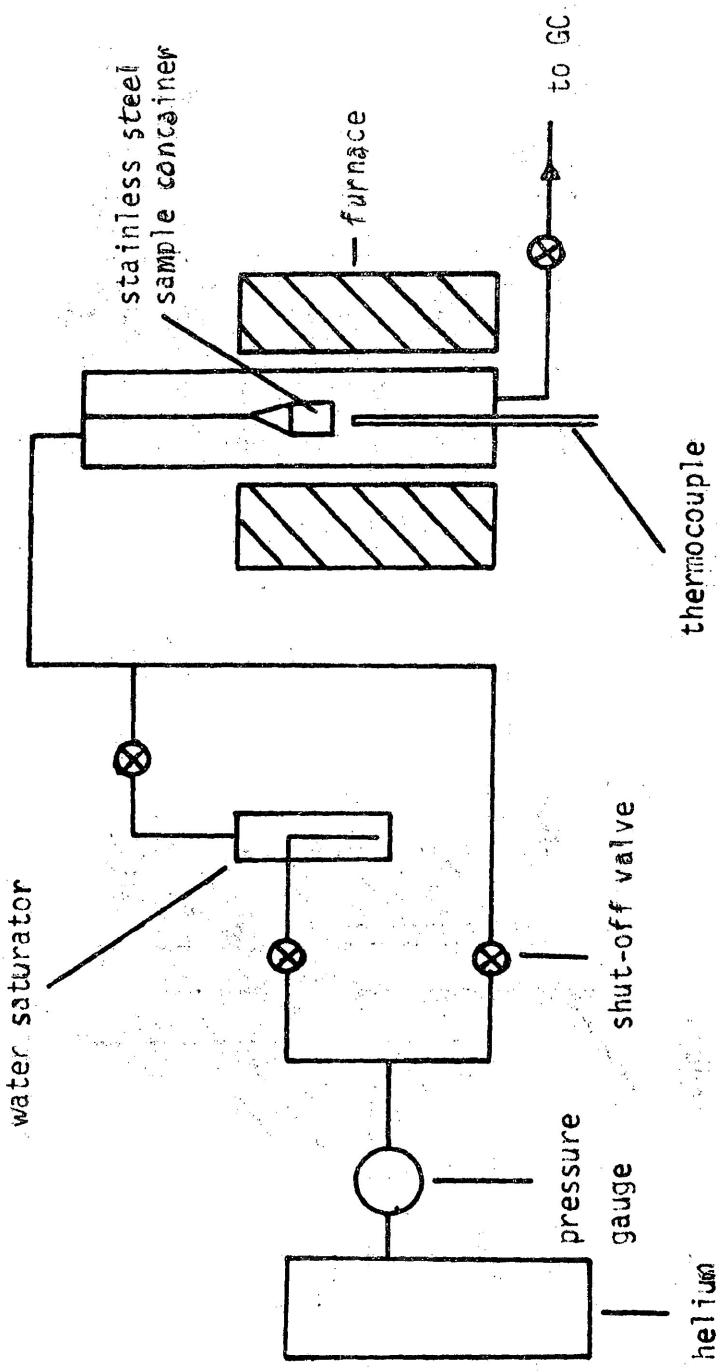

Figure 5 High-pressure 'static system'.

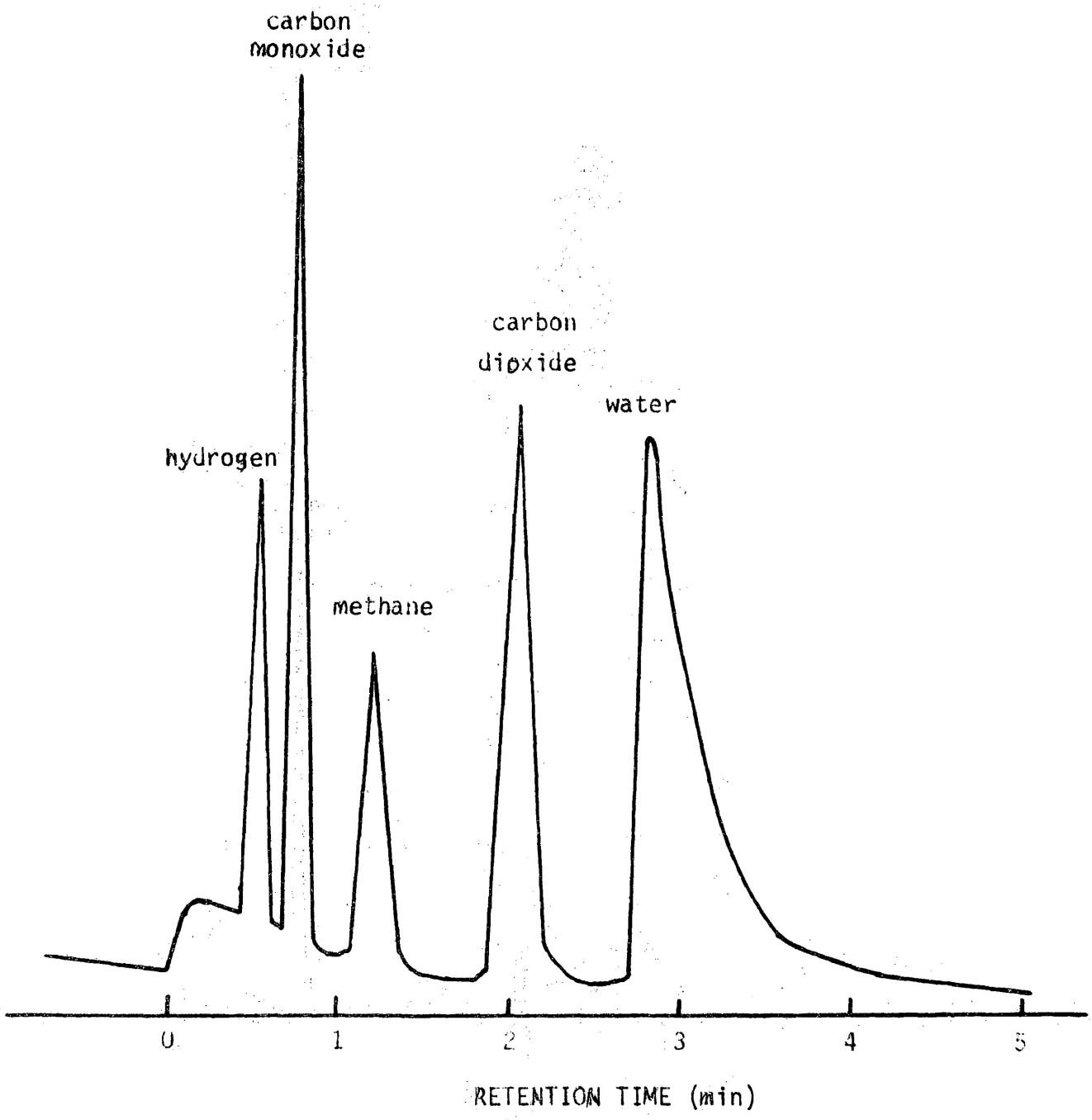

Figure 6 Typical chromatogram of the gaseous products.

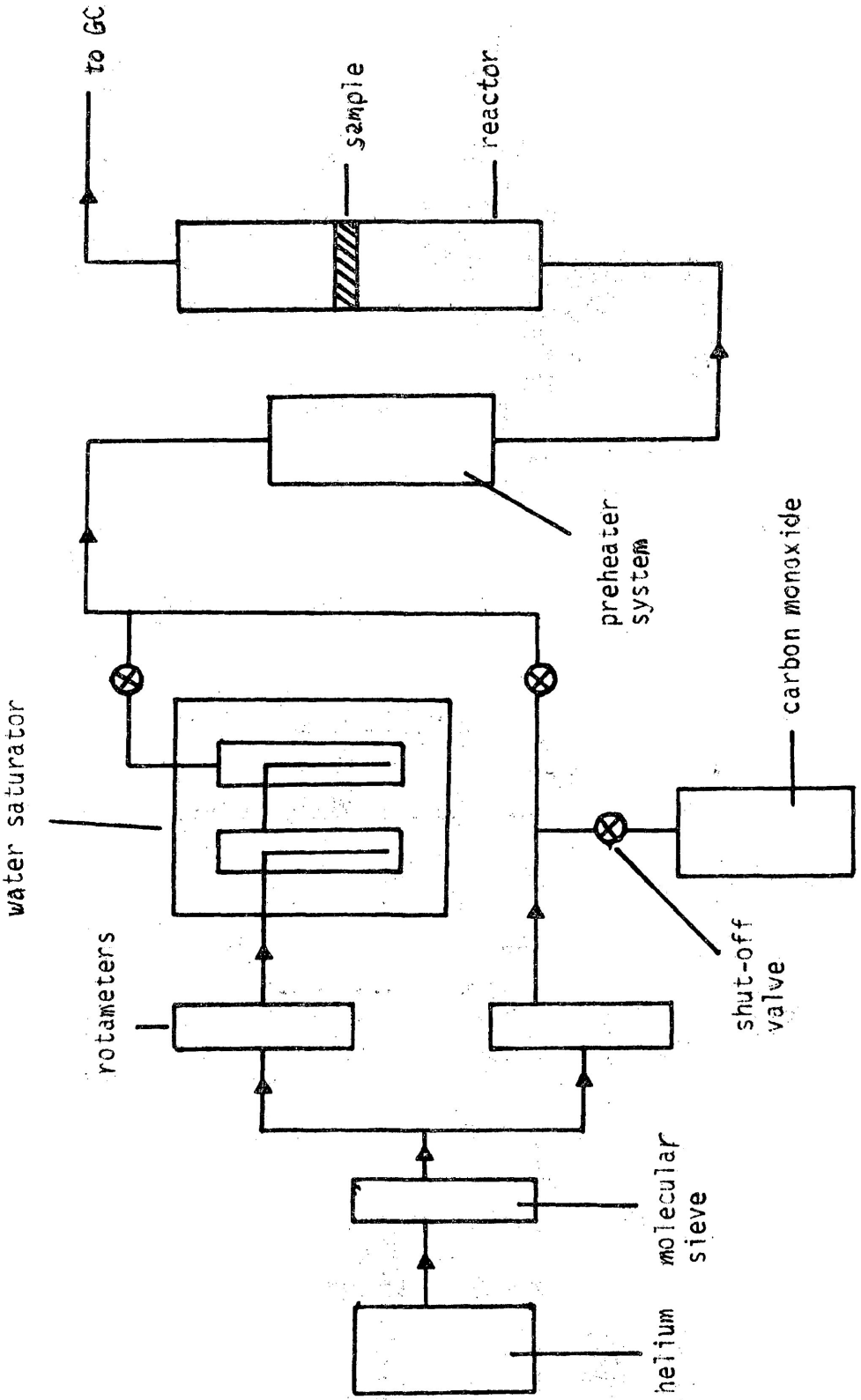

Figure 7 'Flow system'.

Pure helium or a helium/carbon monoxide mixture was passed through line (b) depending on the experimental requirements. The flow through the water saturator was maintained at 70 ml min^{-1} (NTP), while a total flow rate of 100 ml min^{-1} (NTP) was used for all the experiments.

About 0.4 g of sample was placed in the reactor which was then flushed with helium for 30 min. The sample temperature was raised to 350°C in 20 min. The final temperature of 650°C was attained by an increase of 25°C every 5 min. The gaseous products produced were monitored at various temperatures.

2.2.6 Calibration for detectors

The thermal conductivity detectors were calibrated for concentrations of H_2, CH_4, CO and CO_2 by the exponential dilution method [65]. A gas sample was injected into a mixing vessel of known volume with a constant flow of helium passing through it. Equation (19) was used to calculate the concentration of the gas at any given time t.

$$c_t = C_o \cdot \exp^{-(F/V)t} \qquad (19)$$

where C_o is the concentration of the gas at t = o, F is the flow of helium and V is the volume of the vessel. Then a calibration curve of peak height versus the concentration of the gases was constructed.

2.2.7 X-ray analysis

X-ray powder diffraction patterns of samples were obtained with a Philipps X-ray generator which operated at 40 kV and 20 mA, using a nickel-filtered, copper-K_α radiation source, equipped with a 114.8 mm Debye-Scherrer camera. The samples were finely ground and sealed in a capillary tube. X-ray powder diffraction patterns were recorded on strips of photographic film, whence the interplanar spacing was calculated and the samples identified by comparison with standards in the usual manner [66].

2.2.8 Residue analysis

The carbon, hydrogen and nitrogen compositions of samples were analysed by a Perkin Elmer model 240 elemental analyser. About 1.5 to 3.5 mg of sample was combusted in pure oxygen at 1000°C and analysed by difference for N_2, CO_2 and H_2O using thermal conductivity cells.

2.2.9 Scanning electron microscopy

Samples were characterised by scanning electron microscopy (SEM) using a Cambridge Stereoscan 600. They were coated with a thin layer of gold by a standard flash evaporation technique at 10^{-4} Torr. Pictures were taken with a 35 mm or Polaroid camera attached to the CRT screen.

2.2.10 Electron diffraction analysis

Transmission electron micrographs were obtained with a Philips EM 300 instrument. Samples were air pressed onto grids with carbon substrates and were examined at 100 kV. Selected area electron diffraction (SAED) micrographs were taken with a 35 mm or Polaroid camera.

2.2.11 Surface area measurement

The technique involves the measurement of the amount of gas necessary to form a monolayer on a solid surface. The surface area can be determined from the number of molecules adsorbed and the area occupied by each molecule.

The general BET equation (20) was used in the calculation [67]:

$$\frac{p}{V(p_o-p)} = \frac{1}{V_m c} + \frac{(c-1)p}{V_m c p_o} \qquad (20)$$

where V_m is the monolayer volume, p_o is the saturation pressure of the absorbate gas, V is the total volume of gas absorbed, p is pressure measured and c is a constant related to the heats of absorption and liquefaction of the gas.

About 10 mg of sample was weighed into the sample tube which was then positioned on the apparatus, Figure 8, and evacuated at 10^{-4} Torr for 12 h at 10°C. Krypton the absorbate, was then admitted to V_a and the pressure measured on the McLeod gauge. The gas was expanded into the sample tube which was immersed in liquid nitrogen. After equilibrium was achieved, approximately 30 min , the pressure was again measured and the volume of krypton adsorbed was calculated in the usual way [68].

3. Results

3.1 Cellulose

3.1.1 Dynamic thermogravimetry (TG)

The TG curves obtained for the thermal decomposition of cellulose and cellulose plus additives in nitrogen are shown in Figure 9.

The curve for pure cellulose showed an initial loss of 3.0% below 280°C. The major weight loss commenced at 300°C and increased linearly to 82% at 380°C. The final weight loss at 900°C was 91%. The curve for cellulose containing zinc (II) chromite was similiar to that of plain cellulose.

The curve for cellulose with iron (III) oxide showed that major weight loss commenced at 285°C, reaching 77% loss at 355°C. The total loss at 900°C was 95%.

In general, the samples containing potassium carbonate showed a much less abrupt response to temperature increase than the others. The major loss started at a lower temperature, 175°C for the 5% potassium carbonate sample and about 200°C for the rest, than that for pure cellulose and those samples containing the transition metal compounds. The rapid weight-loss region reached a value at 350°C of 62.5% for cellulose with 5% potassium carbonate, dry-mixed and ball-milled, and 57.5% for ball-milled cellulose

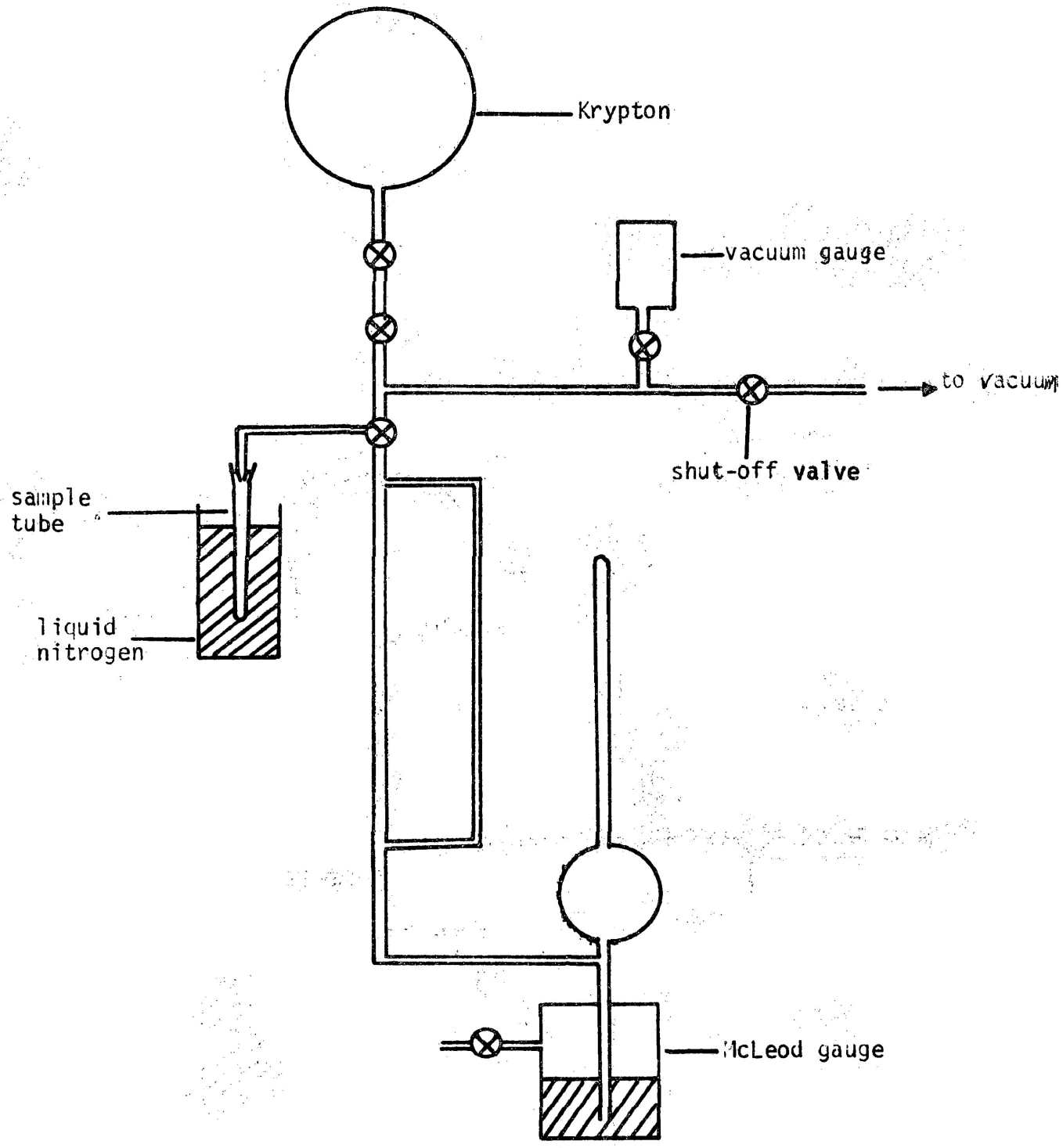

Figure 8 Krypton BET apparatus.

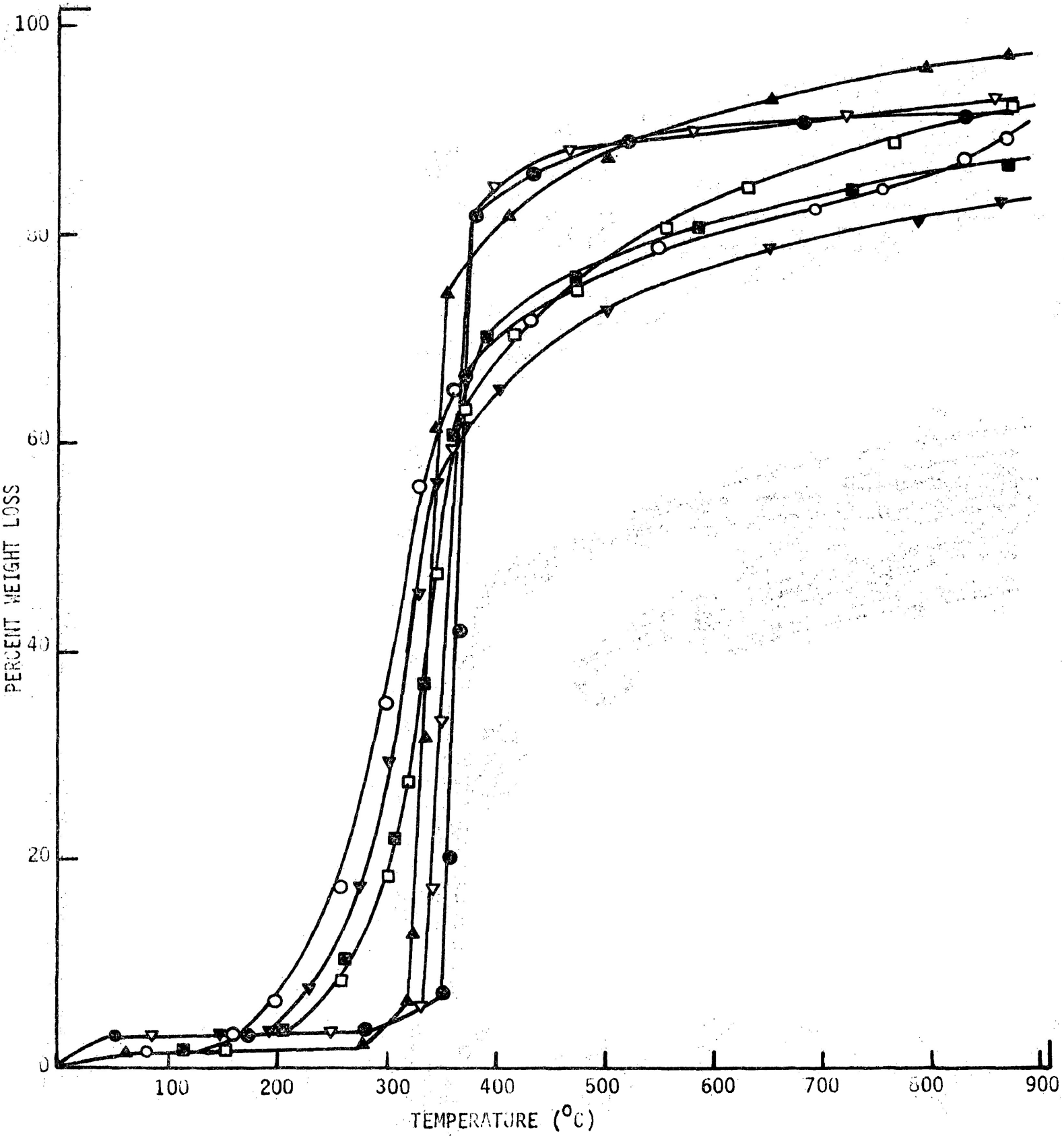

Figure 9 Thermograms for the various cellulose preparations in nitrogen. ● =ball-milled pure cellulose; ▲= ●+10.2% w/w iron(III)oxide (dry mix); □ = cellulose + 0.7% w/w impregnated K_2CO_3; ▼= ●+ 0.7% w/w impregnated K_2CO_3; ○= ●+ 5.0% w/w K_2CO_3 (dry mix); ■= ● + 0.7% w/w K_2CO_3 (dry mix); ▽ = ● + 14.2% w/w zinc(II)chromite (dry mix).

containing 0.7% impregnated potassium carbonate. Total weight loss at 900°C varied from 92% for plain cellulose with 0.7% potassium carbonate impregnated to 85% for ball-milled cellulose with 0.7% potassium carbonate impregnated.

3.1.2 Isothermal pyrolysis

Isothermal weight-change experiments were carried out on cellulose powder in flowing nitrogen from 299 to 330°C. Plots of weight per cent loss versus time confirmed earlier data [26,46] by showing a linear response up to approximately 5% loss followed by a rapid loss and then a slow approach to constant weight.

Kinetic parameters were derived in the manner established earlier [26,46]. The standard kinetic plot α versus $t/t_{0.5}$ is shown in Figure 10. α is the weight loss at time t divided by the final weight loss and $t_{0.5}$ is the time when $\alpha = 0.5$. The pyrolysis was described by two regions. An initial region - defined by $\alpha < 0.05$ - followed simple zero order kinetic behaviour, while the following region, $\alpha = 0.05$ to 0.85, exhibited kinetics which were described by: -

$$[1 - (1 - \alpha)^{0.5}] = (u/r)t \qquad (21)$$

Equation (21) describes a reaction rate controlled by the movement of an interface at constant velocity, u, through a cylinder of radius r [69]. The rate constant, u/r, was obtained from the slope of the plots of the L.H.S. of (21) versus time. Kinetic parameters were then obtained in the standard way from the Arrhenius plot, Figure 10, and are summarized in Table 2.

Cellulose samples containing iron (III) oxide and zinc (II) chromite obeyed the same kinetic expressions for pyrolysis data as those for pure cellulose. The addition of zinc (II) chromite showed no measurable effect on the parameters, in contrast to iron (III) oxide which lowered the value of E_a from 161.0 to 153.0 kJ mol^{-1} in the initial region and from 207.5 to

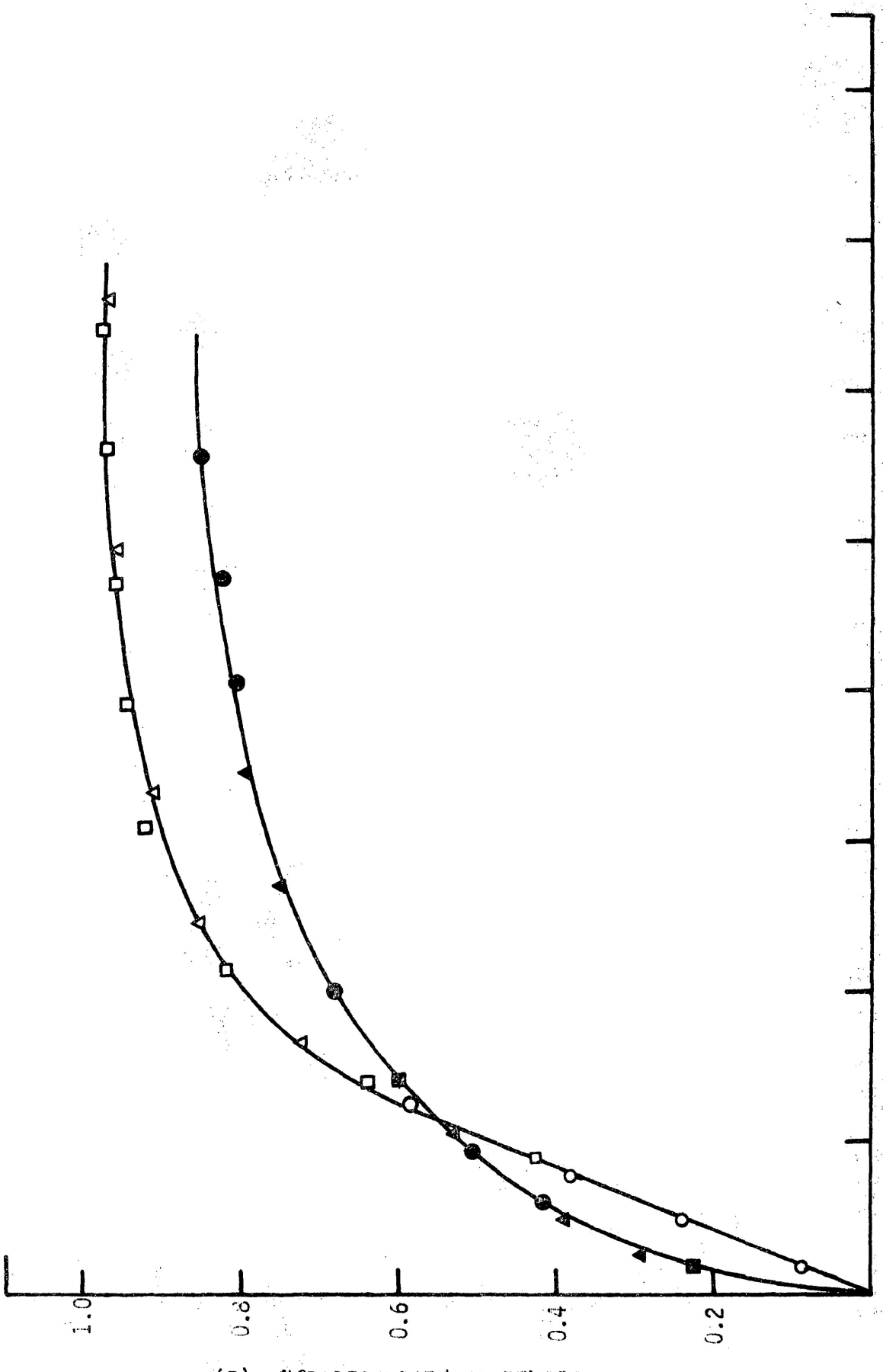

Figure 10 Reduced time plots for cellulose and cellulose containing 5.0% w/w K_2CO_3 in nitrogen at various temperatures.

○ = cellulose at 299°C; △ = cellulose at 320°C; □ = cellulose at 330°C; ● = cellulose + K_2CO_3 at 295°C; ▲ = cellulose + K_2CO_3 at 258°C; ■ = cellulose + K_2CO_3 at 285°C.

Table 2. Kinetic parameters for pyrolysis of the various cellulose samples in nitrogen.

egion	Material	Temperature (°C)	Rate constant $k \times 10^{-2}$ (min^{-1})	Frequency factor A (min^{-1})	Apparent activation energy E_a ($kJ\ mol^{-1}$)
	cellulose	299 315 320 330	26.7 86.1 111.1 200.0	1.4×10^{14}	161.0 ± 8.9
1	cellulose + 14.2% zinc (II) chromite	295 309 325 339	25.4 65.1 110.5 271.8	1.4×10^{14}	161.0 ± 8.9
	cellulose + 10.2% iron (III) oxide	295 317 322 336	44.3 117.7 173.0 350.0	3.4×10^{13}	153.0 ± 20.6
	cellulose	299 315 320 330	0.4 1.7 2.4 5.2	3.9×10^{16}	207.5 ± 8.5
2	cellulose + 14.2% zinc (II) chromite	295 309 325 339	0.4 1.0 2.7 7.8	3.9×10^{16}	207.5 ± 8.5
	cellulose + 10.2% iron (III) oxide	295 317 322 336	0.5 2.6 2.8 6.3	5.1×10^{14}	187.0 ± 30.9

187.0 kJ mol^{-1} in the second region.

The curve obtained for cellulose with 5% potassium carbonate from the standard kinetic plot, Figure 10, differed from that given by pure cellulose. It closely resembles the pattern expected for two-dimensional (D_2) and three-dimensional (D_3) diffusion-controlled reactions [70]. Thus the kinetics could be described by equations (22) and (23): -

$$D_2\ (\alpha) = (1 - \alpha)\ \ell n\ (1 - \alpha) + \alpha = (k/r^2)t \qquad (22)$$

$$D_3\ (\alpha) = [1 - (1 - \alpha)^{1/3}]^2 = (k/r^2)t \qquad (23)$$

Plots of the left-hand side of equation (22) and (23) versus time were linear for values of $\alpha < 0.75$ and the slopes of these lines were used to obtain the rate constant, $k_d = k/r^2$. The values of activation energy, E_a, derived from the Arrhenius plots, Figure 11, are summarized in Table 3. The comparable E_a for cellulose of 207.5 kJ mol^{-1} was lowered to 107.6 and 113.9 kJ mol^{-1} for the two and three-dimensional models, respectively.

3.1.3 Gaseous products analysis

Cellulose samples were pyrolyzed in helium or helium saturated with water vapour in the high pressure 'static system' apparatus. The pressure of the system varied from 101.3 to 2532.5 kPa.

3.1.3.1 The effect of additives

The concentration of the various products obtained from pyrolysis in helium, 101.3 kPa, of the various cellulose samples from 400 to 650°C are shown in Figures 12 and 13.

For most samples, carbon monoxide production decreased with temperature until around 550°C when it began to increase slowly. A rapid increase in carbon monoxide evolution was observed from 450 to 650°C with the samples

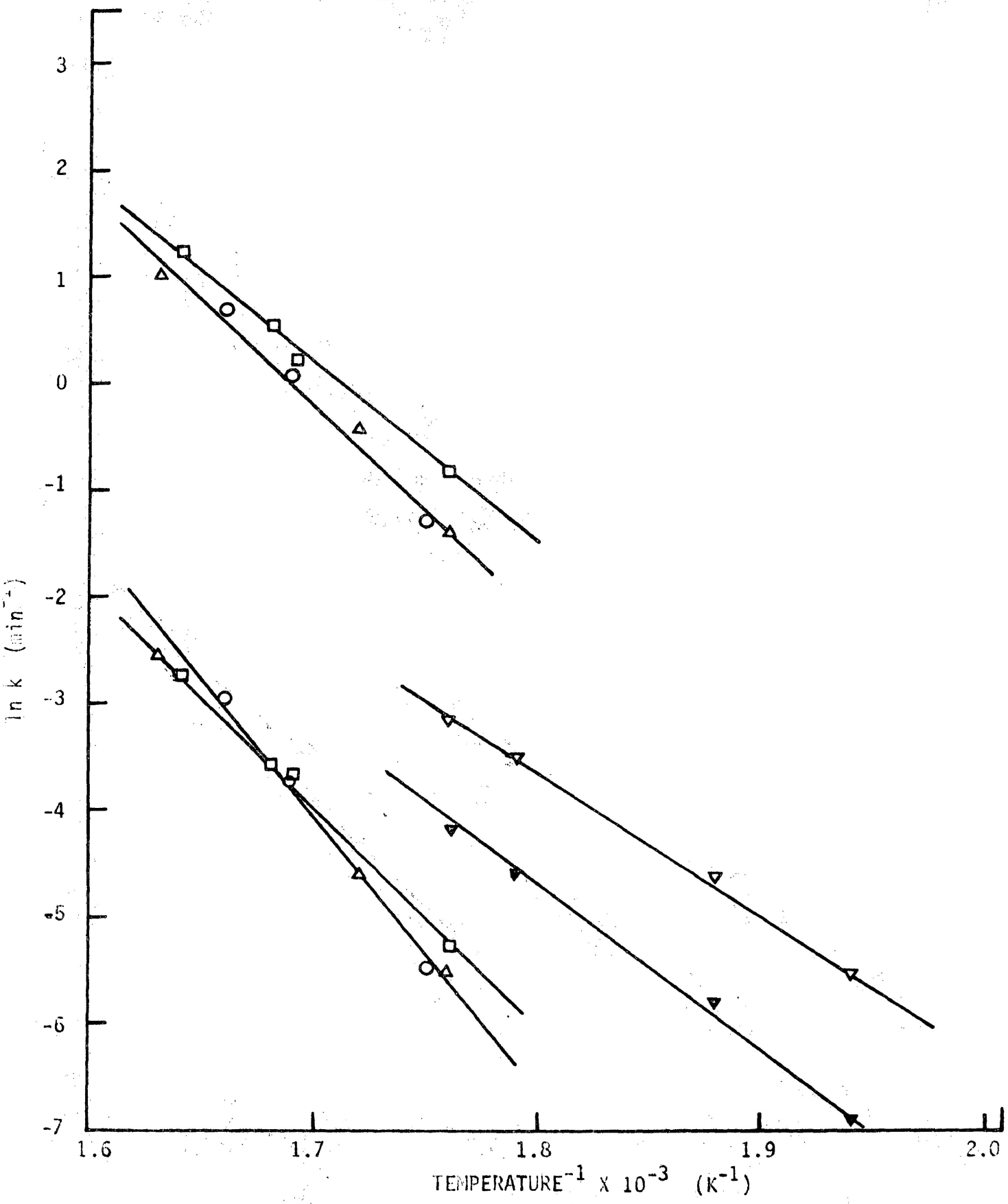

Figure 11 Arrhenius plots for the various cellulose samples in nitrogen from 242 to 340°C.

O = cellulose; △ = O + 14.2% w/w zinc(II)chromite; □ = O + 10.2% w/w iron (III)oxide; ▽ = O + 5.0% w/w potassium carbonate (D-2 model); ▼ = O + 5.0% w/w potassium carbonate (D-3 model).

Table 3. Kinetic parameters for pyrolysis of cellulose + 5% w/w K_2CO_3 in nitrogen.

Model	Temperature	Rate constant $k \times 10^{-2}$ (min^{-1})	Frequency factor A (min^{-1})	Apparent activation energy E_a (kJ mol^{-1})
Two-dimensional	242 258 285 295	0.4 1.0 3.0 4.3	3.3×10^8	107.6 ± 8.1
Three-dimensional	242 258 285 295	0.1 0.3 1.0 1.5	4.3×10^8	113.9 ± 10.4

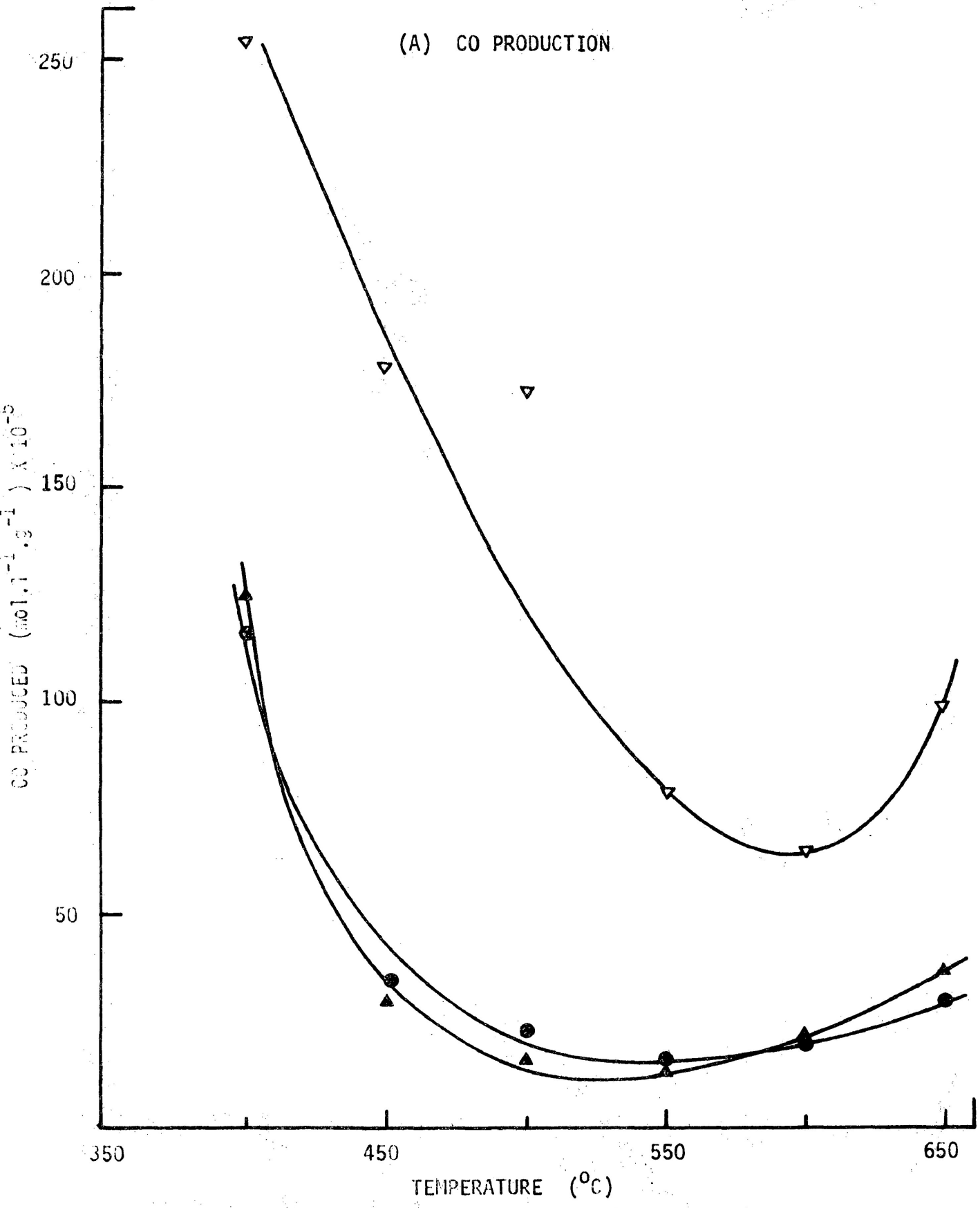

Figure 12(A) The effect of additives on the concentration of various gaseous products from cellulose samples in helium at 101.3 kPa.

● = cellulose; ▲ = ● + 10.2% w/w iron(III)oxide;
▽ = ● + 14.2% w/w zinc(II)chromite.

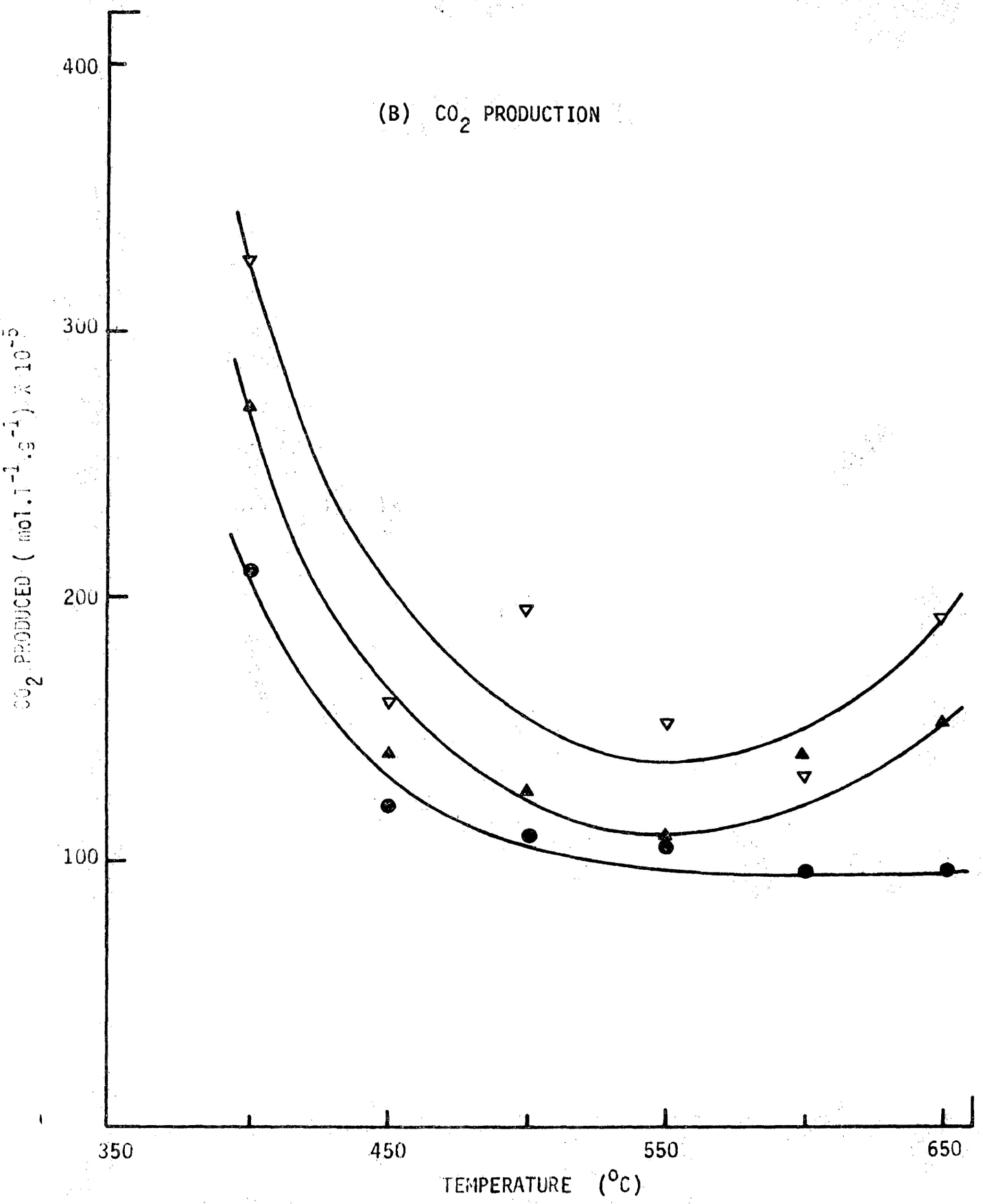

Figure 12(B) The effect of additives on the concentration of various gaseous products from cellulose samples in helium at 101.3 kPa.

● = cellulose; ▲ = ● + 10.2% w/w iron(III)oxide;
▽ = ● + 14.2% w/w zinc(II)chromite.

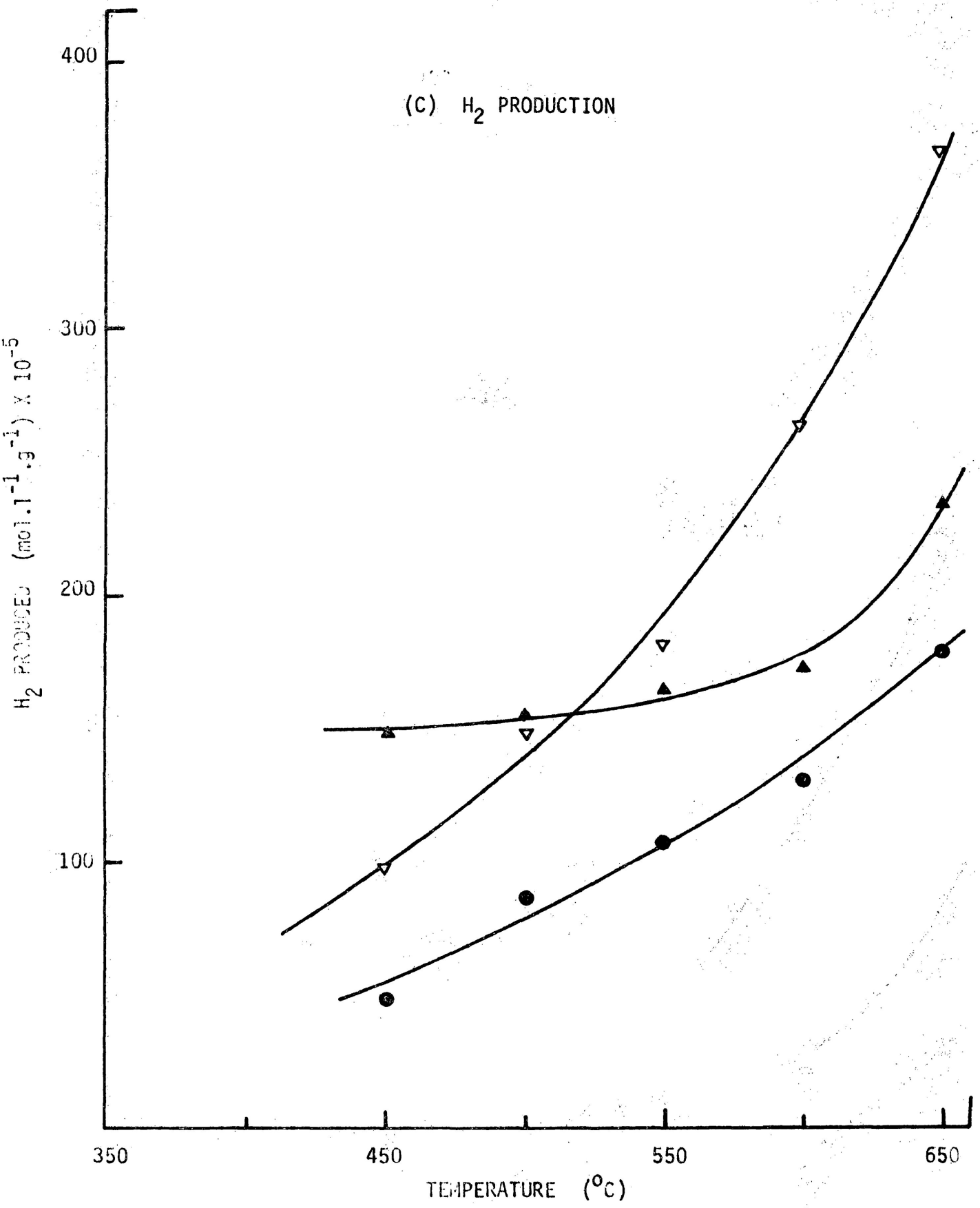

Figure 12(C) The effect of additives on the concentration of various gaseous products from cellulose samples in helium at 101.3 kPa.

● = cellulose; ▲ = ● + 10.2% w/w iron(III)oxide;
▽ = ● + 14.2% w/w zinc(II)chromite.

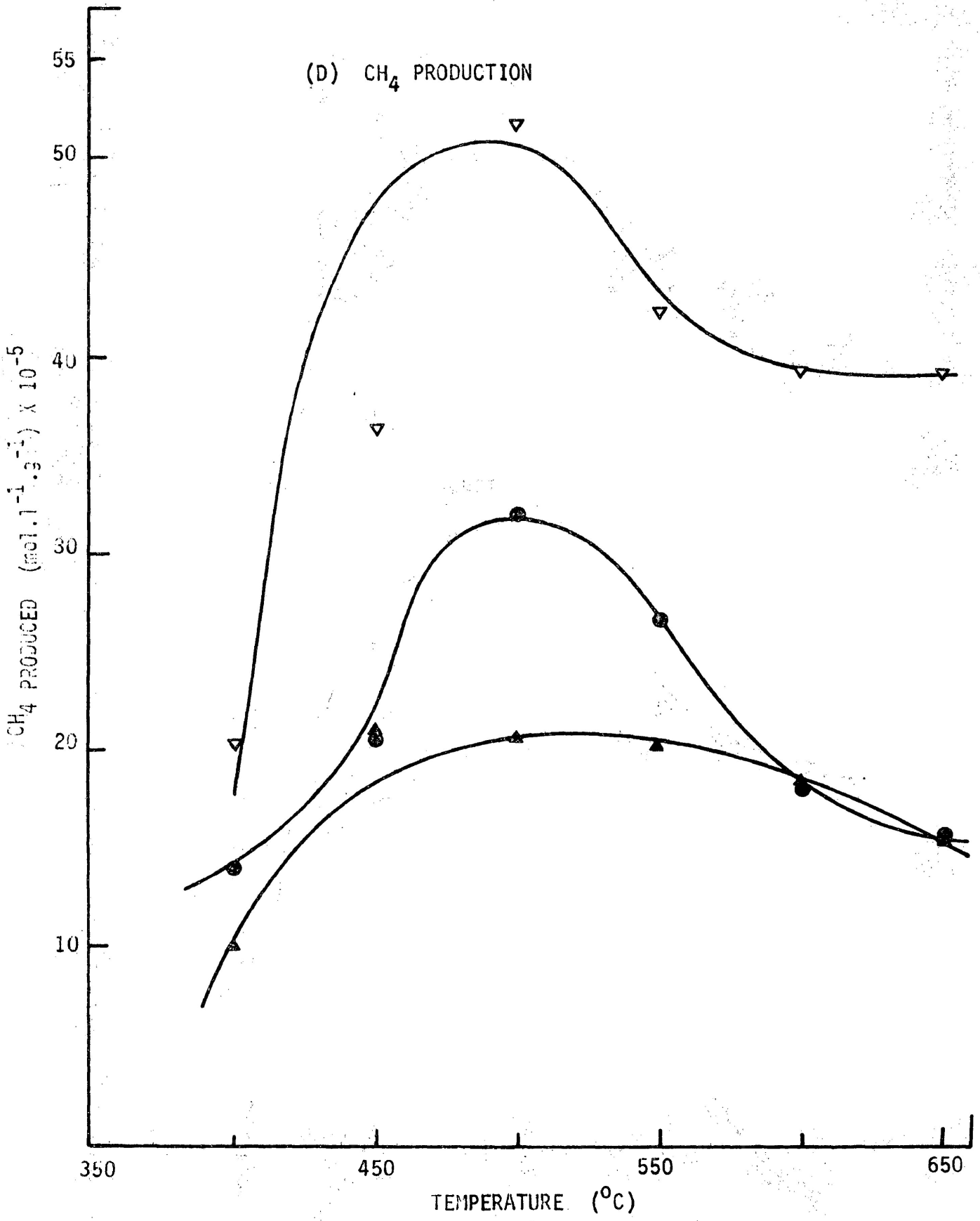

Figure 12(D) The effect of additives on the concentration of various gaseous products from cellulose samples in helium at 101.3 kPa.

● = cellulose; ▲ = ● + 10.2% w/w iron(III)oxide;
▽ = ● + 14.2% w/w zinc(II)chromite.

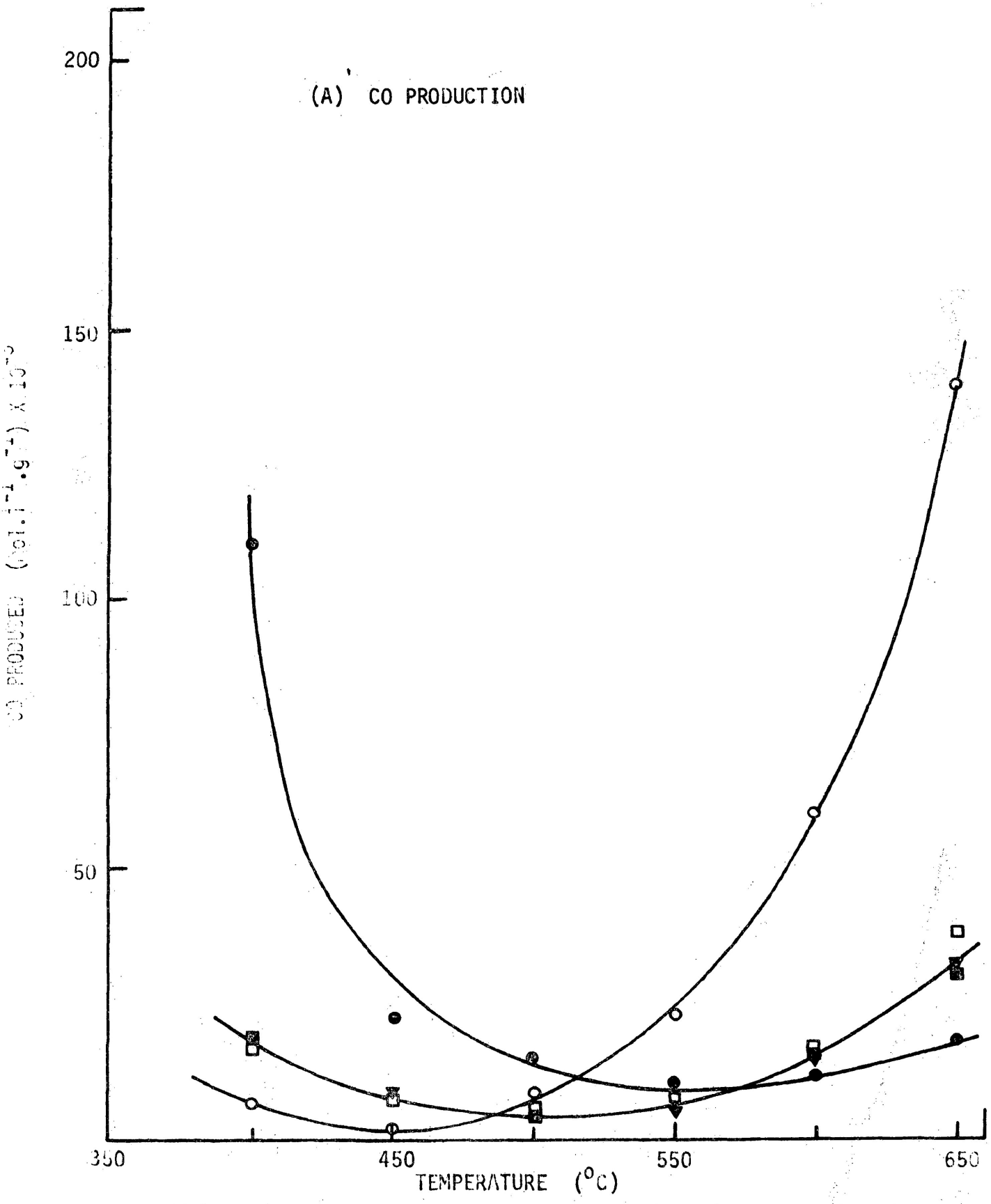

Figure 13(A) The effect of preparative procedure and different concentrations of K_2CO_3 on the concentration of the various gases formed in helium at 101.3 kPa.

● = ball-milled cellulose; □ = cellulose + 0.7% w/w impregnated K_2CO_3; ▼ = ● + 0.7% w/w impregnated K_2CO_3; ○ = ● + 5.0% w/w K_2CO_3 (dry mix); ■ = ● + 0.7% w/w K_2CO_3 (dry mix).

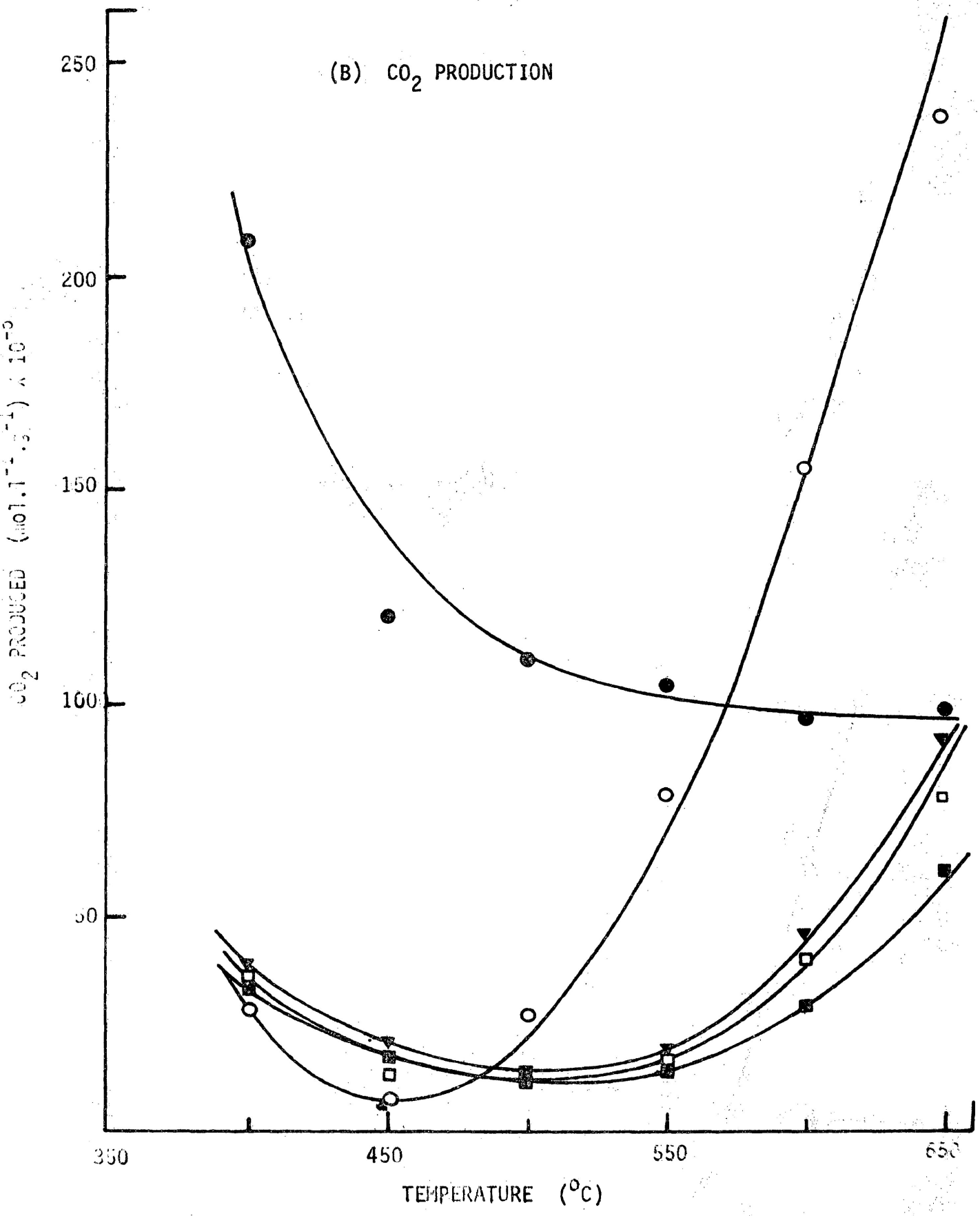

Figure 13(B) The effect of preparative procedure and different concentrations of K_2CO_3 on the concentration of the various gases formed in helium at 101.3 kPa.

● = ball-milled cellulose; □ = cellulose + 0.7% w/w impregnated K_2CO_3; ▼ = ● + 0.7% w/w impregnated K_2CO_3; ○ = ● + 5.0% w/w K_2CO_3 (dry mix), ■ = ● + 0.7% w/w K_2CO_3 (dry mix).

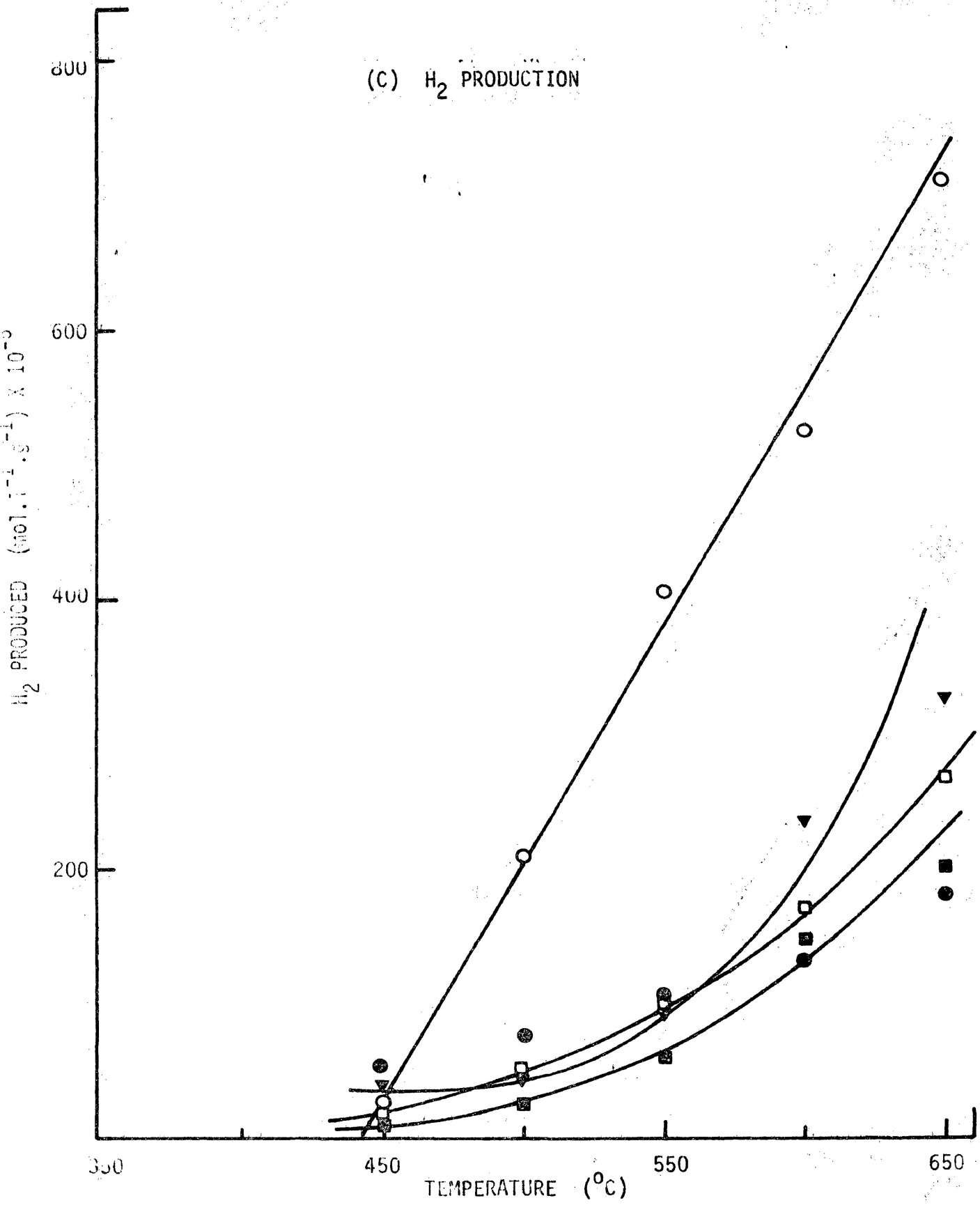

Figure 13(C) The effect of preparative procedure and different concentrations of K_2CO_3 on the concentration of the various gases formed in helium at 101.3 kPa.

● = ball-milled cellulose; □ = cellulose + 0.7% w/w impregnated K_2CO_3; ▼ = ● + 0.7% w/w impregnated K_2CO_3; ○ = ● + 5.0% w/w K_2CO_3 (dry mix); ■ = ● + 0.7% w/w K_2CO_3 (dry mix).

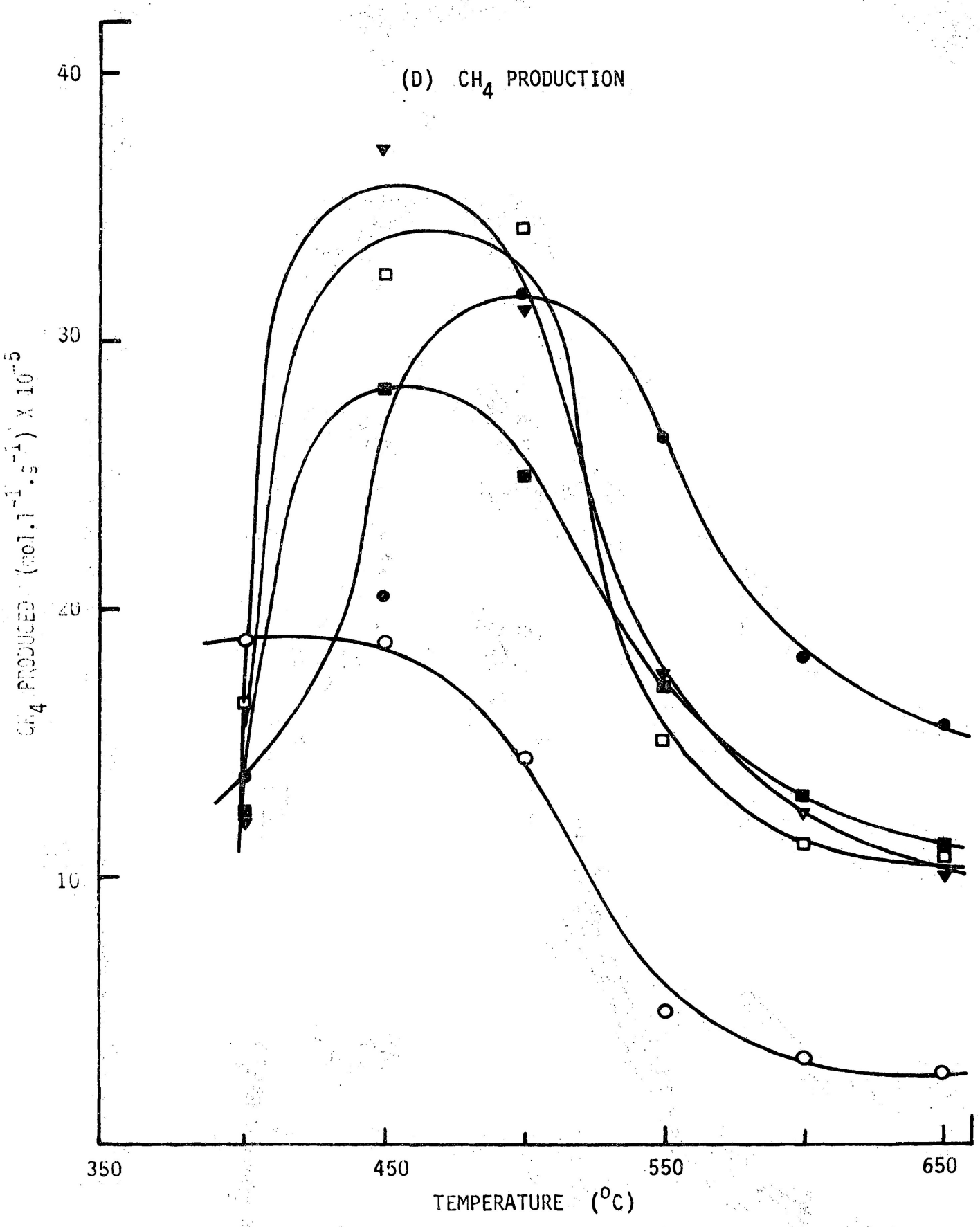

Figure 13(D) The effect of preparative procedure and different concentrations of K_2CO_3 on the concentration of the various gases formed in helium at 101.3 kPa.

● = ball-milled cellulose; □ = cellulose + 0.7% w/w impregnated K_2CO_3; ▼ = ● + 0.7% w/w impregnated K_2CO_3; ○ = ● + 5.0% w/w K_2CO_3 (dry mix), ■ = ● + 0.7% w/w K_2CO_3 (dry mix).

containing 5% potassium carbonate. The pattern of production of carbon dioxide followed the same general trend as those noted for carbon monoxide.

For all samples, methane evolution increased rapidly with temperature to a maximum between 450 and 500°C whence it began to decrease rapidly. A noticeably slow increase in hydrogen formation from 450 to 600°C was observed with iron (III) oxide admixtures and, comparatively, an unusually high yield of hydrogen was measured over the entire temperature range with samples containing 5% potassium carbonate.

3.1.3.2 The effect of pressure

Absolute concentrations of the various gaseous products could not be obtained at elevated pressures since the pressure of the gas injected in the gas chromatograph could not be measured with acceptable accuracy in the present apparatus. However, the product ratios: - CH_4/CO, CO_2/CO and H_2/CO could be obtained by comparing their peak heights with those obtained from a standard gas sample containing CO(0.105%), CO_2(0.104%), H_2(0.10%) and CH_4(0.105%) with helium making up the balance.

The effects of pressure, from 101.3 to 2532.5 kPa, on the product ratios obtained from cellulose and cellulose with 5% potassium carbonate from 400 to 650°C are shown in Figures 14 and 15. The maximum values of product ratios and the temperatures, T_{max}, at which these maxima occurred for all samples are summarized in Tables 4 and 5.

For cellulose and cellulose samples with zinc (II) chromite and iron (III) oxide, no trend was observed for H_2/CO and CO_2/CO ratios. However, the CH_4/CO ratio decreased with increasing pressure. For samples containing potassium carbonate, the product ratios decreased with increasing pressure.

It may be noted that increase of pressure tended to increase the value of T_{max} for all samples.

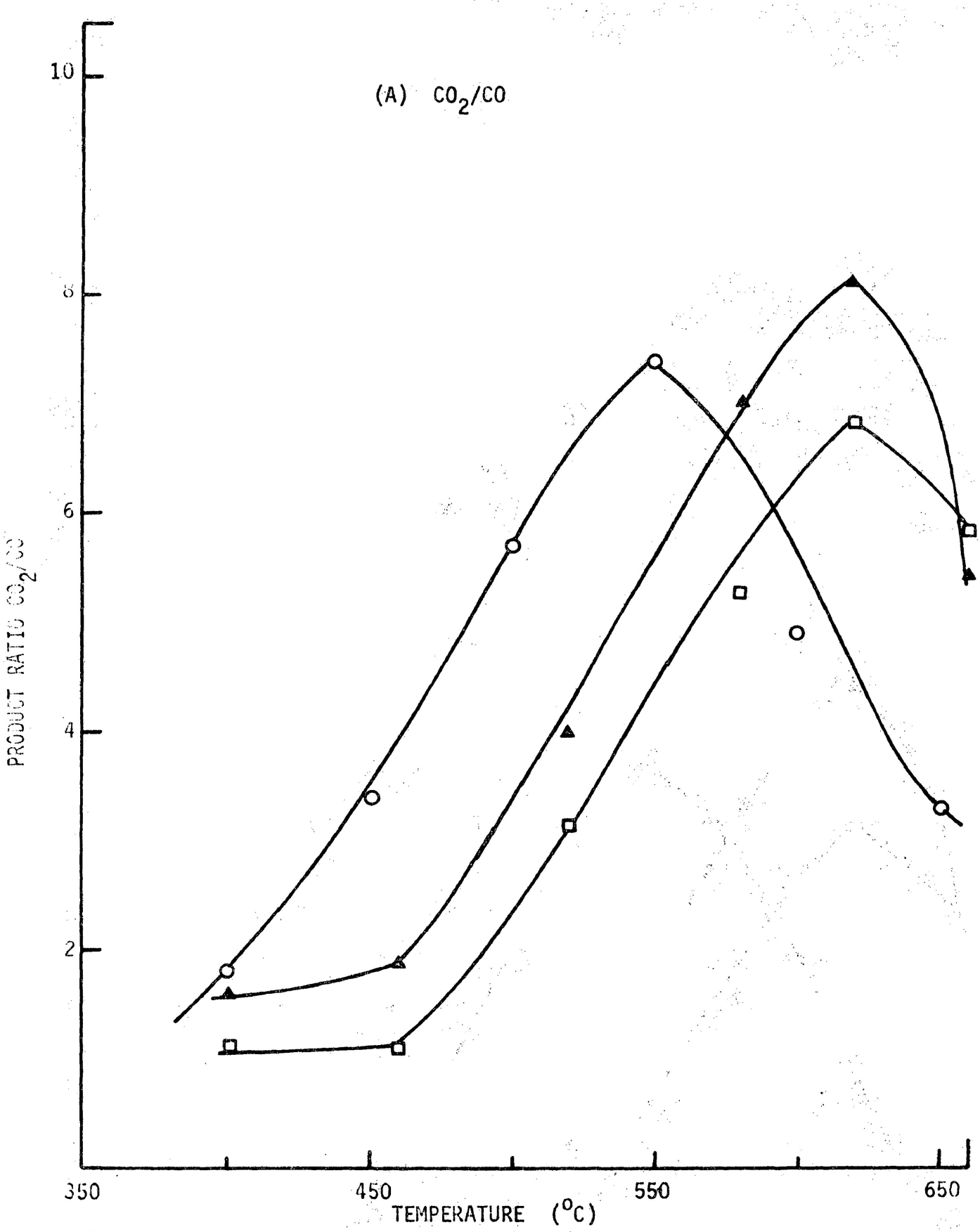

Figure 14(A) The effect of pressure on the product ratios of the various gases formed in helium for cellulose.

○ = 101.3 kPa; ▲ = 607.8 kPa; □ = 1013.0 kPa.

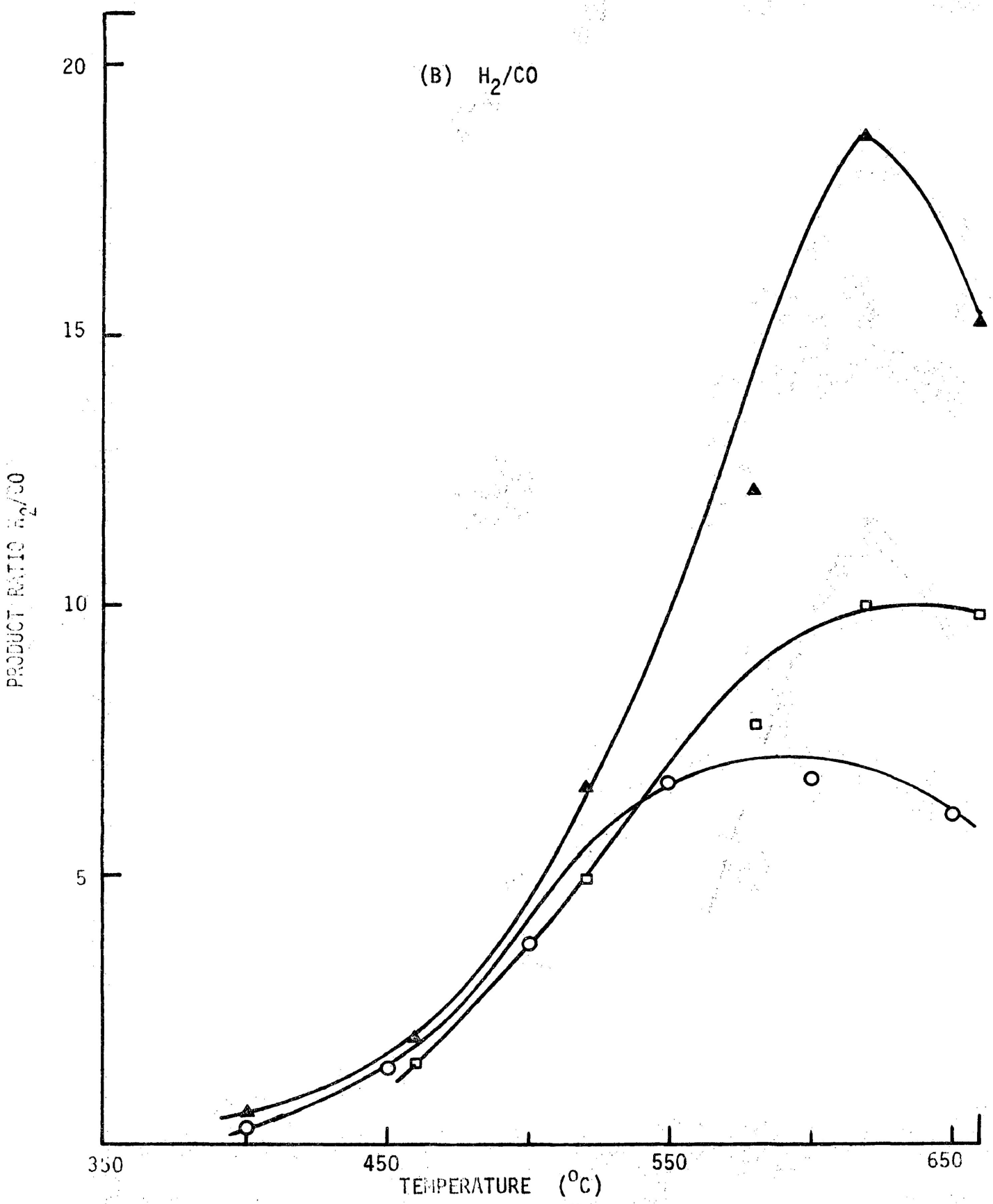

Figure 11(B) The effect of pressure on the product ratios of the various gases formed in helium for cellulose.

○ = 101.3 kPa; ▲ = 607.8 kPa; □ = 1013.0 kPa.

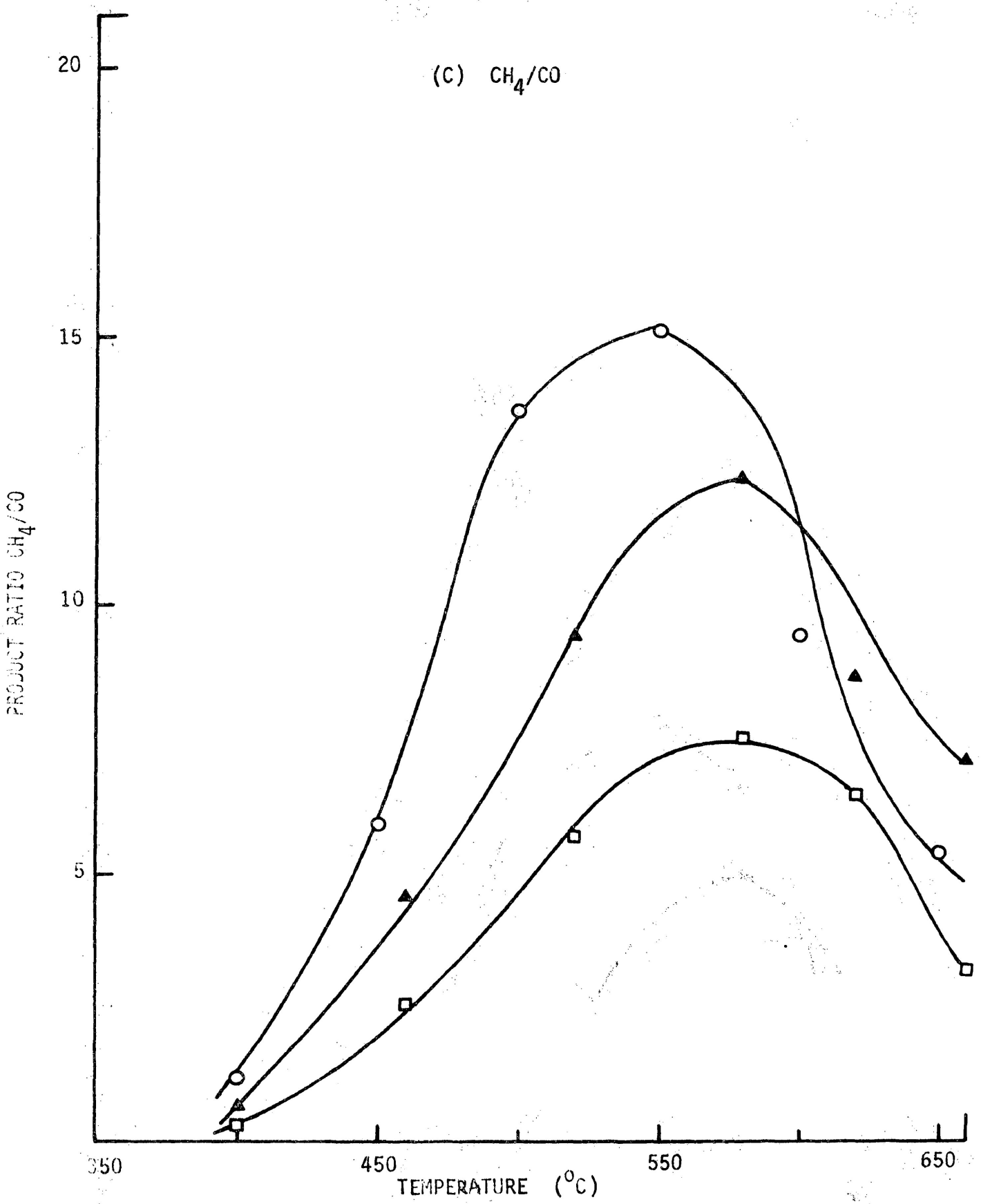

Figure 14(C) The effect of pressure on the product ratios of the various gases formed in helium for cellulose.

○ = 101.3 kPa; ▲ = 607.8 kPa; □ = 1013.0 kPa.

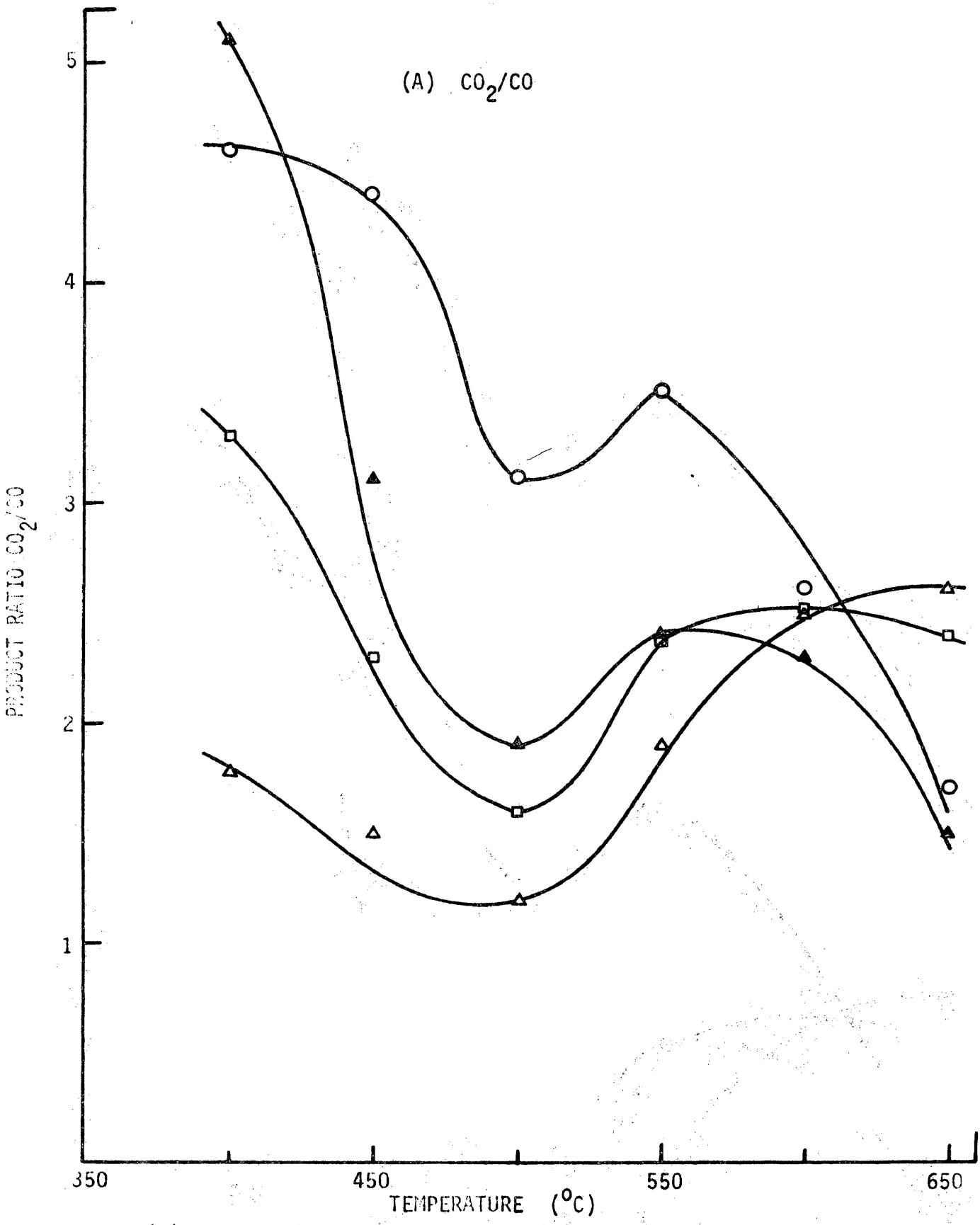

Figure 15(A) The effect of pressure on the product ratios of the various gases formed in helium for cellulose with 5.0% w/w K_2CO_3 (dry mix).
○ = 101.3 kPa; ▲ = 607.8 kPa; □ = 1013.0 kPa; △ = 2532.5 kPa.

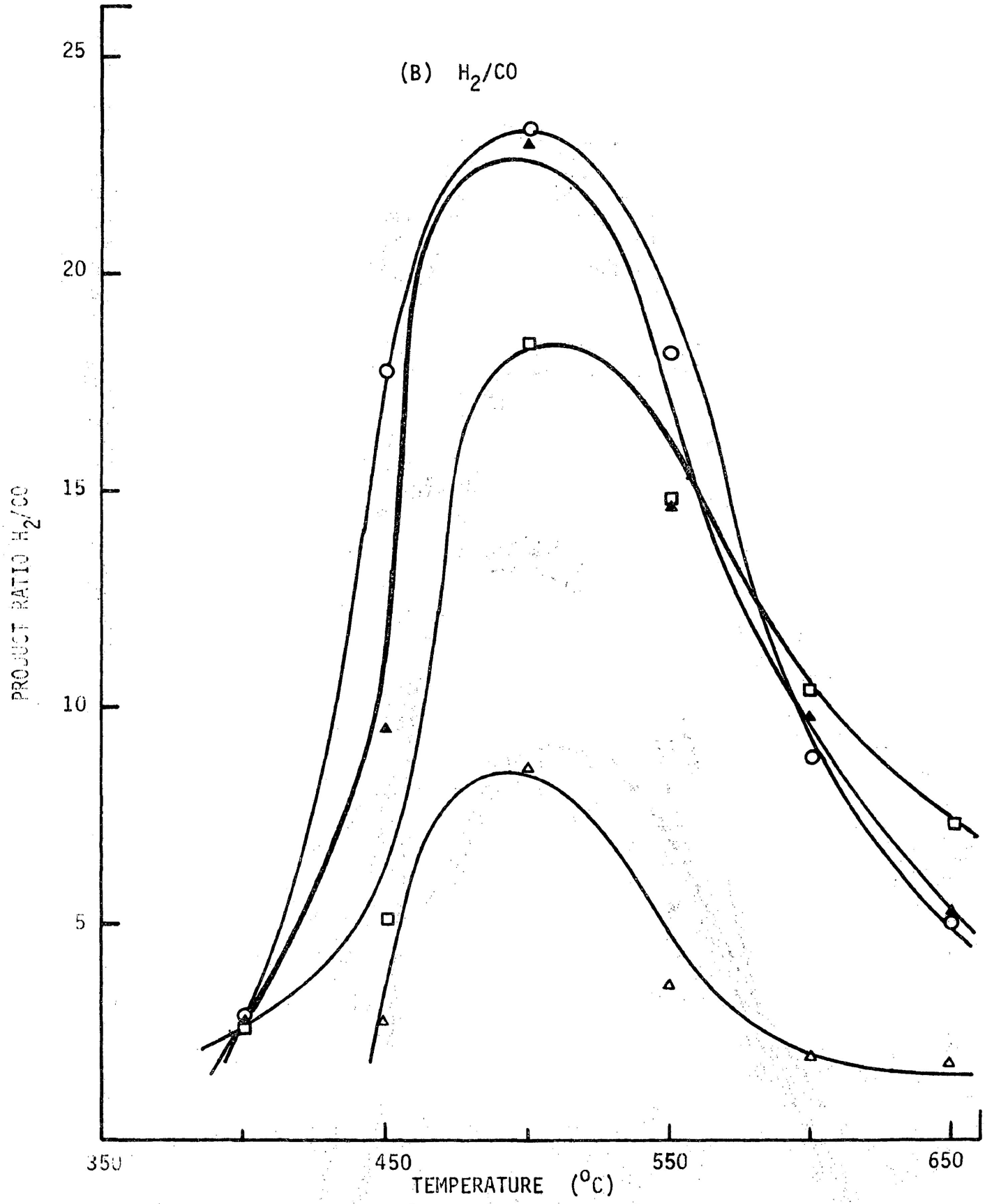

Figure 15(B) The effect of pressure on the product ratios of the various gases formed in helium for cellulose with 5.0% w/w K_2CO_3 (dry mix).
○ = 101.3 kPa; ▲ = 607.8 kPa; □ = 1013.0 kPa; △ = 2532.5 kPa.

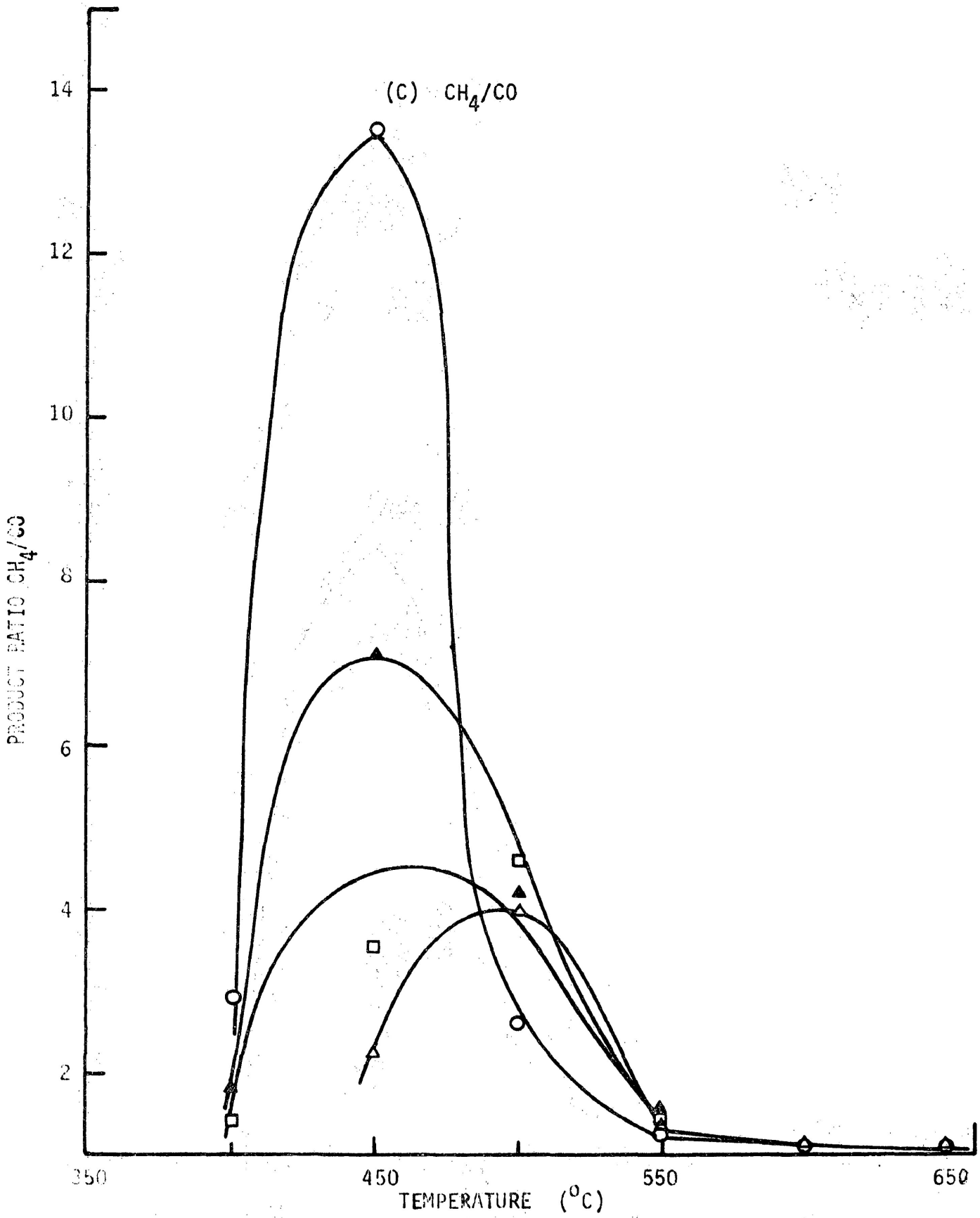

Figure 15(C) The effect of pressure on the product ratios of the various gases formed in helium for cellulose with 5.0% w/w K_2CO_3 (dry mix).

○ = 101.3 kPa; ▲ = 607.8 kPa; □ = 1013.0 kPa; △ = 2532.5 kPa.

Table 4. Peak product ratios obtained from the pyrolysis of cellulose samples.

Atmosphere	Material	Pressure (kPa)	Maximum values of product ratios					
			H_2/CO	Temp. (°C)	CH_4/CO	Temp. (°C)	CO_2/CO	Temp. (°C)
0	cellulose	101.3	12.4	>650	1.6	>650	8.8	>650
		607.8	52.5	>650	4.4	590	26.0	>650
		1013.0	58.2	>650	3.8	580	31.2	>650
Helium/ water vapour (2.1 kPa)	cellulose + 10.2% w/w iron (III) oxide	101.3	30.7	>650	3.5	590	20.7	590
		607.8	52.5	>650	2.6	580	24.4	>650
		1013.0	66.7	>650	1.6	520	28.3	>650
	cellulose + 14.2% w/w zinc (II) chromite	101.3	22.0	600	3.2	590	16.7	585
		607.8	34.4	580	3.1	540	18.5	570
		1013.0	15.1	590	2.4	545	9.3	590
Helium	cellulose	101.3	7.3	570	1.6	540	7.4	550
		607.8	19.7	640	1.3	580	8.6	610
		1013.0	10.8	640	0.8	580	7.0	625
	cellulose + 10.2% w/w iron (III) oxide	101.3	13.5	570	1.6	545	10.9	540
		607.8	20.2	580	1.6	560	10.0	565
		1013.0	11.8	620	1.2	580	9.4	585
	cellulose + 14.2% w/w zinc (II) chromite	101.3	4.5	630	0.6	600	2.1	600
		607.8	17.3	630	0.7	580	5.5	600
		1013.0	13.3	620	0.4	580	4.8	580

Table 5. Peak product ratios obtained from the pyrolysis of cellulose samples.

Atmosphere	Material	Pressure (kPa)	Maximum values of product ratios					
			H_2/CO	Temp. (°C)	CH_4/CO	Temp. (°C)	CO_2/CO	Temp. (°C)
Helium/ water vapour (2.1 kPa)	cellulose + 5.0% w/w K_2CO_3	607.8	8.3	>650	0.9	580	3.6	>650
		1013.0	9.2	>650	0.4	620	3.3	>650
		2532.5	9.6	>650	0.4	620	3.8	>650
	cellulose + 0.7% w/w K_2CO_3 impregnated	1013.0	25.1	>650	1.2	>650	7.7	>650
	cellulose + 0.7% w/w K_2CO_3 impregnated & ball-milled	1013.0	25.1	>650	1.2	>650	7.7	>650
	cellulose + 0.7% w/w K_2CO_3 dry-mix	1013.0	14.8	>650	0.6	>650	5.1	>650
Helium	cellulose + 5.0% w/w K_2CO_3	101.3	23.6	510	13.0	460	3.5	550
		607.8	23.6	510	6.8	460	2.5	570
		1013.0	19.5	510	3.9	490	2.5	600
		2532.5	9.2	510	3.1	510	3.2	630
	cellulose + 0.7% w/w K_2CO_3 impregnated	101.3	13.2	570	5.2	500	2.2	600
		1013.0	8.7	610	2.2	520	2.6	>650
	cellulose + 0.7% w/w K_2CO_3 impregnated & ball-milled	101.3	18.7	570	6.6	510	3.6	550
		1013.0	11.3	570	2.7	520	1.4	550
	cellulose + 0.7% w/w K_2CO_3 dry-mix	101.3	12.0	580	5.0	510	2.8	500
		1013.0	5.2	620	1.6	520	2.0	>650

3.1.3.3 The effect of water vapour

The effect of water vapour (2.1 kPa) on the product ratios of cellulose and cellulose containing 5% potassium carbonate at 101.3 kPa from 400 to 650°C is shown in Figure 16. The maximum values of the product ratios and T_{max} data are summarized in Tables 4 and 5.

The product ratios increased for cellulose, cellulose plus iron (III) oxide and cellulose plus zinc (II) chromite. CO_2/CO and H_2/CO ratios increased while CH_4/CO decreased with samples containing 0.7% potassium carbonate. All of the product ratios were observed to decrease for cellulose with 5% potassium carbonate.

T_{max} tended to increase in this atmosphere for all samples.

3.1.4 Residue analysis

The carbon and hydrogen contents of the residues of isothermally-pyrolyzed cellulose and cellulose with iron (III) oxide and zinc (II) chromite at 340°C in nitrogen showed little variation. The carbon content was 72 to 73%, hydrogen 3.5 to 4.0%, on a residue mass about 12% of the initial cellulose sample.

3.1.5 Scanning electron microscopy

Micrographs of various cellulose samples taken before and after pyrolysis are shown in Figures 17, 18 and 19. Plain cellulose powder consisted of long, cylindrical fibres. After mixing, iron (III) oxide was distributed more evenly on the fibre surface than the other additives, Figure 17. No significant differences were observed between the original cellulose and cellulose samples impregnated with potassium carbonate.

Pyrolysis of cellulose samples at 300°C induced fibre twists as previously demonstrated [46] but no significant differences were noted in

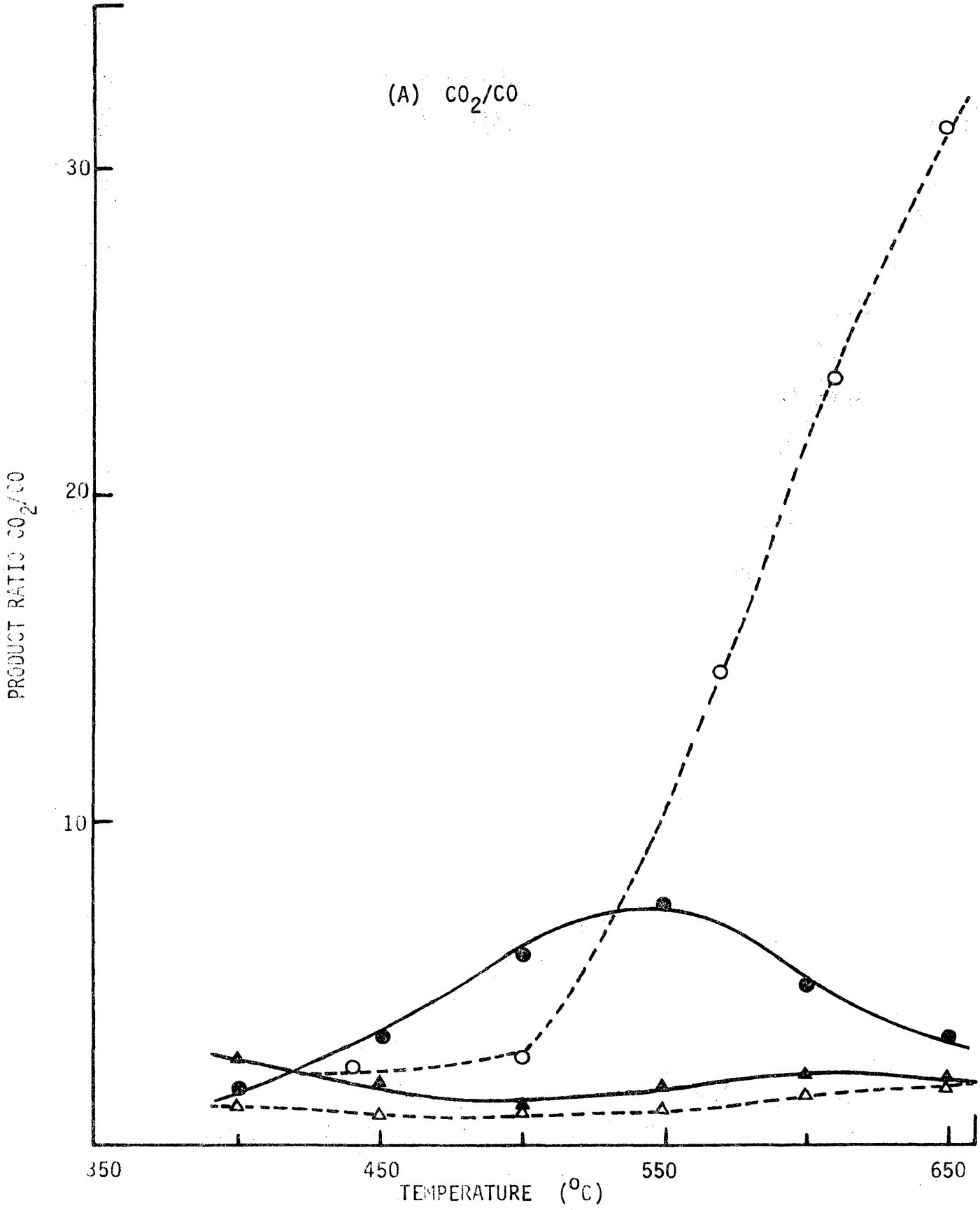

Figure 16(A) The effect of water vapour on the product ratios of the various gases formed in helium at 1013.0 kPa for cellulose and cellulose with 5.0% w/w K_2CO_3 (dry mix).

● = cellulose in helium; ▲ = ● + 5.0% w/w K_2CO_3; ○ = ● + water vapour (2.1 kPa); △ = ▲ + ○ .

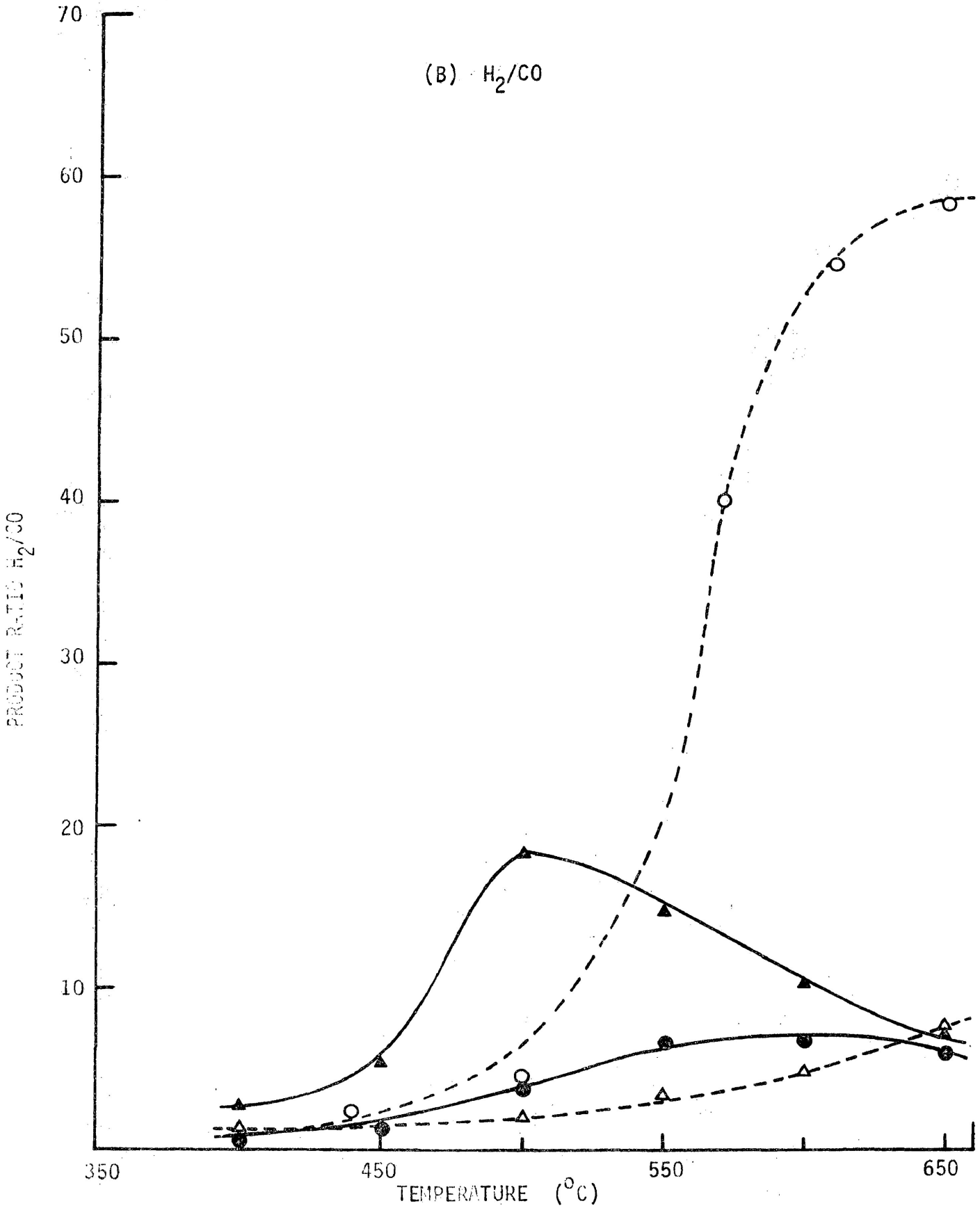

Figure 16(B) The effect of water vapour on the product ratios of the various gases formed in helium at 1013.0 kPa for cellulose and cellulose with 5.0% w/w K_2CO_3 (dry mix).

● = cellulose in helium; ▲ = ● + 5.0% w/w K_2CO_3; ○ = ● + water vapour (2.1 kPa); △ = ▲ + ○ .

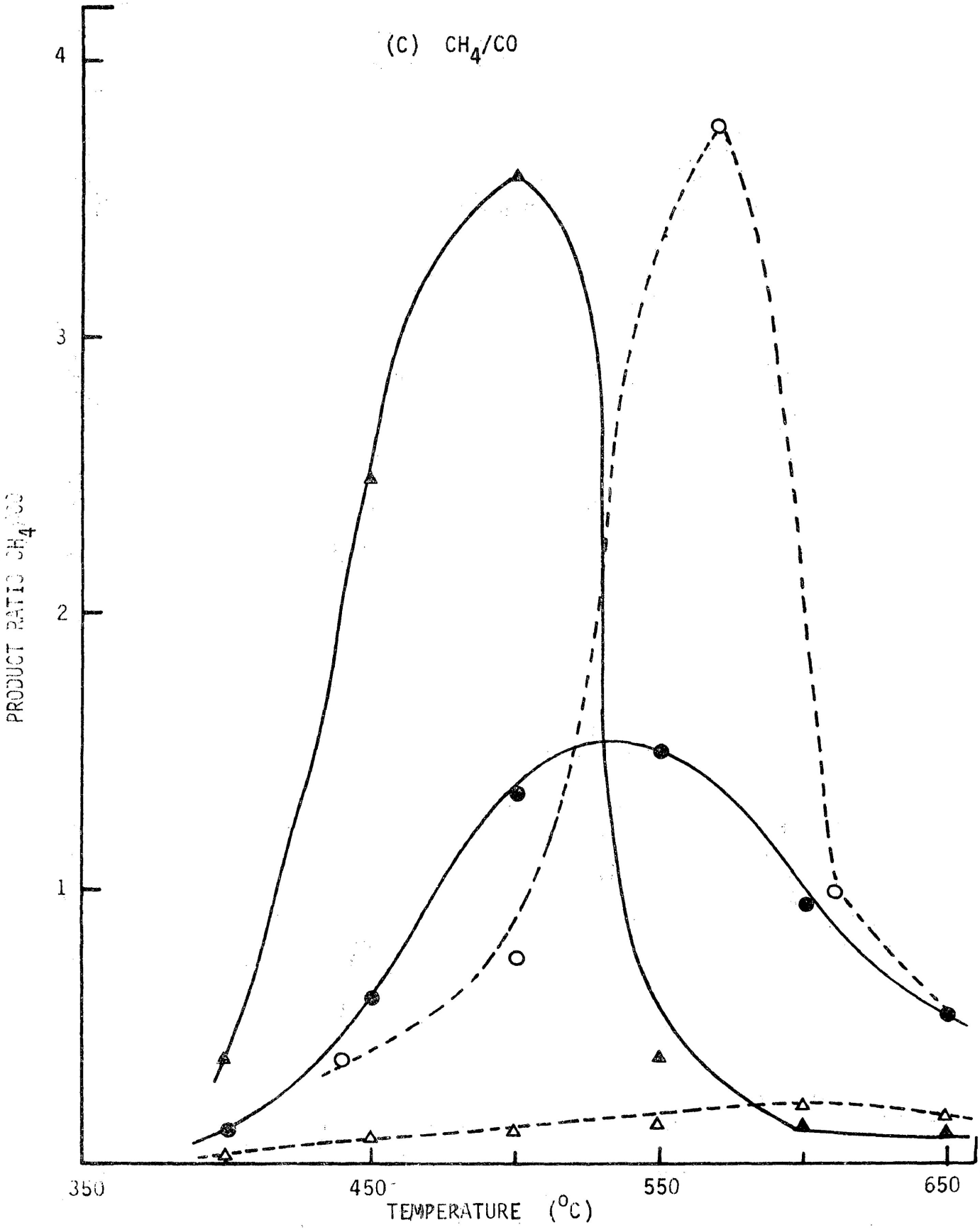

Figure 16(C) The effect of water vapour on the product ratios of the various gases formed in helium at 1013.0 kPa for cellulose and cellulose with 5.0% w/w K_2CO_3 (dry mix).

● = cellulose in helium; ▲ = ● + 5.0% w/w K_2CO_3; O = ● + water vapour (2.1 kPa); △ = ▲ + O .

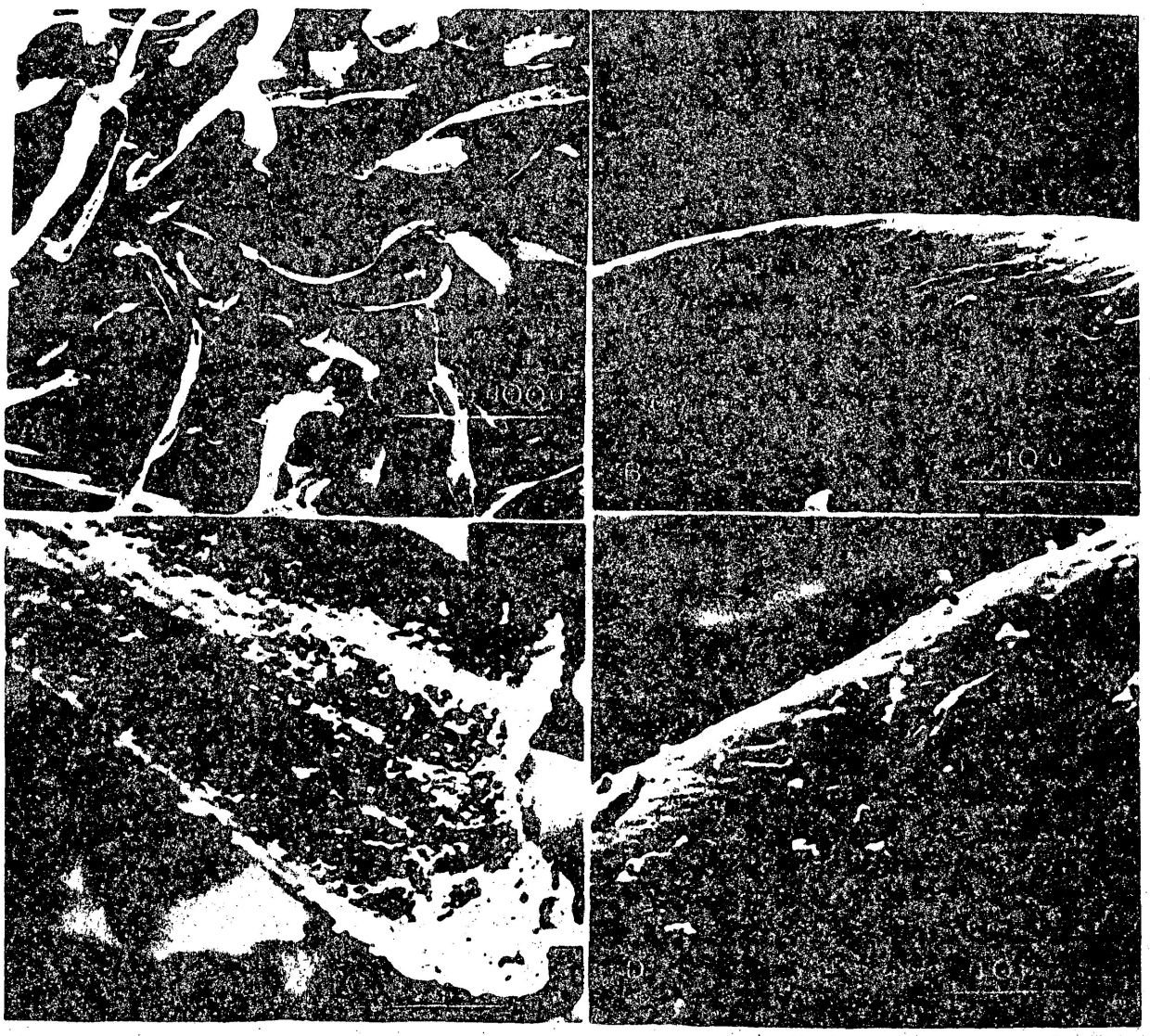

Figure 17 Scanning electron micrographs of cellulose samples. (A) & (B) = cellulose, (C) = cellulose + 10.2% w/w iron(III)oxide, (D) = cellulose + 14.2% w/w zinc (II)chromite.

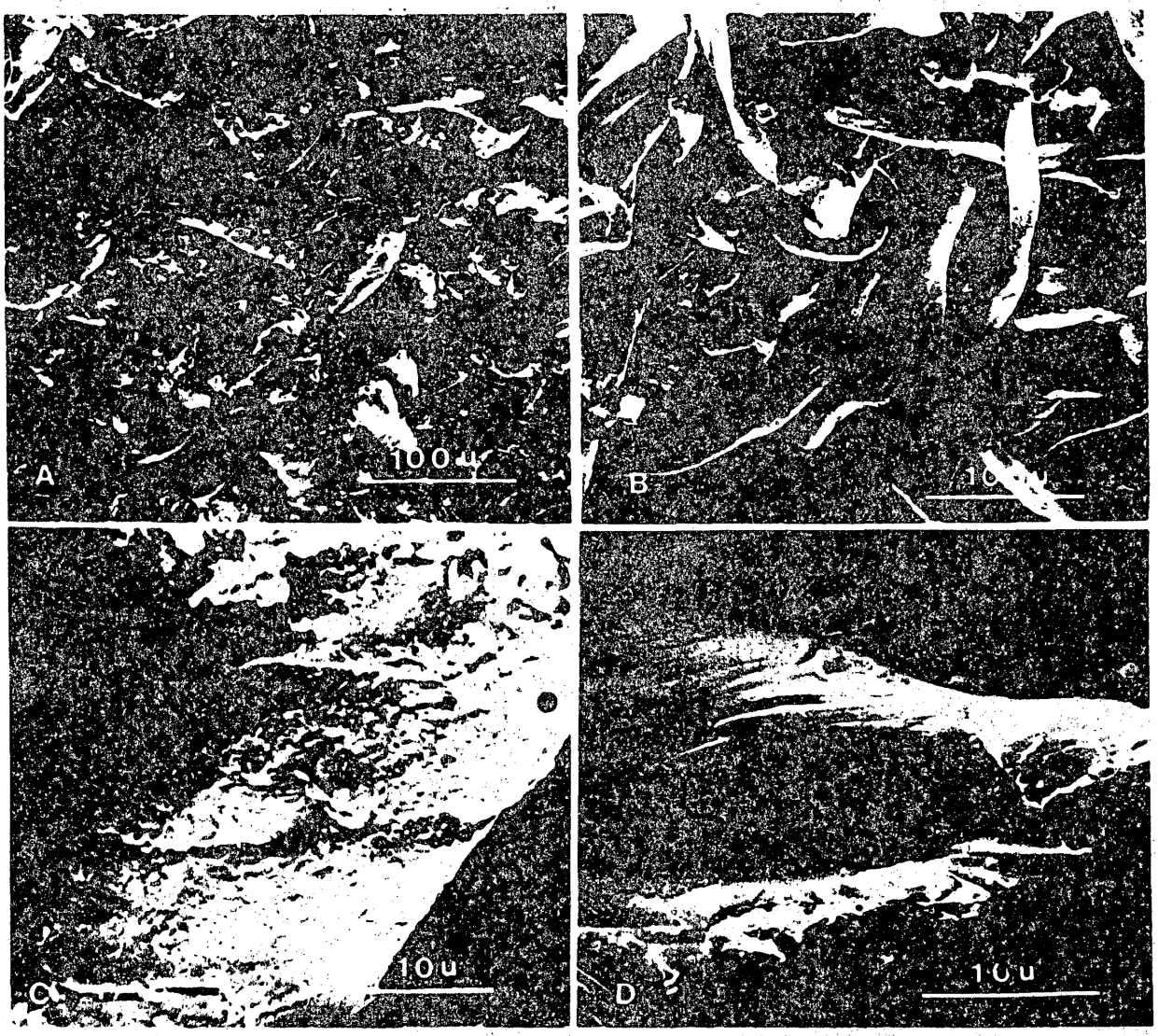

Figure 18 Scanning electron micrographs of cellulose samples containing K_2CO_3.
(A) & (C) = cellulose + 5.0% w/w K_2CO_3 (dry mix);
(B) & (D) = cellulose + 0.7% w/w K_2CO_3 (impregnated).

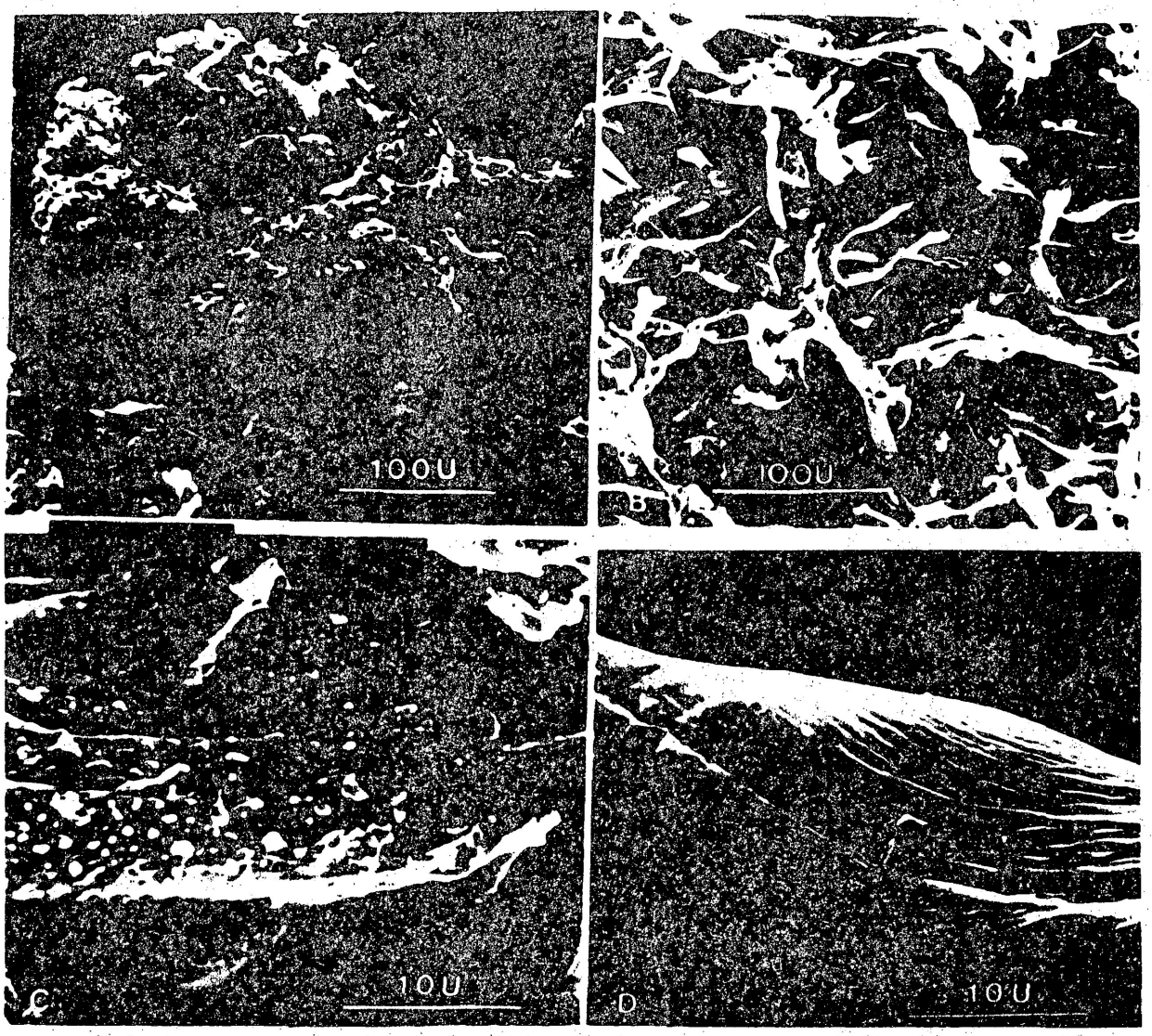

Figure 19 Scanning electron micrographs of cellulose samples after pyrolysis at 101.3 kPa in helium. (A) & (C) = pyrolysis of cellulose + 5.0% w/w K_2CO_3 (dry mix) at 650°C; (B) & (D) = pyrolysis of cellulose at 650°C.

this phenomenon with regard to additive-containing samples.

Figure 19 shows scanning details obtained after pyrolysis at 650°C of cellulose and cellulose with 5% potassium carbonate. The long, cylindrical fibres have split and shortened. Cracks may be noted on the fibre axis through twist compression which results from the comparatively high temperature of heat treatment and additive particles can still be observed on the surfaces of the fibres.

The surfaces of the fibres on the 5% potassium carbonate sample were partially covered by a thin film of an apparently 'glassy' material.

3.1.6 X-ray diffraction

Attempts were made to identify the nature of this 'glassy' surface film by x-ray diffraction which showed that some crystalline deposit was present. Several intense x-ray diffraction lines at 3.68, 2.95, 2.85 and 2.38 Å were recorded as well as a typical amorphous pattern for heat-treated cellulose. These data suggest that potassium hydroxide, potassium bicarbonate and some potassium oxides may have formed but further study would be necessary to identify these compounds precisely.

3.1.7 Surface areas

The surface area of the native cellulose powder has previously been measured [46] to be 0.8 m^2/g. It was further noted that the surface area increased to 29.8 m^2/g after pyrolysis in nitrogen at 332°C.

3.2 White birch sawdust

3.2.1 Dynamic thermogravimetry (TG)

The curves obtained for white birch sawdust and white birch sawdust mixed separately with 14.2% zinc (II) chromite and 10.2% iron (III)

oxide are shown in Figure 20. An initial small weight loss of 2.5% below 200°C was followed by a rapid rate of weight loss. The rapid region reached a value at 400°C of 67% for white birch sawdust, 70% for white birch sawdust with iron (III) oxide and 71% for white birch sawdust with zinc (II) chromite. Total weight loss at 900°C varied from 83% for white birch sawdust with iron (III) oxide and zinc (II) chromite to 80% for plain white birch sawdust.

3.2.2 Isothermal pyrolysis

Isothermal weight-change experiments were carried out on white birch sawdust samples in flowing nitrogen from 225 to 338°C.

Kinetic parameters were derived as described in the previous section. Plots of $\ell n[-\ell n(1 - \alpha)]$ versus ℓnt gave straight lines with an average slope of 0.5 for values of α from 0.2 to 0.8. Therefore, the decomposition could be described by the Avrami-Erofeev equation [71,72] for nucleation and growth with, in this case, $n = 0.5$:

$$[-\ell n(1 - \alpha)]^{1/n} = k_1 t \qquad (24)$$

Values of k_1, the rate constant, obtained from the linear plots of $[-\ell n(1 - \alpha)]^2$ versus time were used to construct the Arrhenius plot, Figure 21, from which the usual kinetic parameters were derived as summarized in Table 6.

3.2.3 Gaseous products analysis

White birch sawdust samples were pyrolyzed in helium and in helium and in helium saturated with water vapour (2.1 kPa) in the high-pressure 'static' apparatus. The total pressure was kept at 607.8 kPa.

The product ratios CH_4/CO, H_2/CO and CO_2/CO for the white birch sawdust samples pyrolyzed from 400 to 650°C are shown in Figure 22. No significant variations of the product ratios were observed with the addition

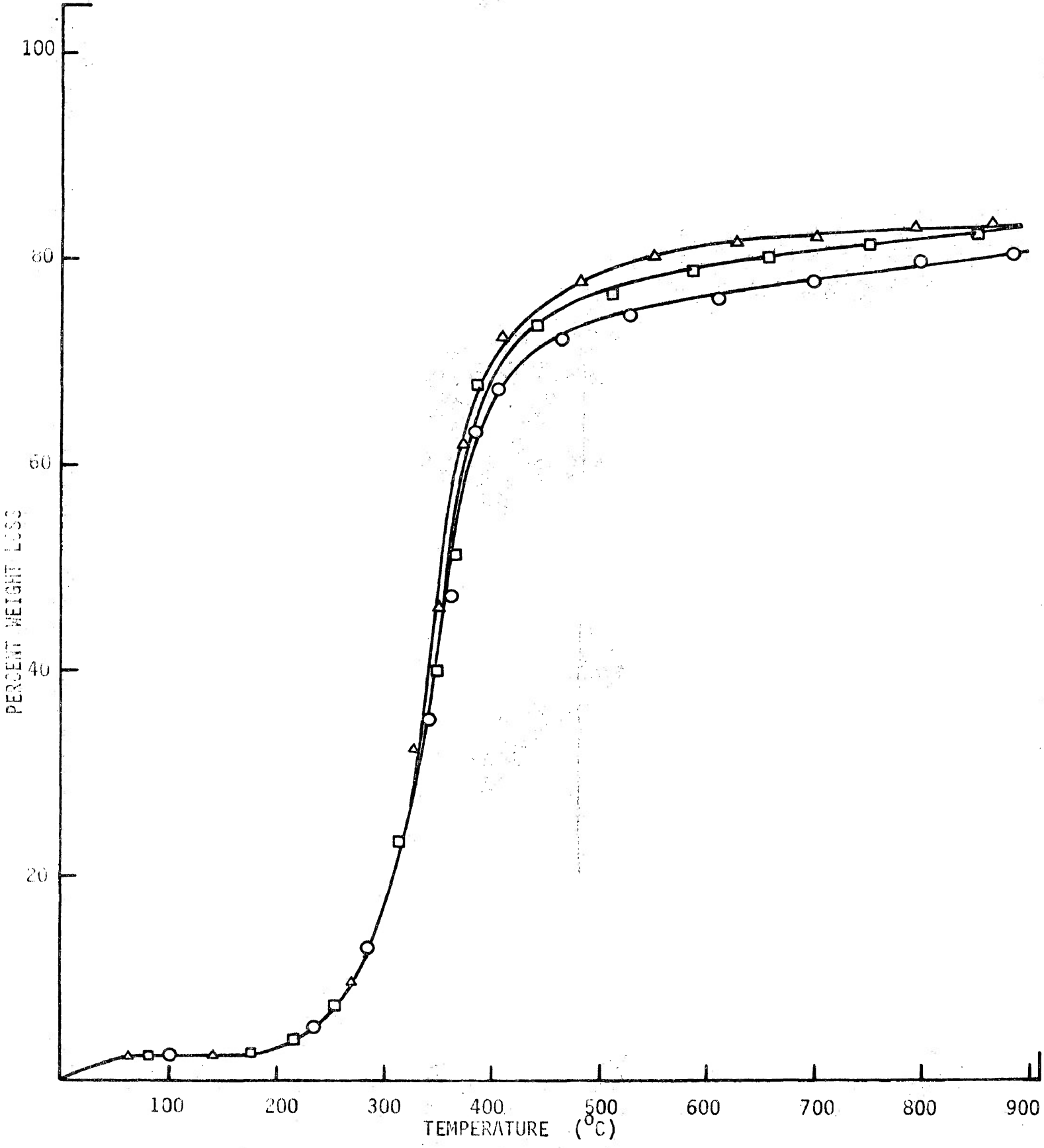

Figure 20 Thermograms for white birch sawdust samples in nitrogen.

○ = white birch sawdust; ● = ○ + 10.2% w/w iron(III)oxide;
△ = ○ + 14.2% w/w zinc(II)chromite.

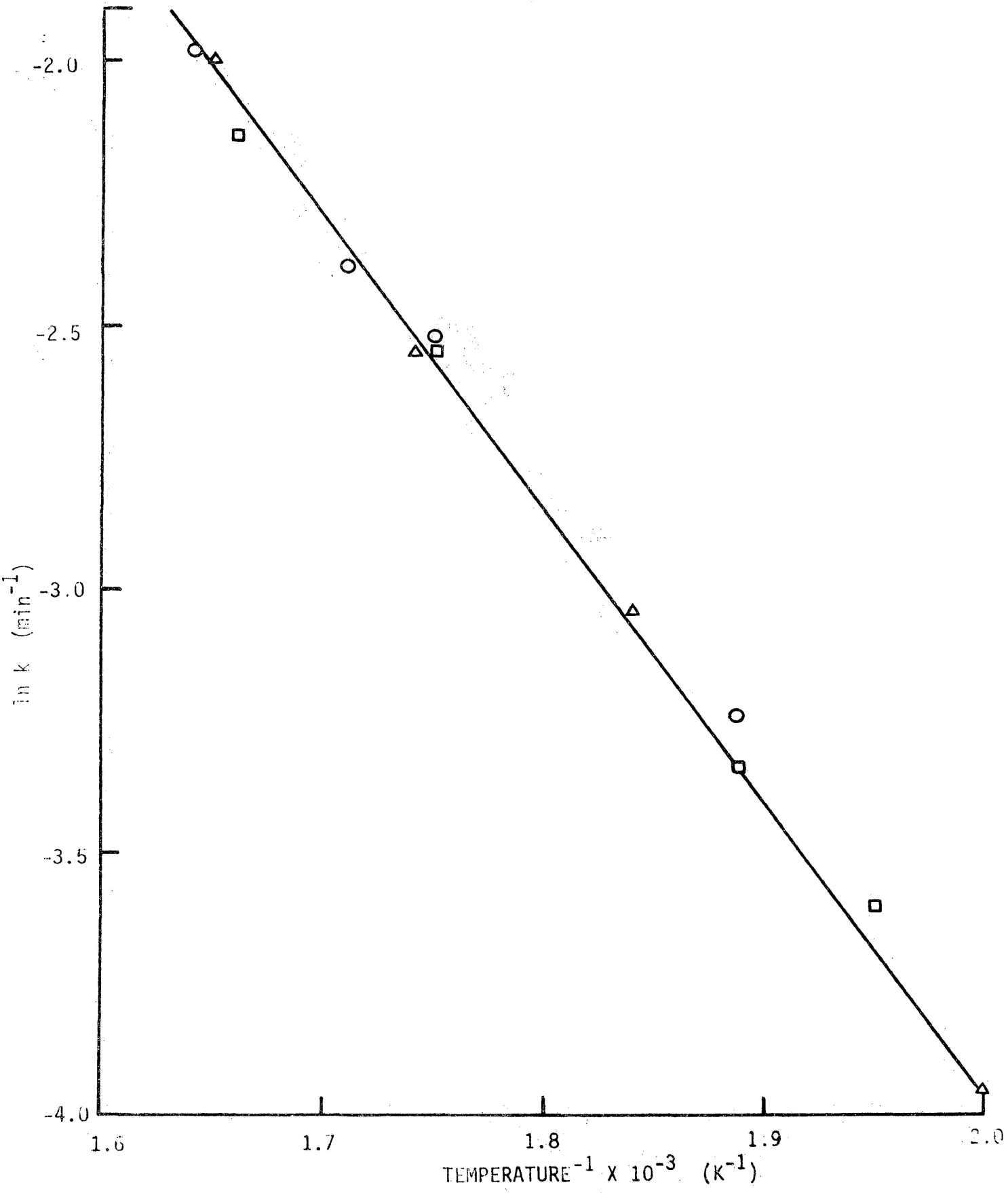

Figure 21 Arrhenius plot for white birch sawdust samples in nitrogen from 225 to 338°C.

○ = white birch sawdust; □ = ○ + 10.2% w/w iron(III)oxide;
△ = ○ + 14.2% w/w zinc(II)chromite.

Table 6. Kinetic parameters for pyrolysis of white birch sawdust samples in nitrogen.

Material	Temperature (°C)	Rate constant k x 10^{-2} (min^{-1})	Frequency factor A (min^{-1})	Apparent activation energy E_a ($kJ\ mol^{-1}$)
white birch sawdust	225 259 299 311 338	1.72 3.93 8.05 9.16 13.84	1030	45.3 ± 2.1
white birch sawdust + 14.2% zinc (II) chromite	226 270 303 332	1.91 4.78 7.81 13.5	1030	45.3 ± 2.1
white birch sawdust + 10.2% iron (III) oxide	239 259 300 329	2.73 3.54 7.81 11.77	1030	45.3 ± 2.1

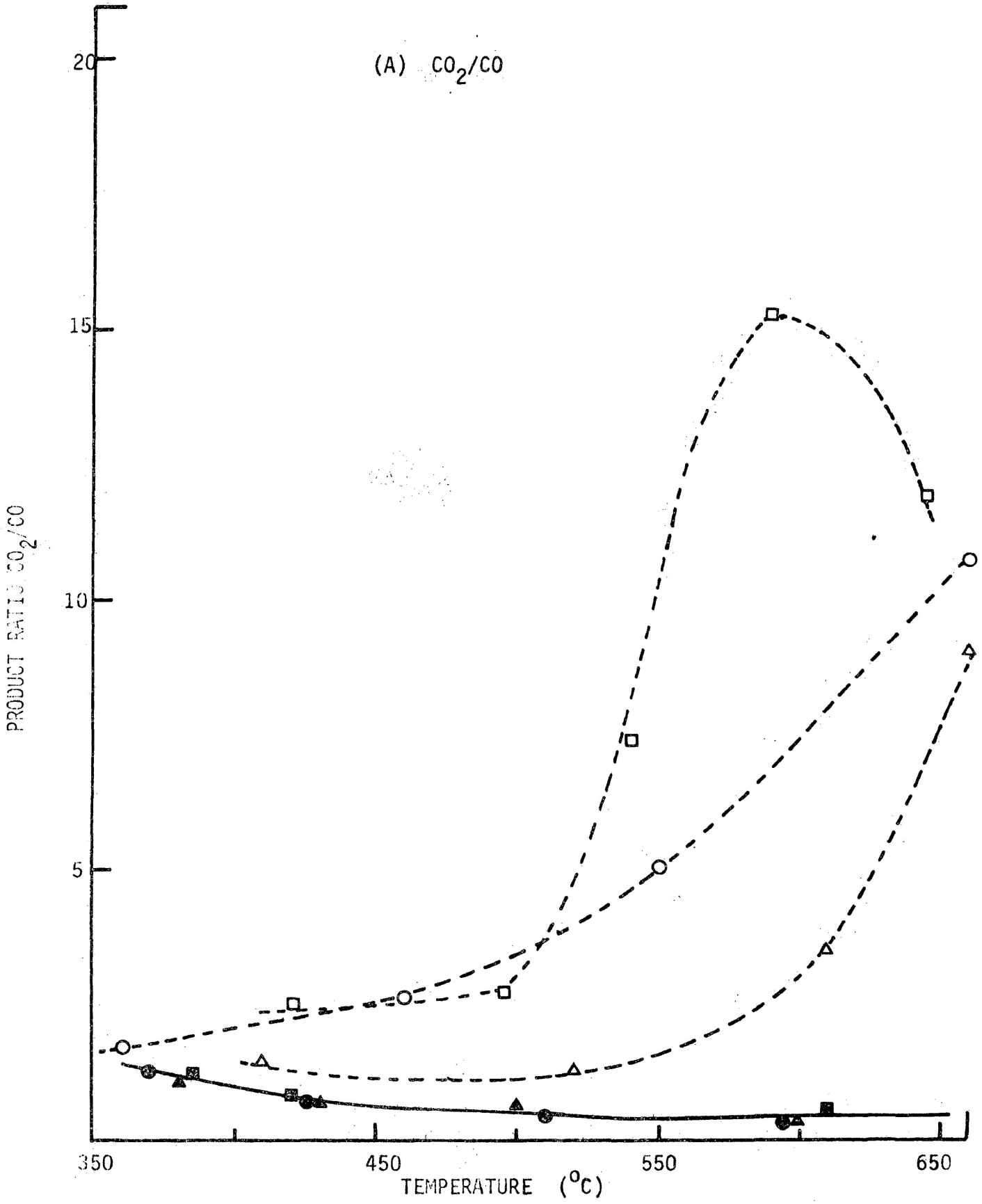

Figure 22(A) The effect of solid additives and water vapour (2.1 kPa) on the product ratios of the gases formed in helium at 1013.0 kPa for white birch sawdust samples.

● = white birch sawdust in helium; ■ = ● + 10.2% w/w iron(III) oxide; ▲ = ● + 14.2% w/w zinc(II)chromite; ○ = ● + water vapour; □ = ○ + ■ ; △ = ○ + ▲ .

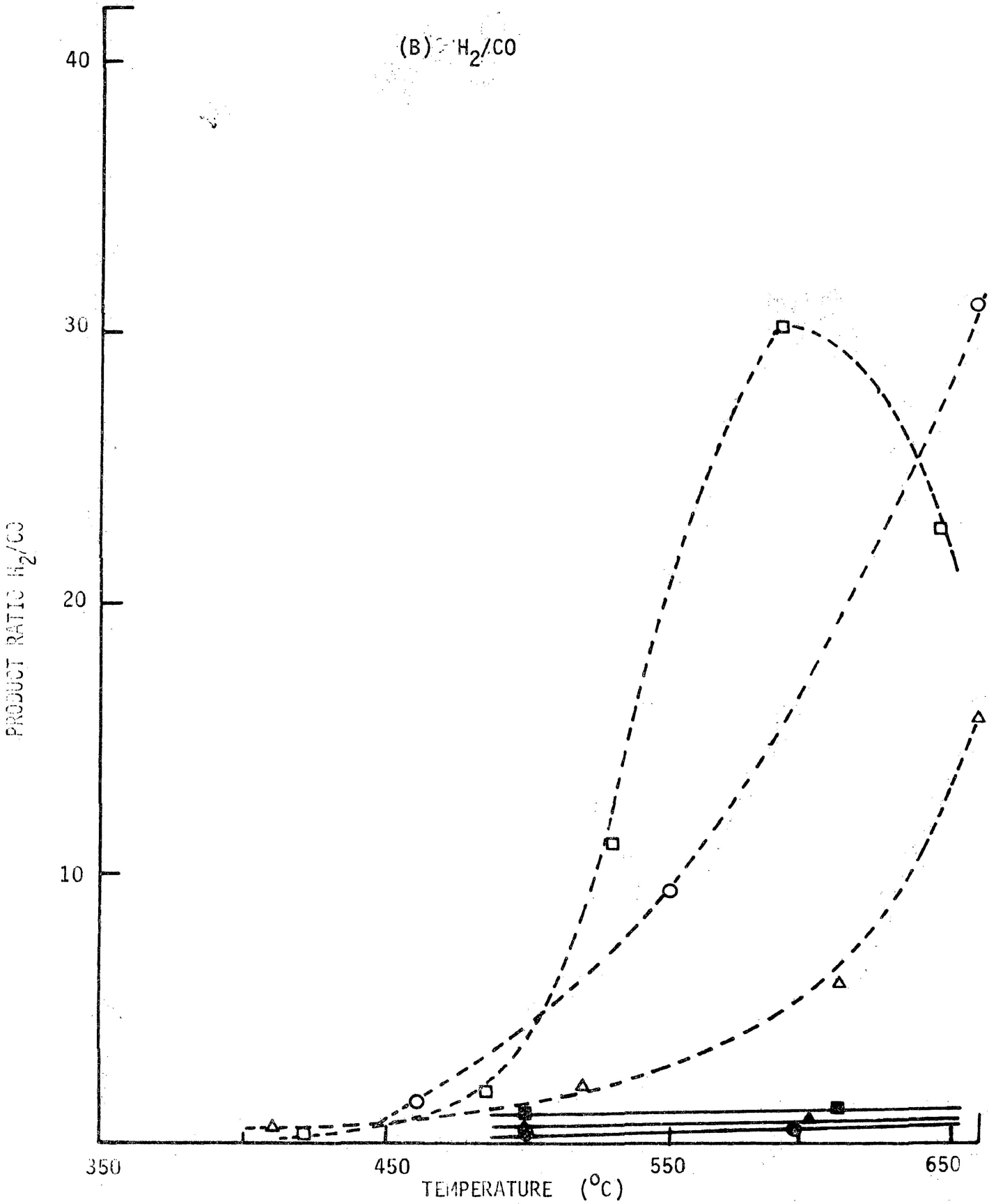

Figure 22(B) The effect of solid additives and water vapour (2.1 kPa) on the product ratios of the gases formed in helium at 1013.0 kPa for white birch sawdust samples.

● = white birch sawdust in helium; ■ = ● + 10.2% w/w iron(III) oxide; ▲ = ● + 14.2% w/w zinc(II)chromite; ○ = ● + water vapour; □ = ○ + ■ ; △ = ○ + ▲ .

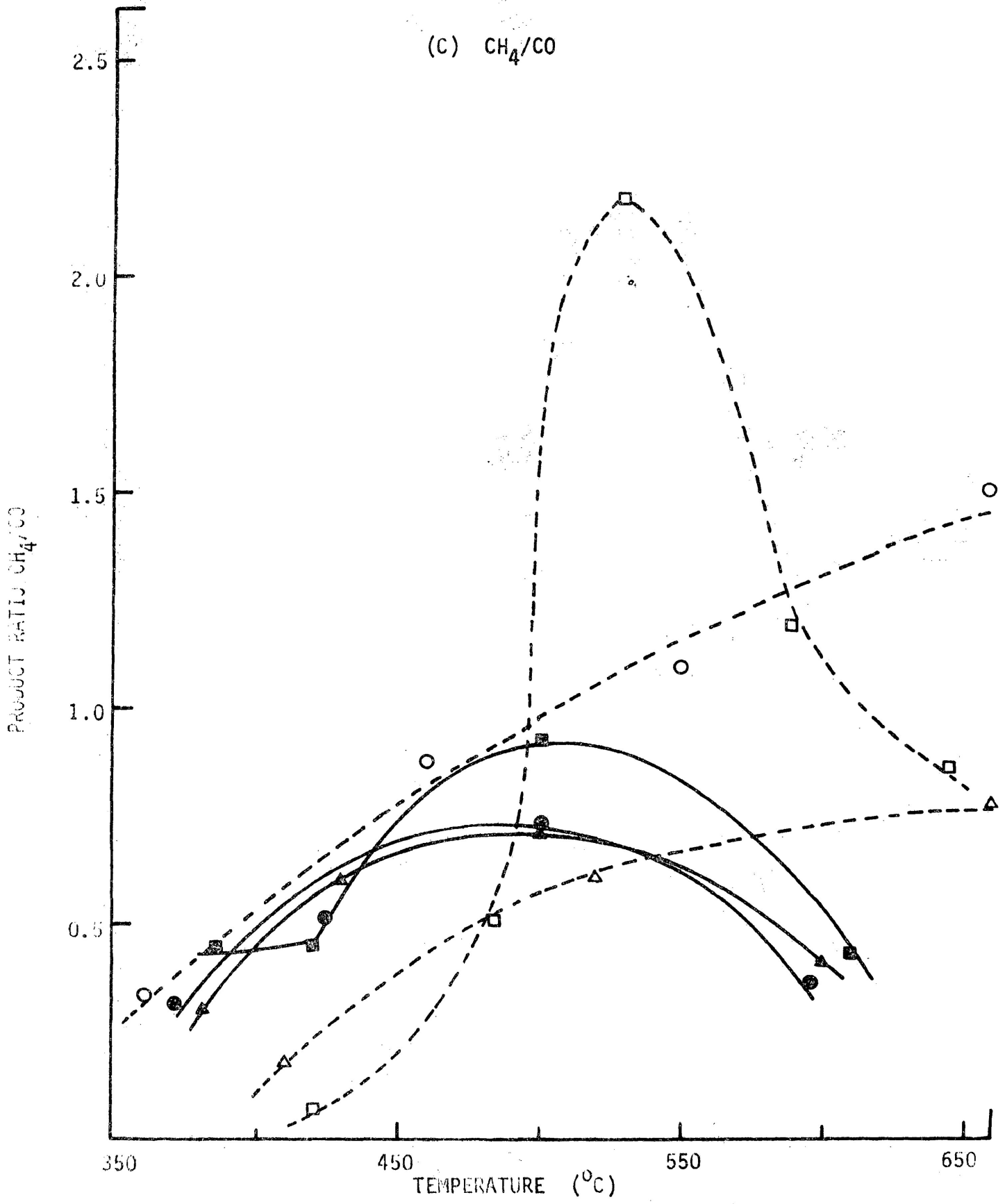

Figure 22(C) The effect of solid additives and water vapour (2.1 kPa) on the product ratios of the gases formed in helium at 1013.0 kPa for white birch sawdust samples.

● = white birch sawdust in helium; ■ = ● + 10.2% w/w iron(III) oxide; ▲ = ● + 14.2% w/w zinc(II)chromite; ○ = ● + water vapour; □ = ○ + ■ ; △ = ○ + ▲ .

of iron (III) oxide and zinc (II) chromite in the helium atmosphere.

Generally, in the saturated water vapour atmosphere, the product ratios from the pyrolysis of plain sawdust increased significantly when compared with the values obtained in dry helium. In the presence of water vapour, iron (III) oxide caused an increase in the product ratios while zinc (II) chromite exerted the opposite effect.

3.2.4 Scanning electron microscopy

Plain white birch sawdust consists of a mixture of long cylindrical fibres and some small particles of no simple or well-defined geometric shape, Figure 23.

Pyrolysis at 300°C induced a few cracks along the fibre axes as illustrated in Figure 24. On pyrolysis at 650°C, the fibre surfaces appear to have roughened considerably, probably as a result of further enlargement of the cracks initiated in the samples at lower temperatures.

3.3 Jack pine bark and char

3.3.1 Dynamic thermogravimetry (TG)

The TG curves obtained for the thermal decomposition of jack pine bark and bark containing additives in nitrogen are shown in Figure 25.

The curve for plain jack pine bark showed an initial weight loss of 6% below 200°C. The major weight loss commenced at 220°C and the decomposition was rapid up to about 400°C after which a decceleration period followed. The total weight loss at 900°C was 80%.

Curves obtained from bark containing additives were similar in shape to that of the plain jack pine bark. The major difference was that, generally, a higher percentage of weight loss was observed after the rapid weight loss region. Thus the final weight losses at 900°C were higher than

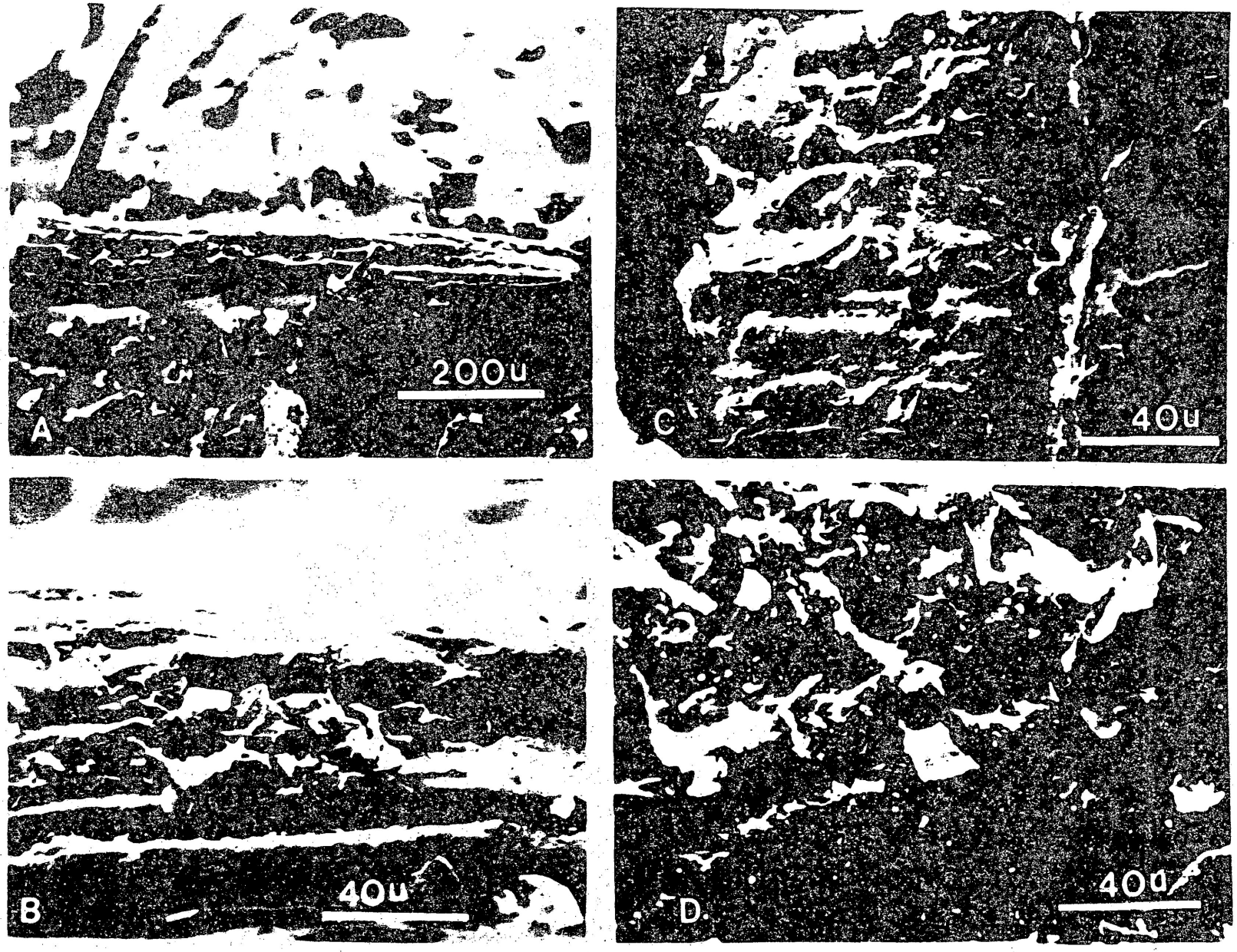

Figure 23 Scanning electron micrographs of white birch sawdust samples.
(A) & (B) = white birch sawdust, (C) = (B) + 10.2% w/w iron(III)oxide;
(D) = (B) + 14.2% w/w zinc(II)chromite.

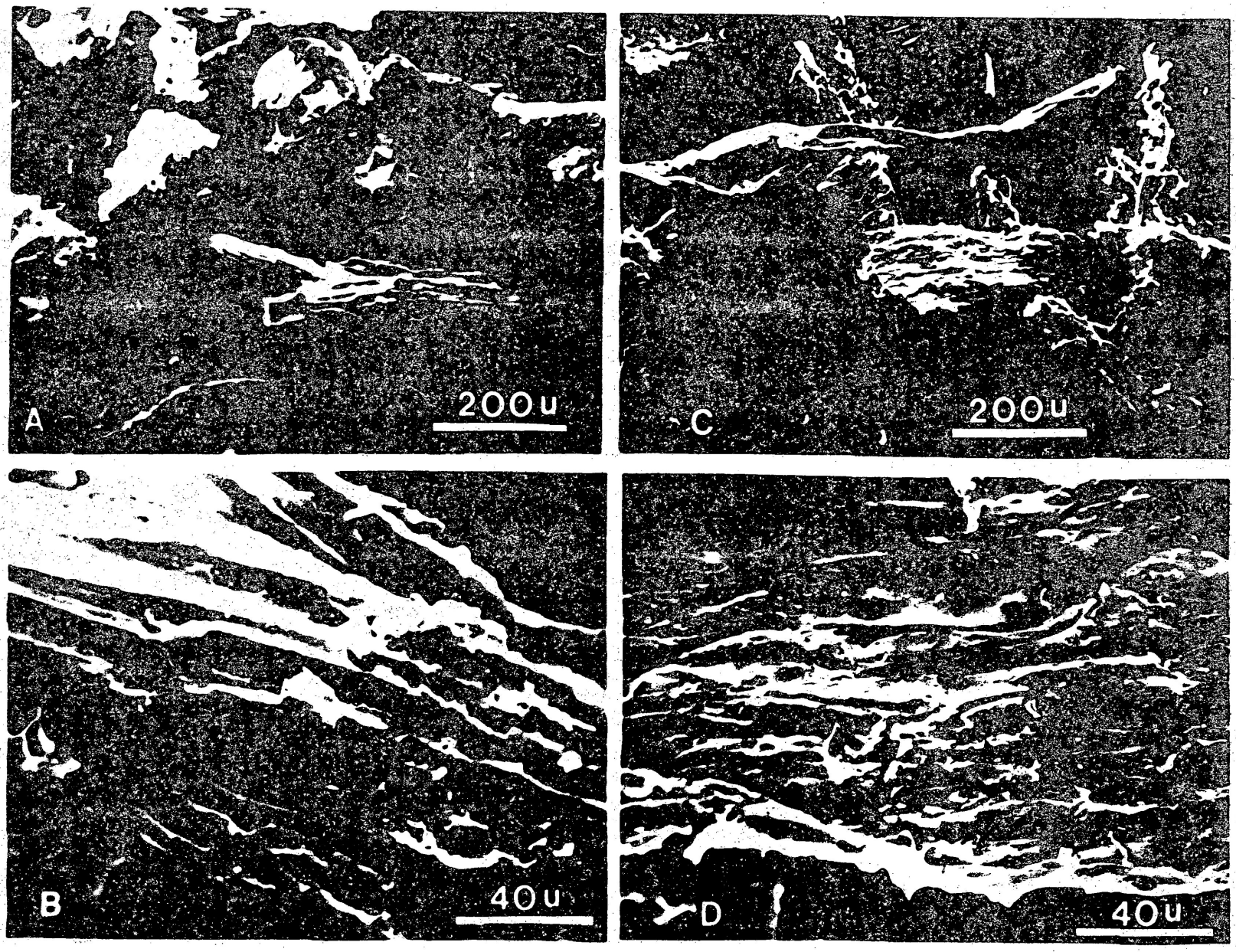

Figure 24 Scanning electron micrographs of white birch sawdust samples after pyrolysis at 607.8 kPa in helium.

(A) & (B) = white birch sawdust + 10.2% w/w iron(III)oxide pyrolysed at 330°C,
(C) & (D) = white birch sawdust pyrolysed at 650°C.

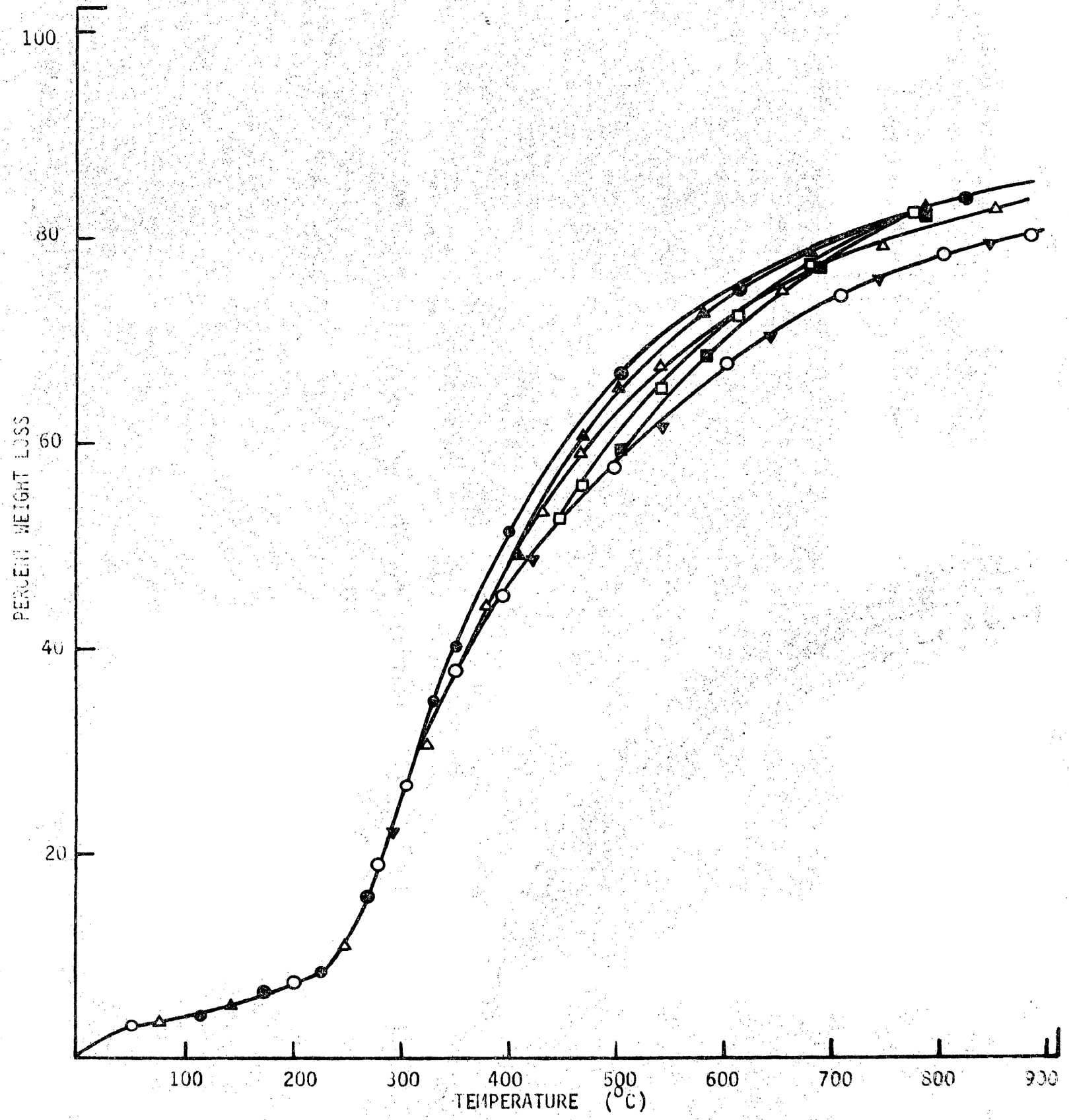

Figure 25 Thermograms for jack pine bark and jack pine bark plus additives in nitrogen.

O = jack pine bark; ● = O + 5.0% w/w K_2CO_3; △ = O + 2.5% w/w K_2CO_3; ▲ = O + 1.3% w/w K_2CO_3; ▼ = O + 0.8% w/w Li_2SO_4; □ = O + 1.3% w/w K_2SO_4; ■ = O + 2.9% w/w $BaCO_3$.

that recorded for plain jack pine bark. In the presence of 5% potassium carbonate the total weight loss increased to 85% at 900°C.

3.3.2 Isothermal pyrolysis

Isothermal weight-changes were determined on jack pine bark containing 5% potassium carbonate in flowing nitrogen from 248 to 310°C.

Kinetic parameters were derived in the manner established earlier [47]. Straight lines with an average slope of 0.5 for α values from 0.2 to 0.8 were obtained from the plot of $\ell n[-\ell n(1 - \alpha)]$ against ℓn t. Thus the decomposition followed the same pattern as that of white birch sawdust and could be described by the Avrami-Erofeev equation [71,72].

$$[-\ell n(1 - \alpha)]^{1/n} = k_1 t \qquad (24)$$

Values of k_1 were obtained from a graph of $[-\ell n(1 - \alpha)]^2$ versus time. The Arrhenius plot is shown in Figure 26 and kinetic parameters derived are summarized in Table 7.

3.3.3 Gaseous products analysis

The preparation of the jack pine char samples has been described in Section 2.1.7. The catalysts used were potassium sulphate, potassium carbonate, lithium sulphate and barium carbonate. Each of these materials was added to the bark by the dry-mix method. Then barks containing 1.3%, 2.5% and 5.0% w/w potassium carbonate were prepared. A constant cation molar concentration equivalent to that of the 1.3% w/w K_2CO_3 sample was maintained for the samples with potassium sulphate, lithium sulphate and barium carbonate in order to provide a more accurate basis for comparison of possible catalytic activity.

The jack pine char samples were pyrolyzed in helium and helium saturated with water vapour in the flow apparatus at 101.3 kPa. Moreover,

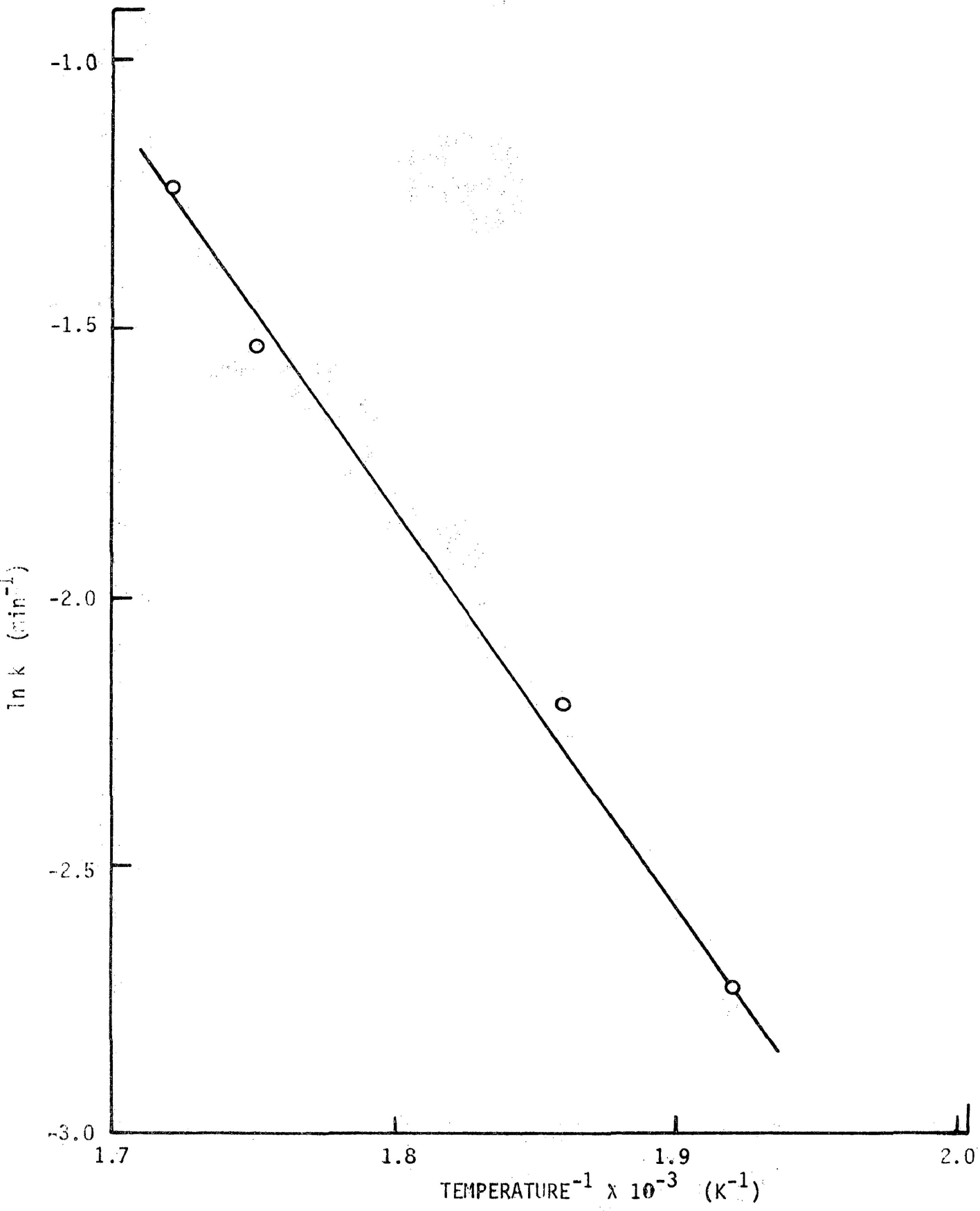

Figure 26 Arrhenius plot for jack pine bark with 5.0% w/w K_2CO_3 in nitrogen from 248 to 310°C.

Table 7. Kinetic parameters for pyrolysis of jack pine bark samples in nitrogen.

Material	Temperature (^{o}C)	Rate constant k x $10^{-2}(min^{-1})$	Frequency factor A (min^{-1})	Apparent activation energy Ea ($kJmol^{-1}$)
jack pine bark + 5.0% w/w K_2CO_3	248 264 300 310	6.5 11.1 21.4 29.0	3.8×10^4	57.4 ± 9.1
* plain jack pine bark	250 257 274 336	5.3 7.6 8.3 24.9	1.1×10^3	43.0 ± 4.7

* data taken from [26] for comparison

char samples were pyrolyzed in the presence of added carbon monoxide.

3.3.3.1. The effect of additives

The effects of the additives on the concentration of the various products obtained in helium, 101.3 kPa, for the various jack pine char samples are shown in Figures 27 and 28.

Carbon monoxide production, Figure 27, increased with temperature reaching a maximum value at 550 to 575°C, then it dropped off at higher temperatures. Two maximum values of carbon dioxide yields were found. The first maximum occurred at 450 to 475°C and then fell rapidly until 575°C, whence the yield increased and maximized at 600°C after which it again decreased rapidly. Methane production was first detected at 375°C and increased rapidly to a maximum at 550 to 575°C. Hydrogen production increased with increasing temperature. The gaseous product yields for all samples containing additives followed the same patterns as those determined for jack pine char.

In general, the additives decreased the yields of gaseous products with the exception of the potassium carbonate addition. Chars modified with this component gave decreased yields of carbon monoxide and methane as the concentration of potassium carbonate was increased. However, hydrogen production increased with increasing concentration of potassium carbonate while carbon dioxide yields did not appear to be affected by the material.

3.3.3.2 The effect of water vapour

The effects of water vapour (34.5 kPa) on the concentrations of the various products obtained in helium, 101.3 kPa, for the various jack pine chars are shown in Figures 27 and 28.

For jack pine bark and jack pine bark with 1.3% potassium sulphate,

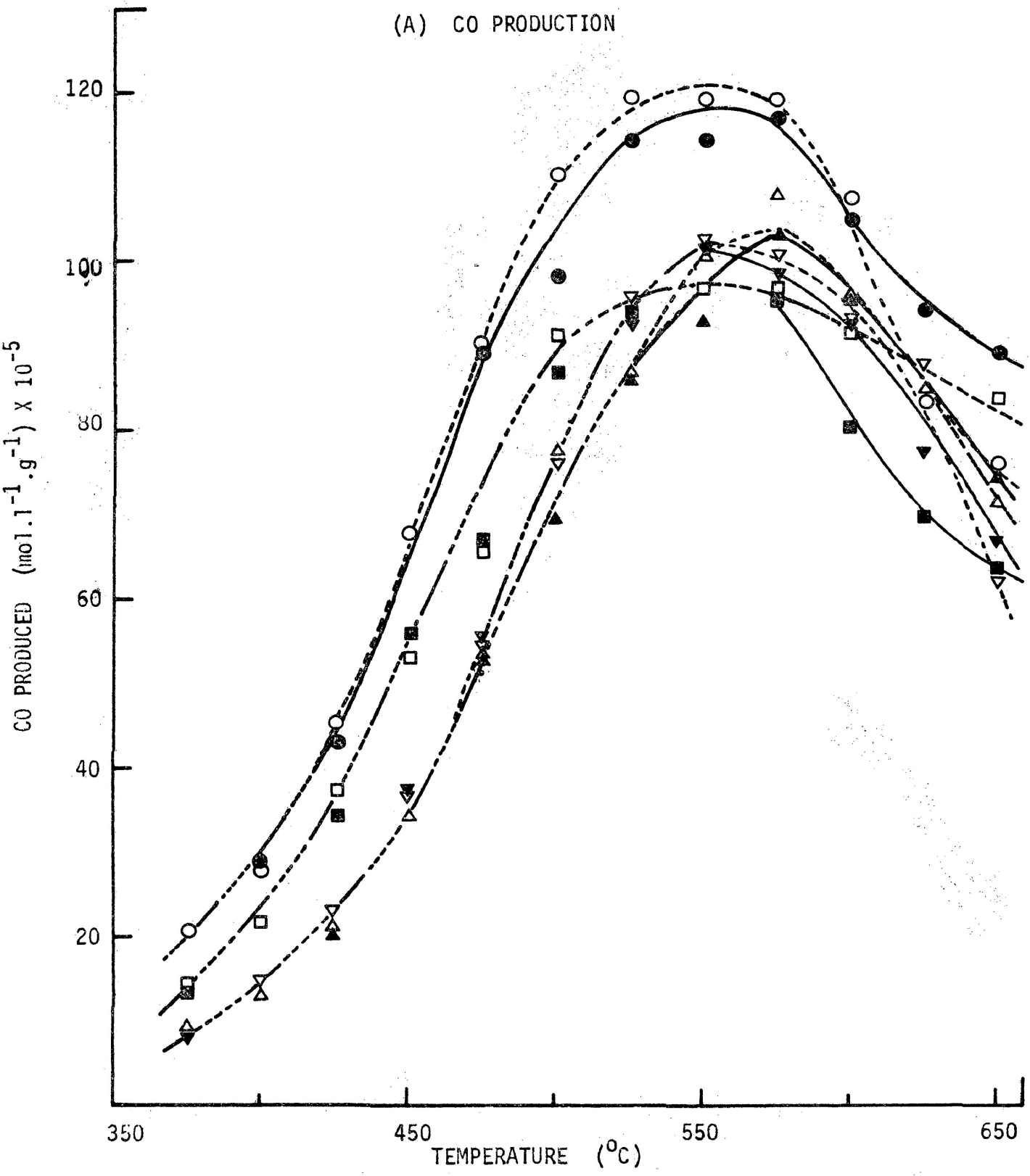

Figure 27(A) The effect of solid additives and water vapour (34.5 kPa) on the concentration of the gases formed in helium at 101.3 kPa from jack pine char samples.
● = jack pine char in helium; ▲ = ● + 1.3% w/w K_2SO_4; ■ = ● + 0.8% w/w Li_2SO_4; ▼ = ● + 2.9% w/w $BaCO_3$; ○ = ● + water vapour; △ = ○ + ▲ ; □ = ○ + ■ ; ▽ = ○ + ▼ .

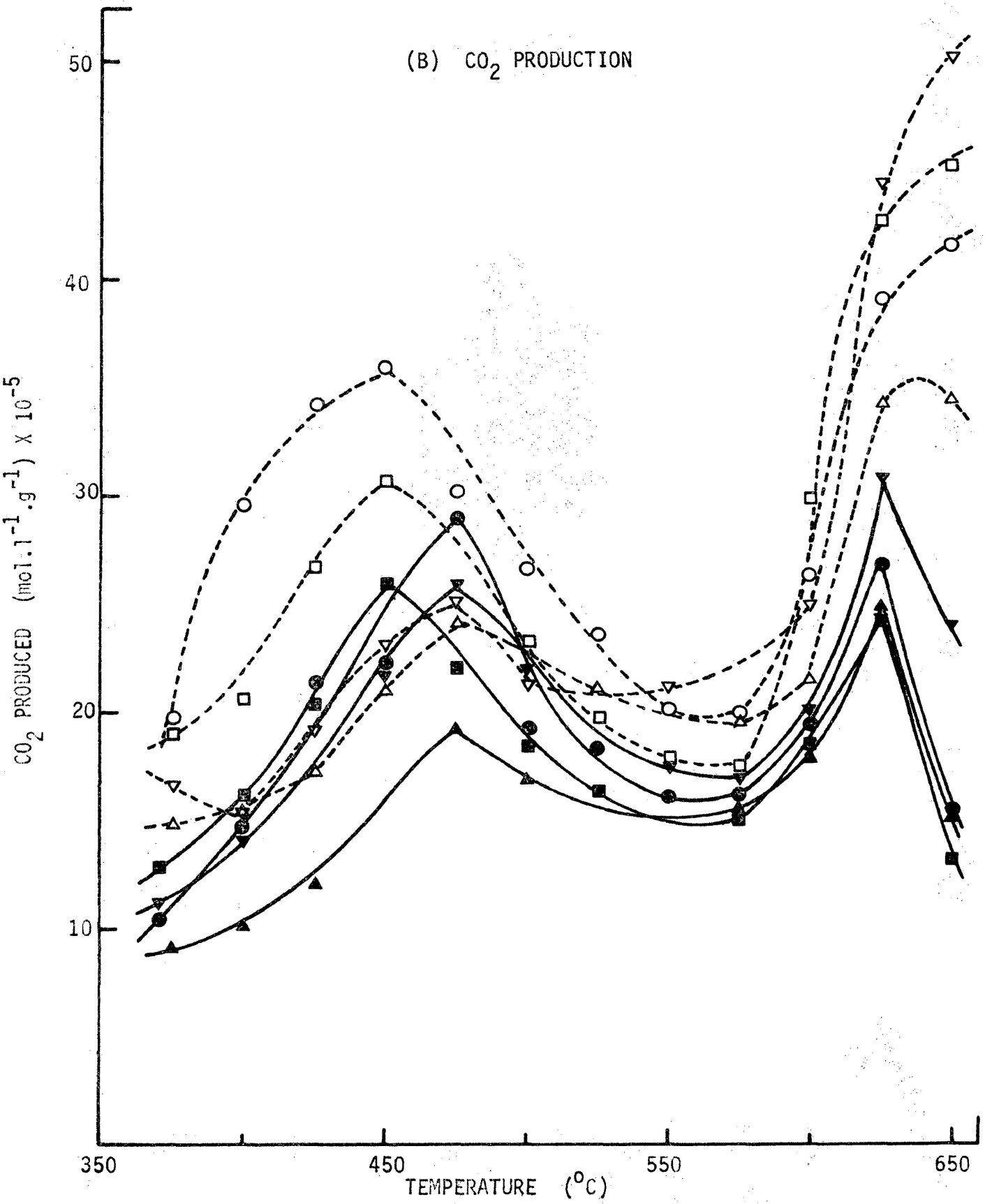

Figure 27(B) The effect of solid additives and water vapour (34.5 kPa) on the concentration of the gases formed in helium at 101.3 kPa from jack pine char samples.
● = jack pine char in helium; ▲ = ● + 1.3% w/w K_2SO_4; ■ = ● + 0.8% w/w Li_2SO_4; ▼ = ● + 2.9% w/w $BaCO_3$; ○ = ● + water vapour; △ = ○ + ▲ ; □ = ○ + ■ ; ▽ = ○ + ▼ .

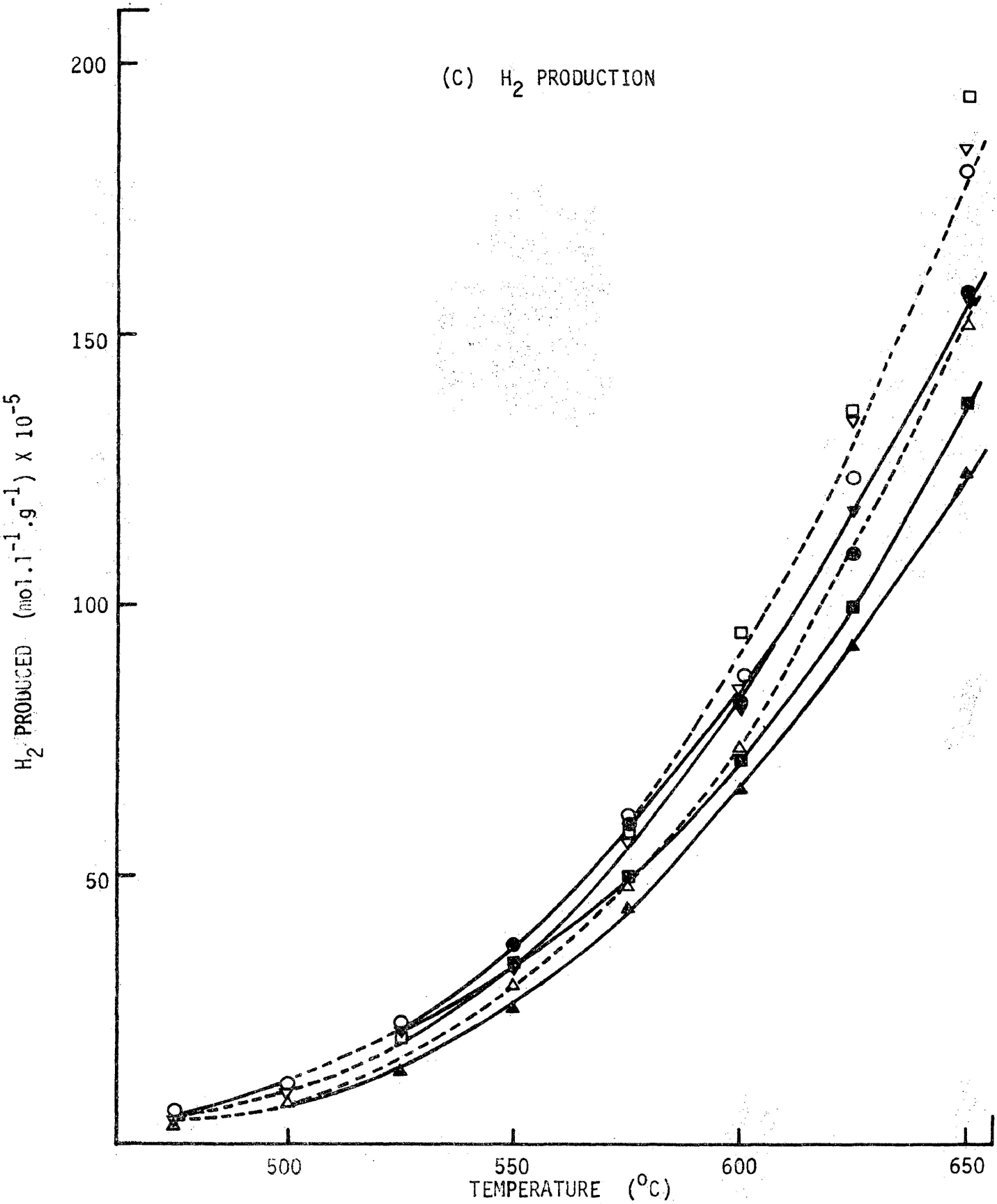

Figure 27(C) The effect of solid additives and water vapour (34.5 kPa) on the concentration of the gases formed in helium at 101.3 kPa from jack pine char samples.
● = jack pine char in helium; ▲ = ● + 1.3% w/w K_2SO_4; ■ = ● + 0.8% w/w Li_2SO_4; ▼ = ● + 2.9% w/w $BaCO_3$; ○ = ● + water vapour; △ = ○ + ▲ ; □ = ○ + ■ ; ▽ = ○ + ▼ .

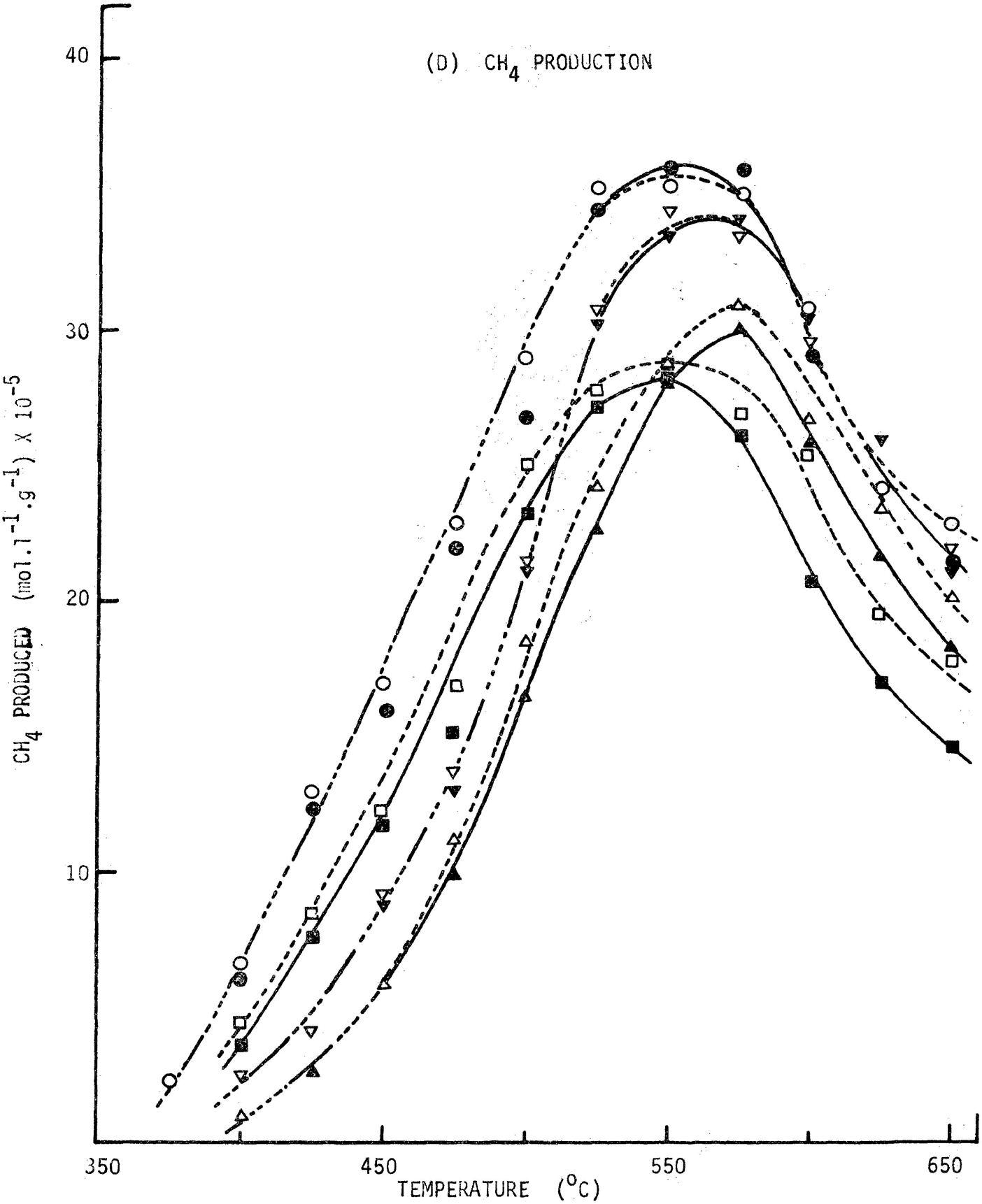

Figure 27(D) The effect of solid additives and water vapour (34.5 kPa) on the concentration of the gases formed in helium at 101.3 kPa from jack pine char samples.
● = jack pine char in helium; ▲ = ● + 1.3% w/w K_2SO_4; ■ = ● + 0.8% w/w Li_2SO_4; ▼ = ● + 2.9% w/w $BaCO_3$; ○ = ● + water vapour; △ = ○ + ▲ ; □ = ○ + ■ ; ▽ = ○ + ▼ .

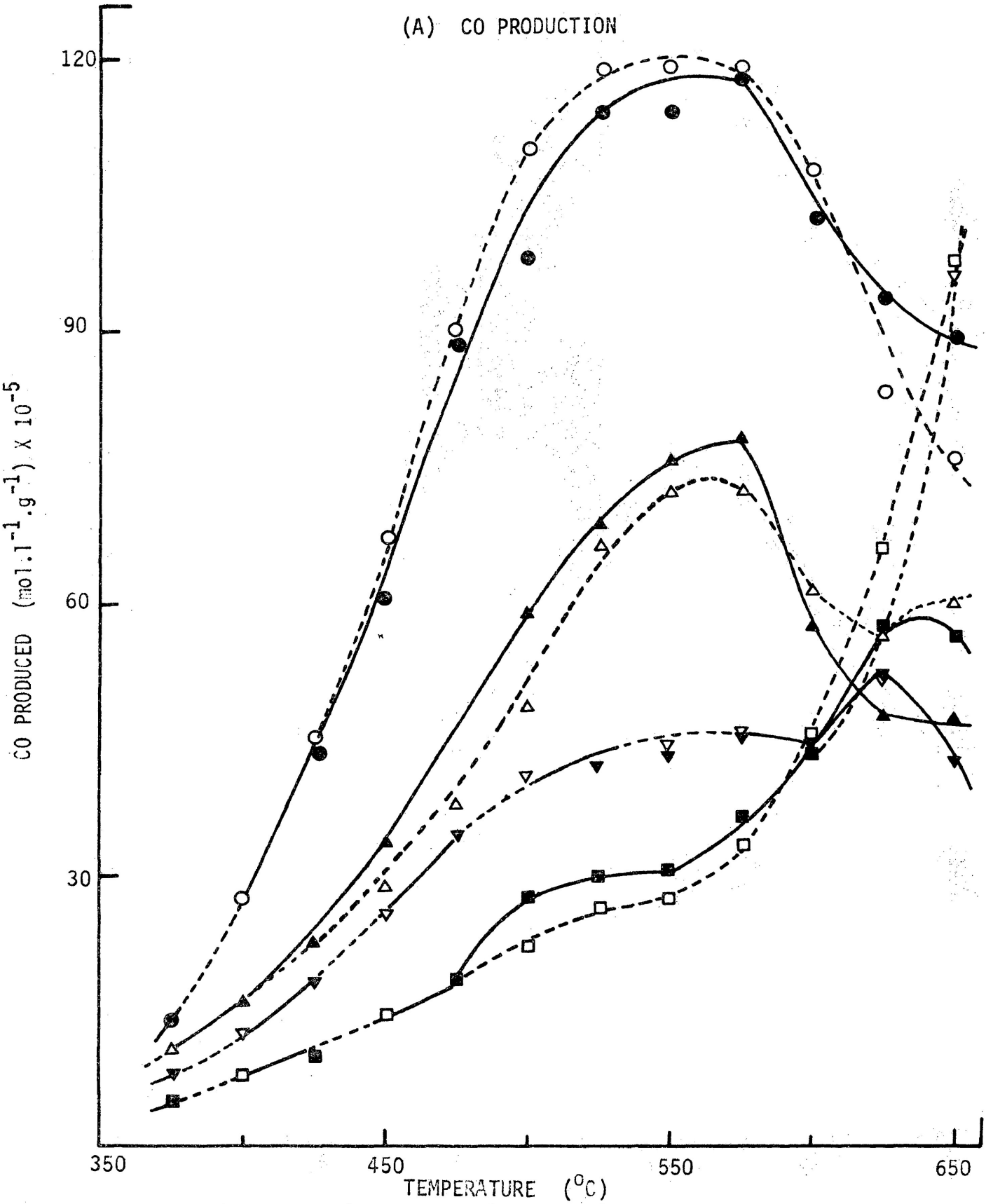

Figure 28(A) The effect of K_2CO_3 and water vapour (34.5 kPa) on the concentration of the various gases formed in helium at 101.3 kPa for jack pine chars.
● = jack pine char in helium; ■ = ● + 5.0% w/w K_2CO_3; ▼ = ● + 2.5% w/w K_2CO_3; ▲ = ● + 1.3% w/w K_2CO_3; ○ = ● + water vapour; □ = ○ + ■ ; ▽ = ○ + ▼ ; △ = ○ + ▲ .

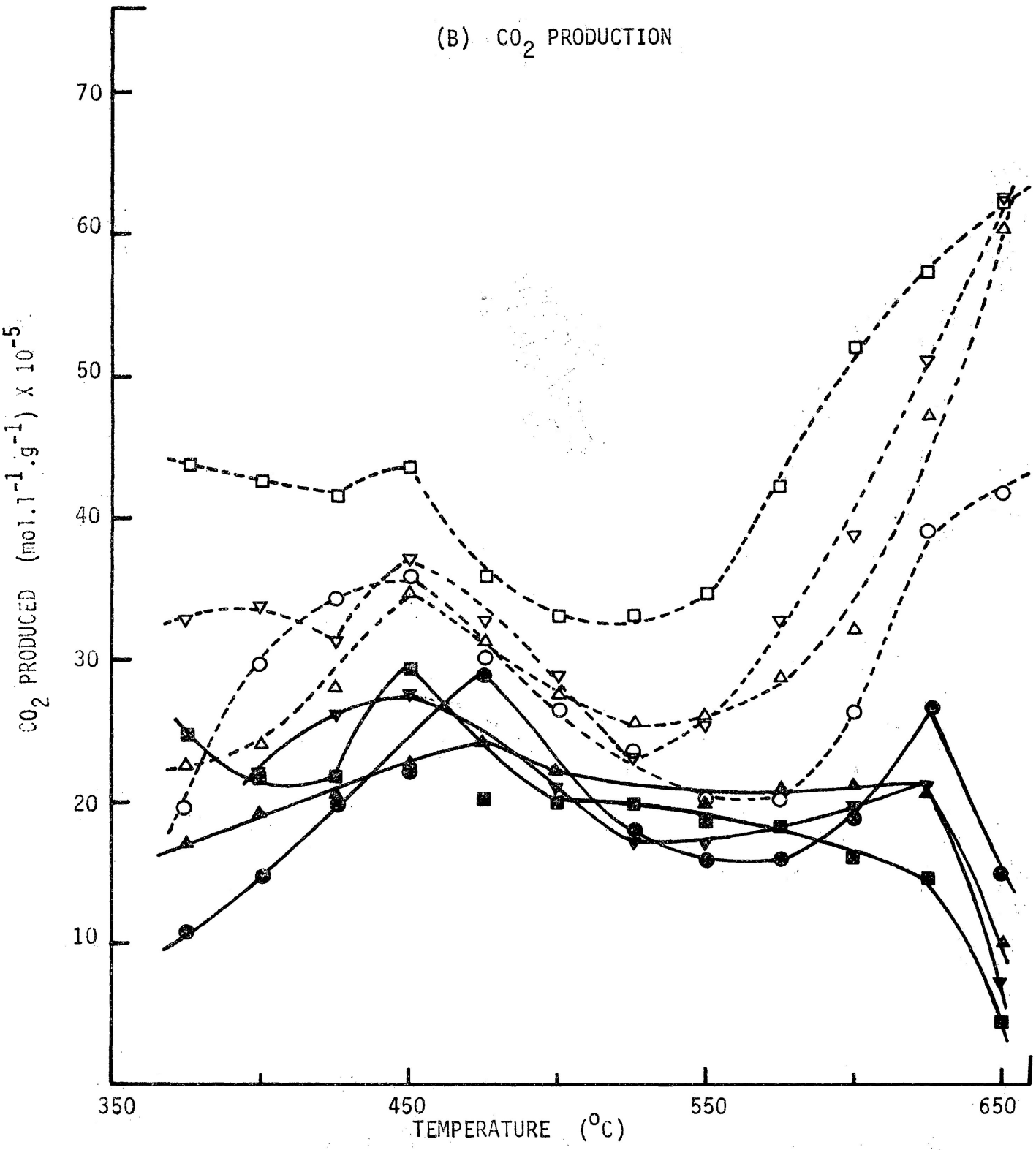

Figure 28(B) The effect of K_2CO_3 and water vapour (34.5 kPa) on the concentration of the various gases formed in helium at 101.3 kPa for jack pine chars.
● = jack pine char in helium; ■ = ● + 5.0% w/w K_2CO_3; ▼ = ● + 2.5% w/w K_2CO_3; ▲ = ● + 1.3% w/w K_2CO_3; ○ = ● + water vapour; □ = ○ + ■ ; ▽ = ○ + ▼ ; △ = ○ + ▲ .

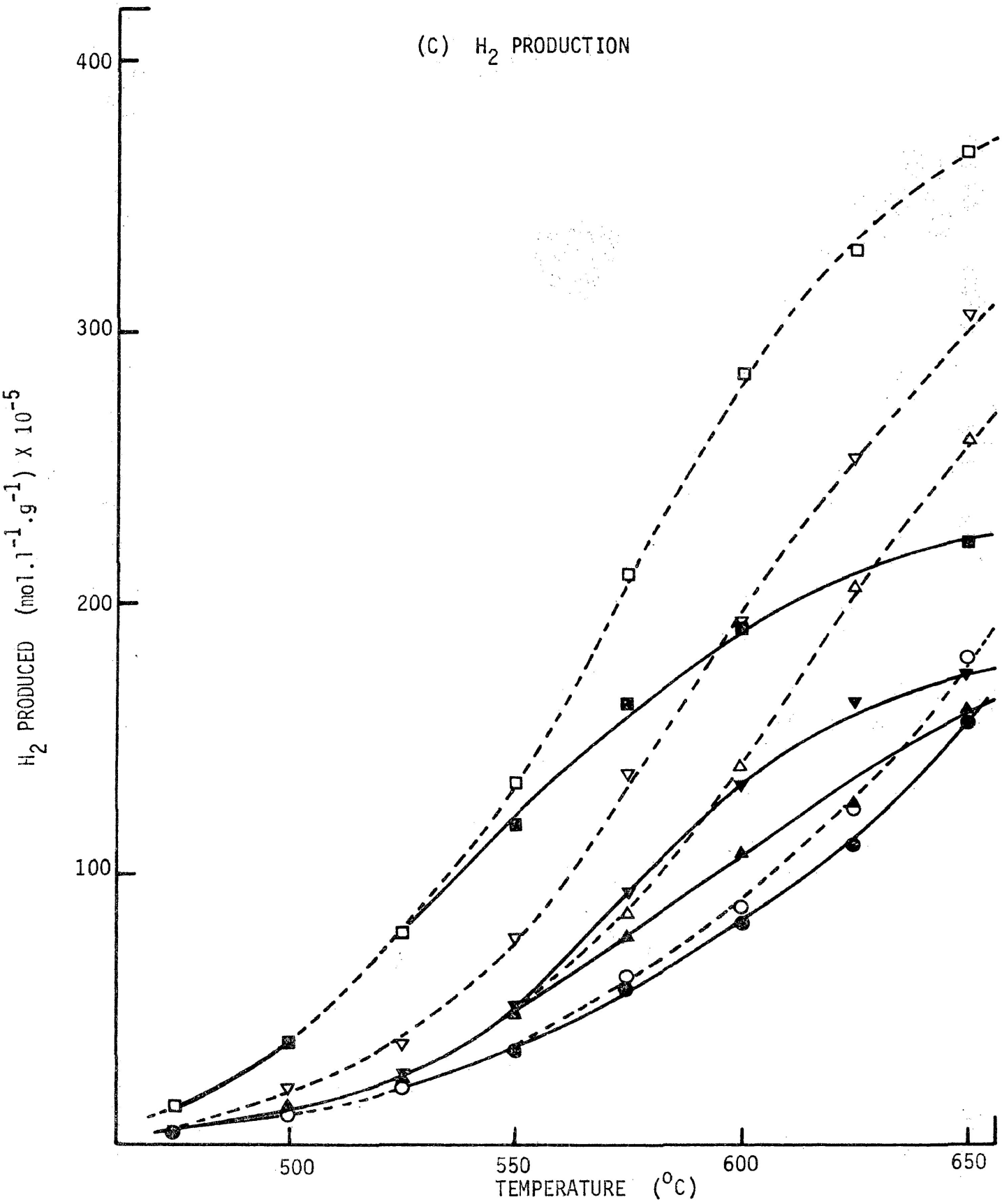

Figure 28(C) The effect of K_2CO_3 and water vapour (34.5 kPa) on the concentration of the various gases formed in helium at 101.3 kPa for jack pine chars.
● = jack pine char in helium; ■ = ● + 5.0% w/w K_2CO_3; ▼ = ● + 2.5% w/w K_2CO_3; ▲ = ● + 1.3% w/w K_2CO_3; ○ = ● + water vapour; □ = ○ + ■ ; ▽ = ○ + ▼ ; △ = ○ + ▲ .

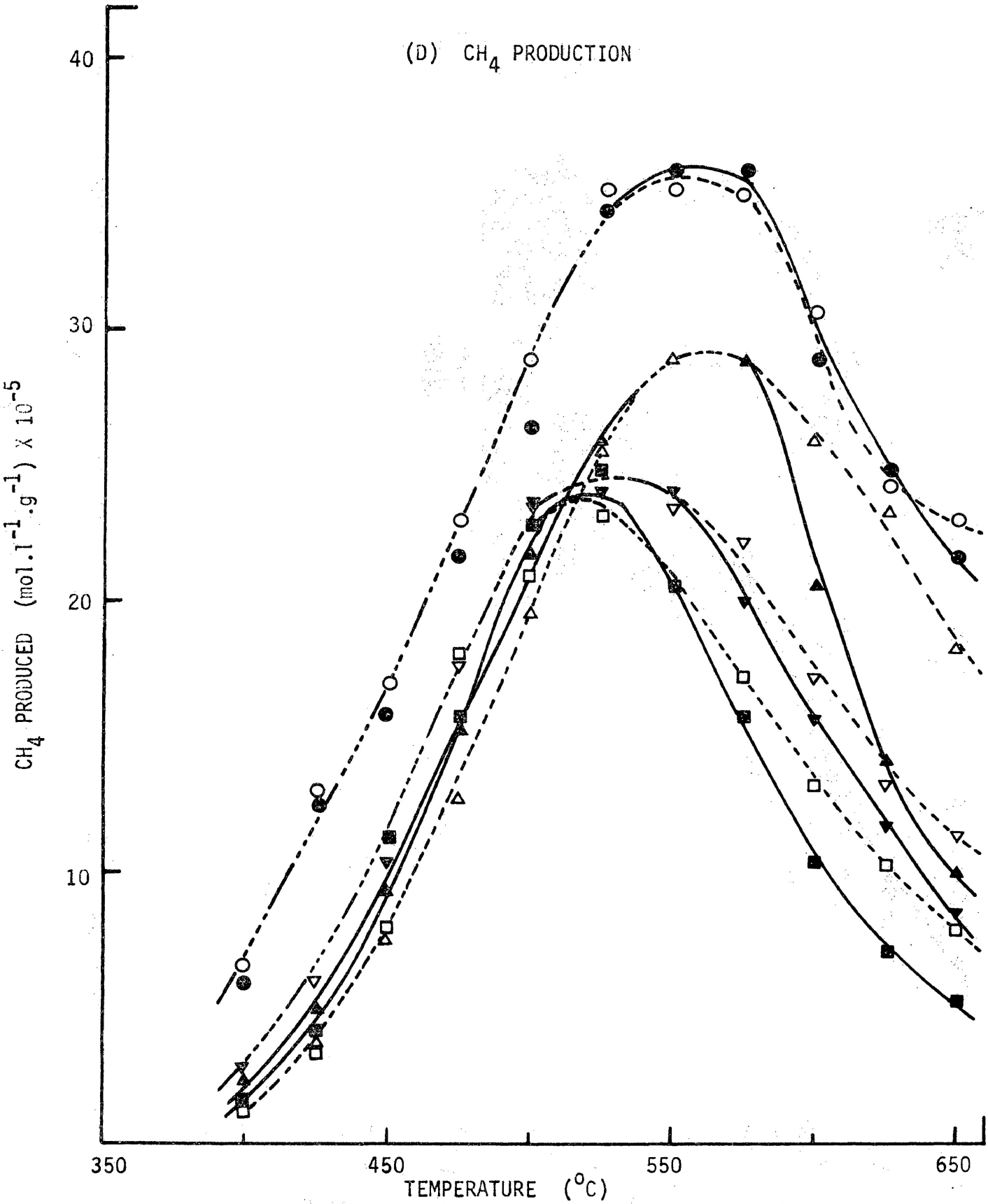

Figure 28(D) The effect of K_2CO_3 and water vapour (34.5 kPa) on the concentration of the various gases formed in helium at 101.3 kPa for jack pine chars.
● = jack pine char in helium; ■ = ● + 5.0% w/w K_2CO_3; ▼ = ● + 2.5% w/w K_2CO_3; ▲ = ● + 1.3% w/w K_2CO_3; ○ = ● + water vapour; □ = ○ + ■ ; ▽ = ○ + ▼ ; △ = ○ + ▲ .

0.8% lithium sulphate and 2.9% barium carbonate no significant differences in the production of carbon monoxide and methane were observed. Carbon dioxide yields increased greatly while the yields of hydrogen improved slightly. For samples containing potassium carbonate, the same effects on methane and carbon dioxide yields were observed. However, carbon monoxide yields increased rapidly above 600°C. Moreover, a much higher increase in hydrogen yield was observed with potassium carbonate when compared to other additives.

3.3.3.3 The effect of carbon monoxide

2.1×10^{-5}, 5.8×10^{-5} and 9.2×10^{-5} mol min^{-1} of carbon monoxide were added in the helium and helium/water vapour flows which corresponded to approximately 50%, 100% and 200% of the maximum rate of carbon monoxide production for 0.4 g of plain jack pine char gasified in helium. The effects of carbon monoxide on the gasification of char and char with 5.0% potassium carbonate are shown in Figures 29 and 30. The major effect was an increase of carbon dioxide yields and a very slight increase of hydrogen production, while methane yields remained constant. Chars containing the other additives demonstrated the same phenomena as these two samples, and thus their gaseous yields are not included in Figures 29 and 30.

3.3.4 Residue analysis

Table 8 shows the elemental analysis of jack pine chars produced from the pyrolysis of the bark in nitrogen at 350°C for 3 h. No significant variation of the carbon and hydrogen contents with the presence of the additives was observed.

3.3.5 Scanning electron microscopy

Scanning electron micrographs showed that jack pine bark samples

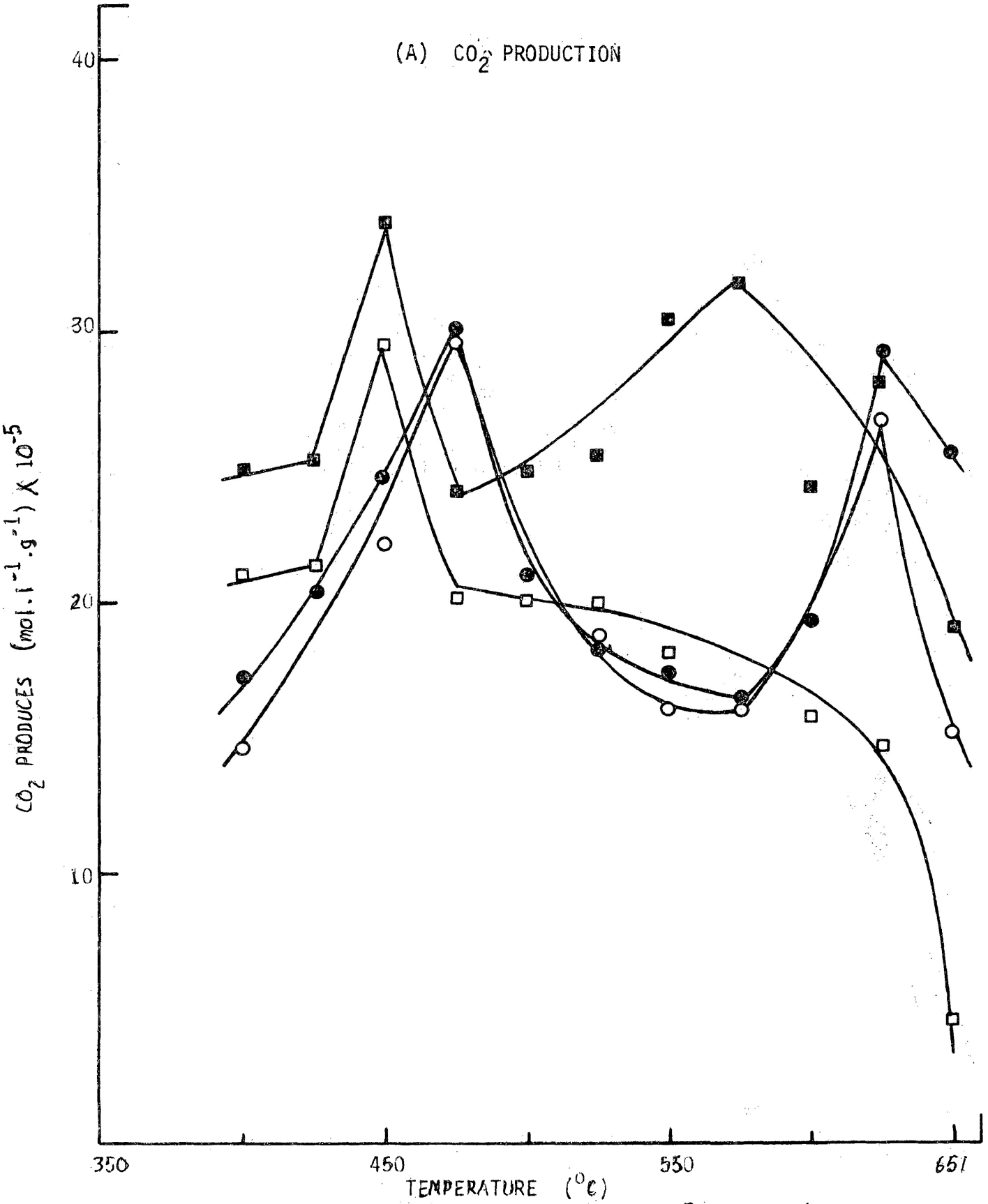

Figure 23(A) The effect of carbon monoxide (9.2×10^{-5} mol.min^{-1}) on the concentration of the various gases formed in helium at 101.3 kPa for (about 0.4 g) jack pine chars.

○ = jack pine char in helium; □ = ○ + 5.0% w/w K_2CO_3;
● = ○ + carbon monoxide; ■ = ● + □ .

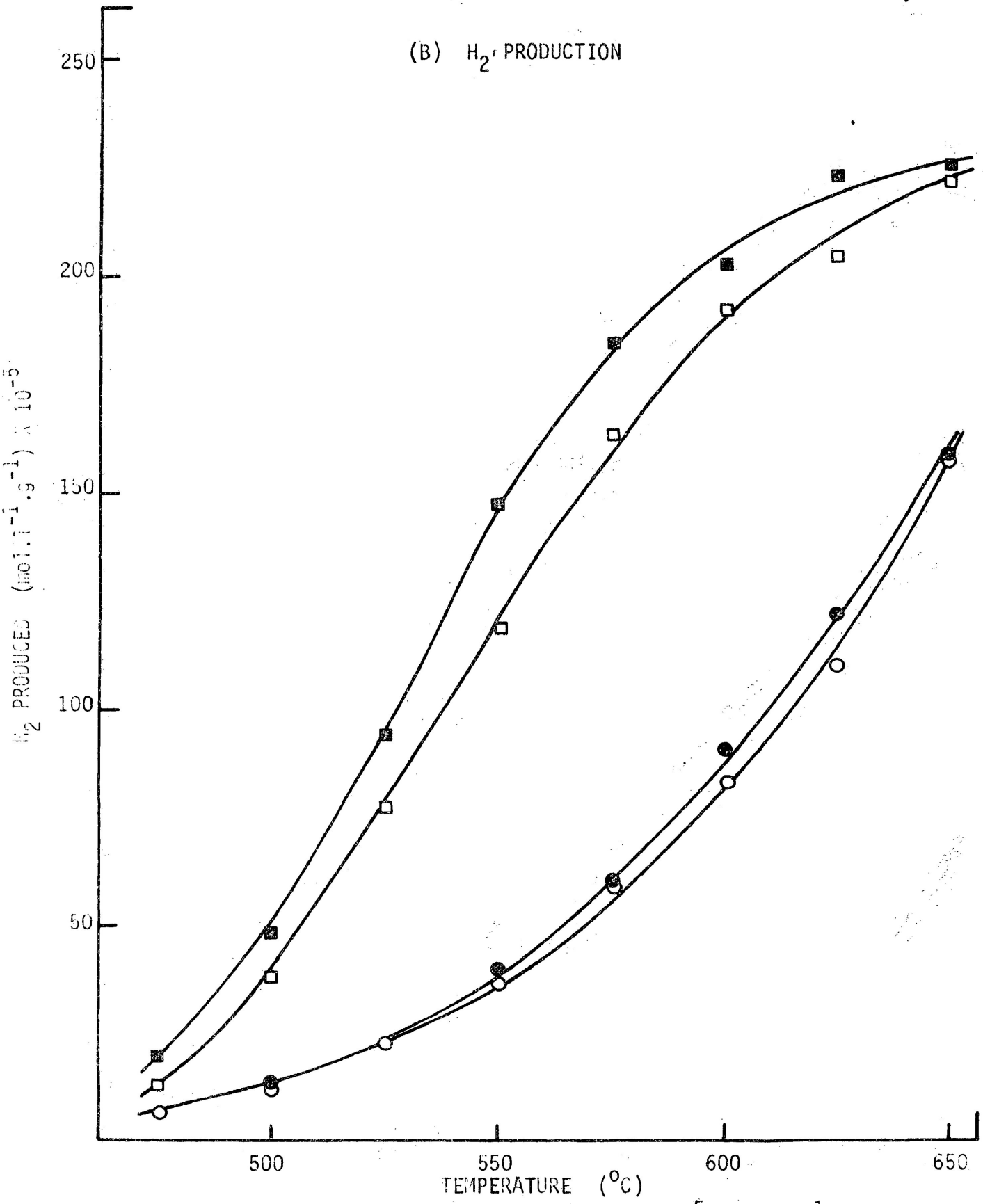

Figure 29(B) The effect of carbon monoxide (9.2 X 10^{-5} mol.min^{-1}) on the concentration of the various gases formed in helium at 101.3 kPa for (about 0.4 g) jack pine chars.

○ = jack pine char in helium; □ = ○ + 5.0% w/w K_2CO_3;
● = ○ + carbon monoxide; ■ = ● + □ .

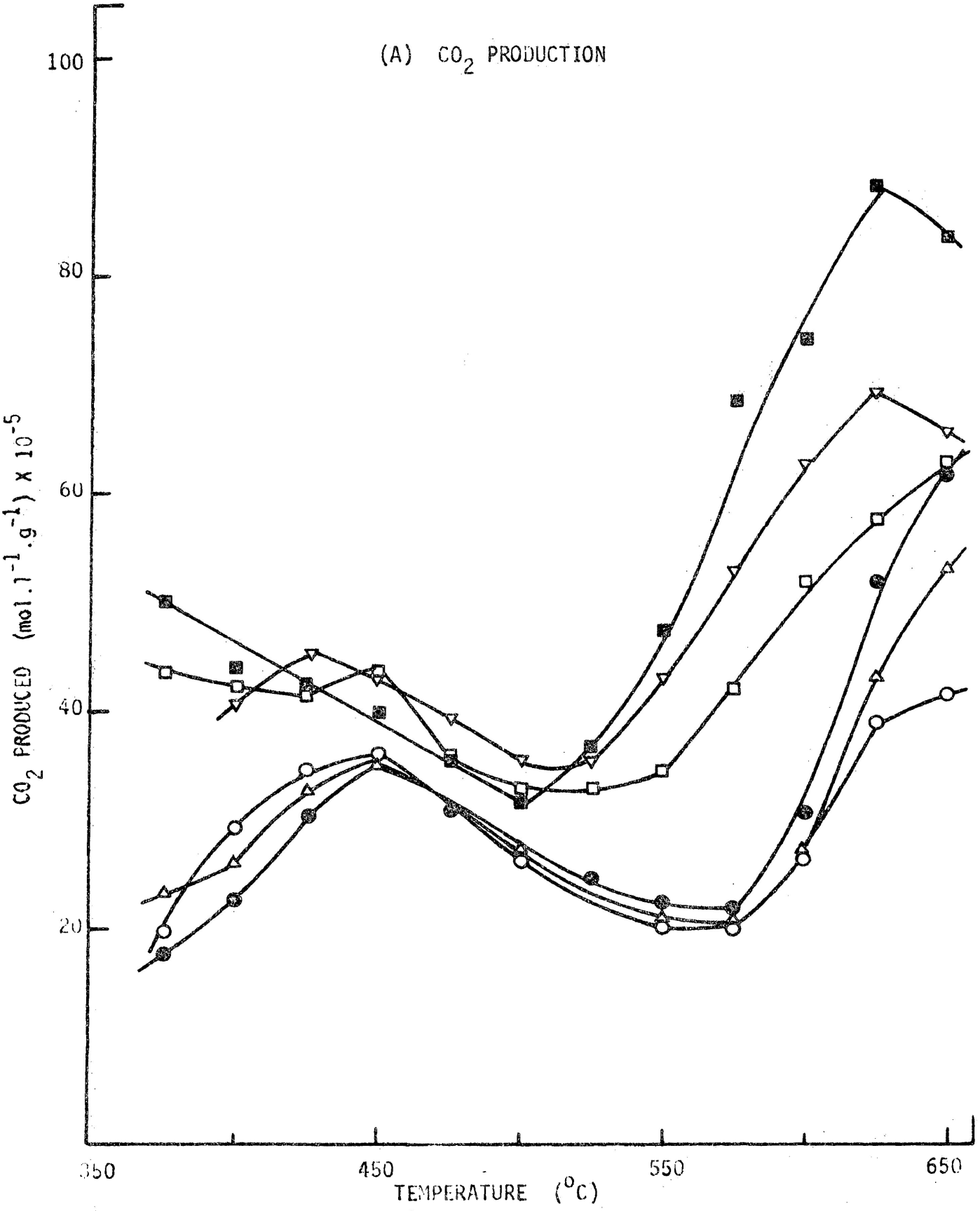

Figure 30(A) The effect of carbon monoxide on the concentration of the various gases formed in helium/water vapour (34.5 kPa) for (about 0.4 g) jack pine chars.

○ = jack pine char in helium/water vapour; □ = ○ + 5.0% w/w K_2CO_3; △ = ○ + (2.1 X 10^{-5} mol.min-1) CO; ▽ = □ + △ ; ● = ○ + (5.8 X 10^{-5} mol.min^{-1}) CO; ■ = ● + □ .

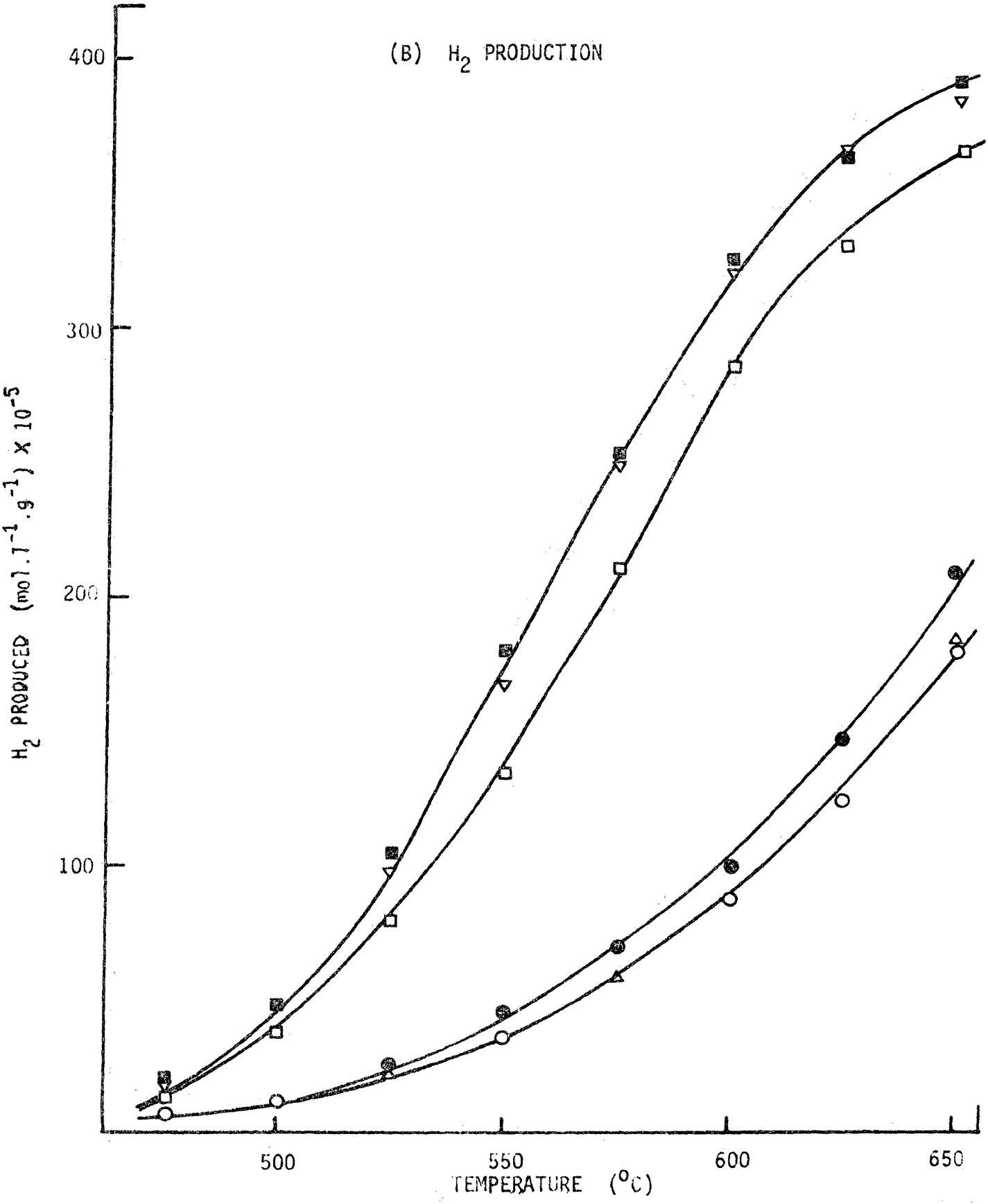

Figure 30(B) The effect of carbon monoxide on the concentration of the various gases formed in helium/water vapour (34.5 kPa) for (about 0.4 g) jack pine chars.

○ = jack pine char in helium/water vapour; □ = ○ + 5.0% w/w K_2CO_3; △ = ○ + (2.1 X 10^{-5} mol.min^{-1}) CO; ▽ = □ + △ ; ● = ○ + (5.8 X 10^{-5} mol.min^{-1}) CO; ■ = ● + □ .

Table 8. Carbon, hydrogen and oxygen contents (%w/w) of the char samples prepared from pyrolysis of jack pine bark in nitrogen at 350°C for 3 h.

Sample	Carbon	Hydrogen	Oxygen
plain jack pine char	67.6	3.75	28.65
char + 1.3% w/w K_2CO_3	69.7	3.39	26.91
char + 2.5% w/w K_2CO_3	68.9	3.53	27.57
char + 5.0% w/w K_2CO_3	68.9	3.32	27.78
char + 1.3% w/w K_2SO_4	68.6	3.34	28.06
char + 0.8% w/w Li_2SO_4	70.0	3.30	26.70
char + 2.9% w/w $BaCO_3$	69.0	3.36	27.64

were irregular with respect to particle size and shape, Figure 31. The distribution of potassium carbonate on the surface of bark particles was not uniform.

After pyrolysis at 650°C in helium, no significant structural change of the bark particles could be observed, Figure 32. However, it appeared that the form of the potassium carbonate on the surface changed from irregular to a rather globular shape. A similar phenomenon was observed in cellulose pyrolysis, Section 3.1.5.

3.3.6 X-ray diffraction

For char with 5.0% potassium carbonate pyrolysed in helium at 650°C, x-ray diffraction lines at 3.65, 3.45, 2.95 and 2.85 Å were recorded which are very similar to the pattern obtained from cellulose samples, Section 3.1.6.

3.3.7 Surface areas

The surface area of native bark was previously measured [45] at 0.3 m^2/g. The value increased to 2.0 m^2/g after heat treatment at 233°C in nitrogen.

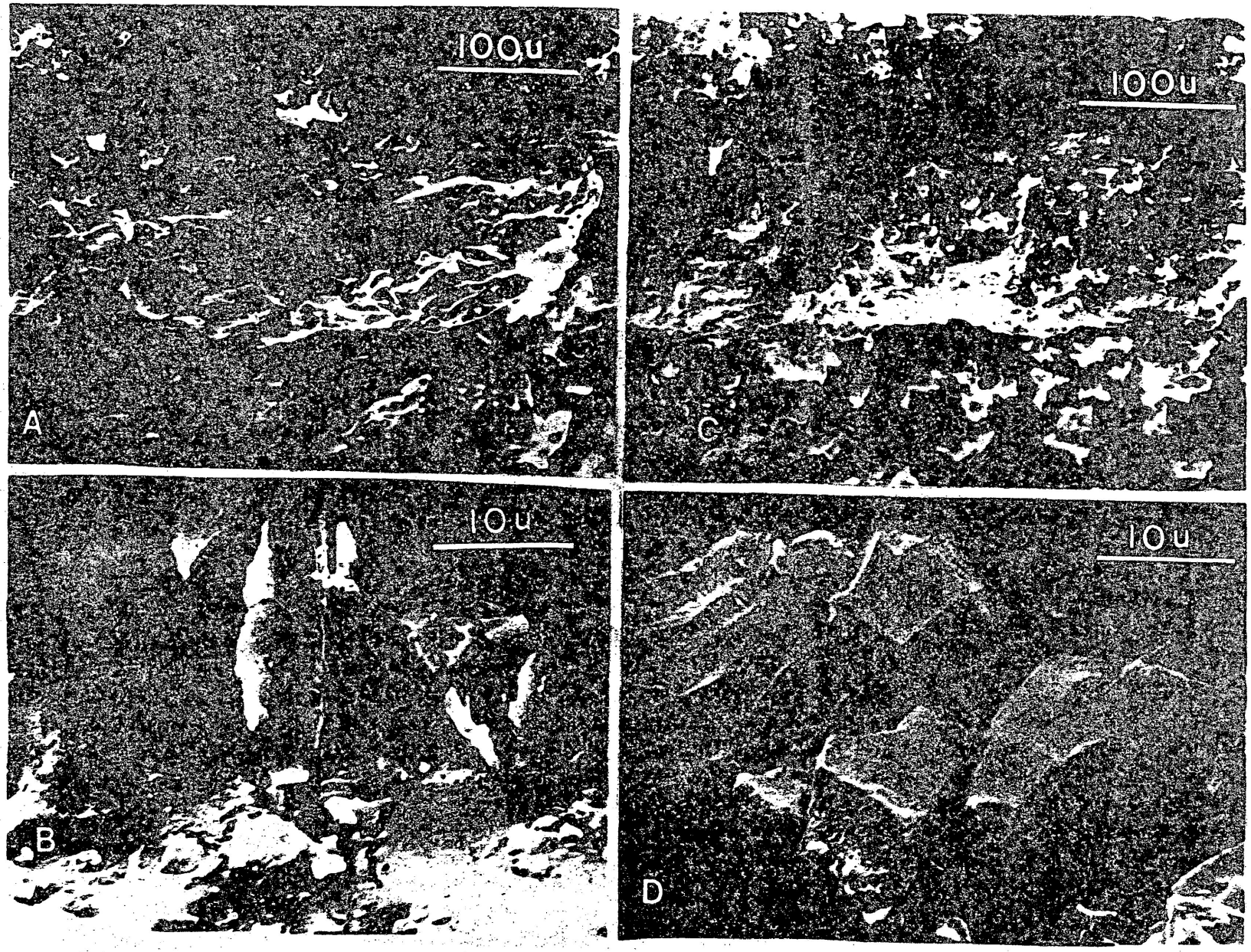

Figure 31 Scanning electron micrographs of jack pine bark samples.
(A) & (B) = jack pine bark; (C) & (D) = jack pine bark + 5.0% w/w K_2CO_3.

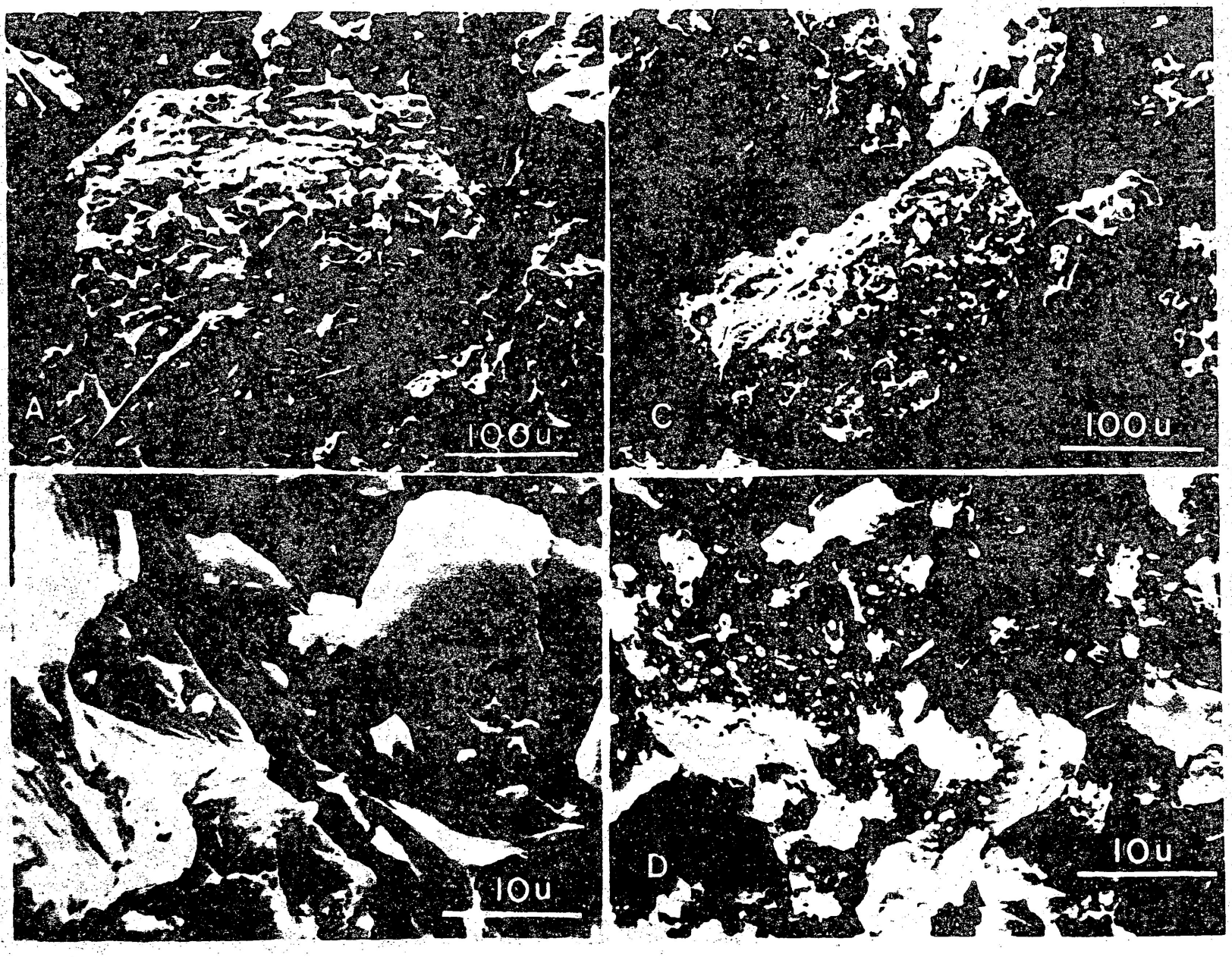

Figure 32 Scanning electron micrographs of jack pine chars after pyrolysis in helium at 650°C. (A) & (B) = jack pine char; (C) & (D) = jack pine char + 5.0% w/w K_2CO_3.

4. Discussion

4.1 Critique of thermobalance methods

Kinetic data could be derived from thermobalance methods by isothermal weight-change determinations and dynamic thermogravimetry. A summary of the computing methods applied in both techniques has been given in Section 1.2.

The two techniques do not always yield the same kinetic results. For example, it has been noted that the effect of heating rates [26] and the usual assumption of first or second order reactions [25] would influence the accuracy of kinetic information derived from dynamic thermogravimetry. Thus it was thought that results obtained from isothermal techniques would be more reliable.

A major drawback of the isothermal technique is that significant sample weight may be lost before thermal equilibrium between the sample and the furnace has been attained. However, in this study, the samples generally reached the reaction termperature with a minimum delay, about 2 min , and only a slight weight loss was observed in this time period.

Thus, in the present study, apparent activation energies were derived from the isothermal technique exclusively. Dynamic thermogravimetric curves were used as indicators regarding the general effects caused by the solid additives.

4.2 The pattern of pyrolysis

The thermal decomposition of wood wastes and allied materials between 20 and 900^{o}C takes place in two stages in dry nitrogen. The first stage involves the loss of water molecules through intra- and inter- molecular dehydration reactions [73]. The subsequent stage occurs as a bulk reaction and includes the loss of low molecular weight fragments to yield tars with additional dehydration, fission and disproportionation reactions forming volatiles such as hydrogen, methane and oxides of carbon with a carbon char residue.

The pyrolysis steps were initiated at 300, 200 and 200°C for cellulose, white birch sawdust and jack pine bark, respectively. The rapid weight-loss region for cellulose lay in a narrow temperature range, 300 to 355°C, where the weight loss was 62.5%. For white birch and jack pine bark, rapid decomposition continued to about 400°C with weight losses of 66 and 46%, respectively. The total weight loss reached a value of 91% for cellulose, in contrast to 80% for both white birch sawdust and jack pine bark at 900°C.

Cellulose, hemicellulose and lignin are the major components of wood and although the proportions of these constituents vary from species to species, elemental analysis figures are generally close to 49.5% for carbon, 6.3% for hydrogen and 44.2% for oxygen [48]. White birch sawdust was obtained from cuts of a debarked log, and thus the carbon, hydrogen and oxygen values would be expected to be similar to those reported. In fact, analysis gave 48.5% for carbon, 6.23% for hydrogen and 45.2% for oxygen in good agreement with the data published on the typical elemental composition of woods [48].

Bark is a general term which includes all tissues outside the cambium, Figure 33, and although a detailed description of the anatomy of bark is outside the scope of this study, it is useful to note that an excellent survey of the topic has been given by Chang [74]. In comparison to wood, bark contains a relatively large amount of lignin and, to a smaller extent, carbohydrates [13]. The CHO composition of jack pine bark is included in Table 9.

Table 9. Carbon, hydrogen and oxygen analysis for the wood waste samples.

Sample	carbon (%)	hydrogen (%)	oxygen (%)
cellulose	43.6	6.66	49.7
white birch sawdust	48.5	6.25	45.3
jack pine bark	53.4	5.96	40.7

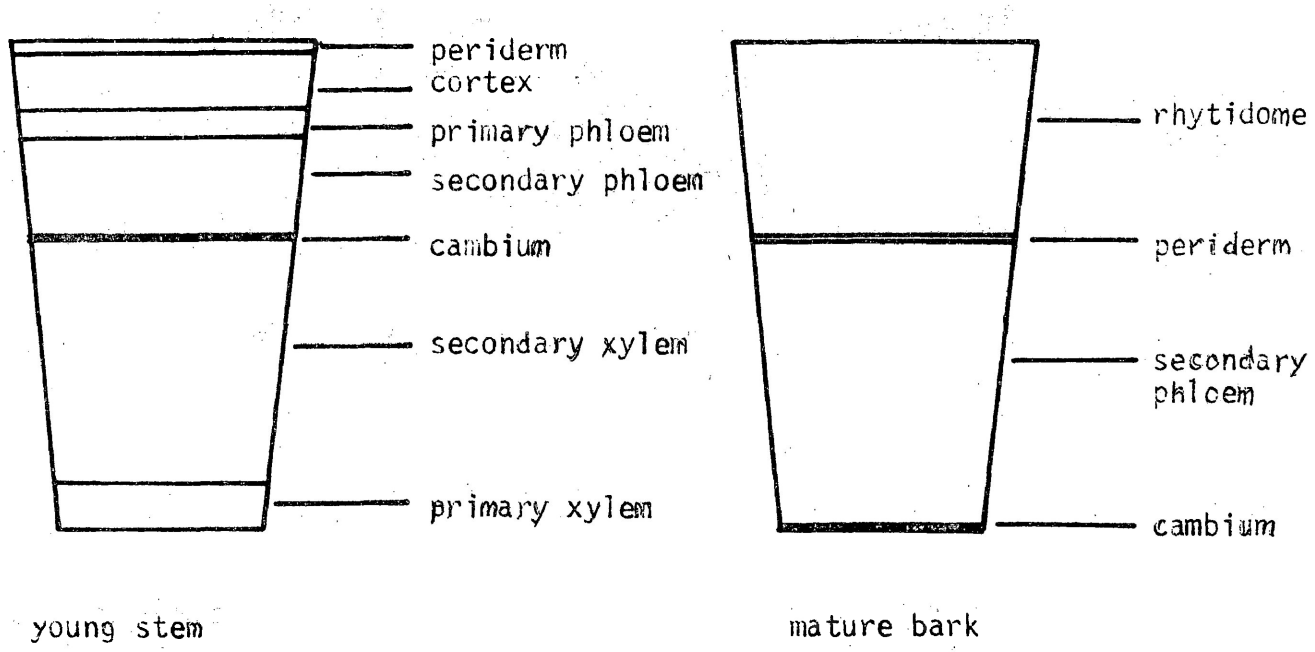

Figure 33 Digrammatic drawings of bark.

It has to be noted that no uniform relationship between chemical composition and anatomical structure has been established for bark.

The breakdown of cellulose, hemicellulose and lignin does not occur simultaneously as observed in studies of relationships between pyrolysing temperatures and mass for samples of woods, α-cellulose and lignin [75]. Hemicellulose was the first material to decompose, largely between 200 to 260°C. Pyrolysis began at about 200°C for lignin and at 275°C for cellulose. The reaction was essentially complete at 360°C for cellulose and 500°C for lignin. The rapid decomposition of cellulose within a relatively narrow temperature range, 275 to 360°C, and the slower pyrolysis of lignin from 200 to 500°C may be explained by the nature of the macromolecules present in cellulose and lignin. In broad terms, the differences in behaviour among the wood, bark and cellulose samples can be related to chemical composition. Thus for bark, which contains a large proportion of lignin, the rapid decomposition was extended over a broad range of temperature, 200 to 400°C in contrast to that for cellulose.

The initiation temperature for cellulose pyrolysis was lowered by the iron (III) oxide addition from 300 to 285°C and, most strikingly, to the region of 200°C for the various samples containing potassium carbonate. Additives did not alter the initiation temperature for either white birch sawdust or jack pine bark. While 5% potassium carbonate lowered the temperature corresponding to the onset of decomposition in cellulose samples to 175°C, it had no effect on the jack pine bark. This difference in behaviour can be attributed to anatomical differences in the samples. Apart from the different compositions of each of the components, anatomy is an important factor in determining the physical and chemical properties of woods.

On the basis of (i) experimental kinetic data on the effects of alkali treatment on wood, (ii) the influence of oxidative destruction on

the lignin network on swelling, and the mechanical properties of wood, a model for the structure of the amorphous ligno-carbohydrate matrix of wood has been proposed [76]. It describes the wood matrix as a heterogenous crosslinked polymer system in which chain-like molecules of carbohydrates intersect and are linked covalently to globular structures of lignin. The differences in behaviour of softwood and hardwood, in general, can be considered to be determined by the differences in density and structure of the lignin networks. For example, after being treated with alkali which destroys the cross-links of lignin and hemicellulose, softwood preserves its elasticity and stiffness in contrast to the increase of plasticity observed in hardwood which has a less dense lignin network than softwood.

4.3 Kinetics of pyrolysis

The kinetics of pyrolysis for the cellulose samples, with the exception of those containing potassium carbonate, showed two distinct regions of behaviour. The initial region followed a simple zero-order kinetic law and the second region was described by equation (21):

$$[1 - (1 - \alpha)^{0.5}] = (u/r)t \qquad (21)$$

An equation derived previously to describe the movement of an interface at constant velocity, u, through a cylinder of radius r, [69].

The results for the kinetics of pyrolysis of cellulose with 5% potassium carbonate added could be explained mathematically by equations similar to those derived for both two- and three-dimensional diffusion-controlled reactions [70] for α values up to 0.8. In practice, however, as the scanning electron micrographs clearly indicate, Figure 17, the fibres have a cylindrical form, rather than spherical, and hence it may be more meaningful, in a physical sense, to predict that the reaction would more likely follow a two-dimensional route. Further, Figure 19 shows that a thin, glass-like layer or film partially covered the surface of these fibres and although it lacks total coherency

of coverage in this micrograph, it may be speculated that the presence of a more coherent film could influence the switch to a diffusion mechanism which might occur, for example, if the reaction rate was controlled by the transport of gaseous reaction products through an adhesive surface film.

The kinetic data for white birch sawdust fit the Avrami-Erofeev equation [71,72] with n = 0.5. However, this equation when applied to a nucleation and growth process is normally only valid when n is a positive integer. Comparison of the reduced-time plot, Figure 34, with known kinetic plots [69] indicates that the curve closely resembles those derived for diffusion-controlled reactions [69]. For low values of α, it is difficult to differentiate between the respective curves for one-, two-, or three-dimensional diffusion-controlled reactions. The scanning electron micrograph, Figure 23, shows that the sawdust samples consisted of cylindrical fibres and particles of different size, 15 to 120 μm in diameter. With the presence of the cylindrical fibres, it is more likely that a two-dimensional diffusion-controlled reaction path would be followed. However, geometric variations as a result of the non-uniformity of particle size distribution would be expected to influence interfacial reaction rates between and within particles [77] and thus affect the form of the reduced-time plot. Hence the deviation of the experimental results from the theoretical curve for a two-dimensional diffusion controlled reaction may be explained. Neither iron (III) oxide nor zinc (II) chromite changed the apparent activation energy determined for the decomposition of the birch sawdust samples.

Kinetic data for the pyrolysis of jack pine bark containing 5% potassium carbonate fell on the same reduced-time plot as that for birch sawdust, and hence would be expected to show the same kinetic behaviour. The scanning electron micrograph of Figure 31 shows that the bark particles are considerably non-uniform, thus diffusion-controlled reactions of one-,

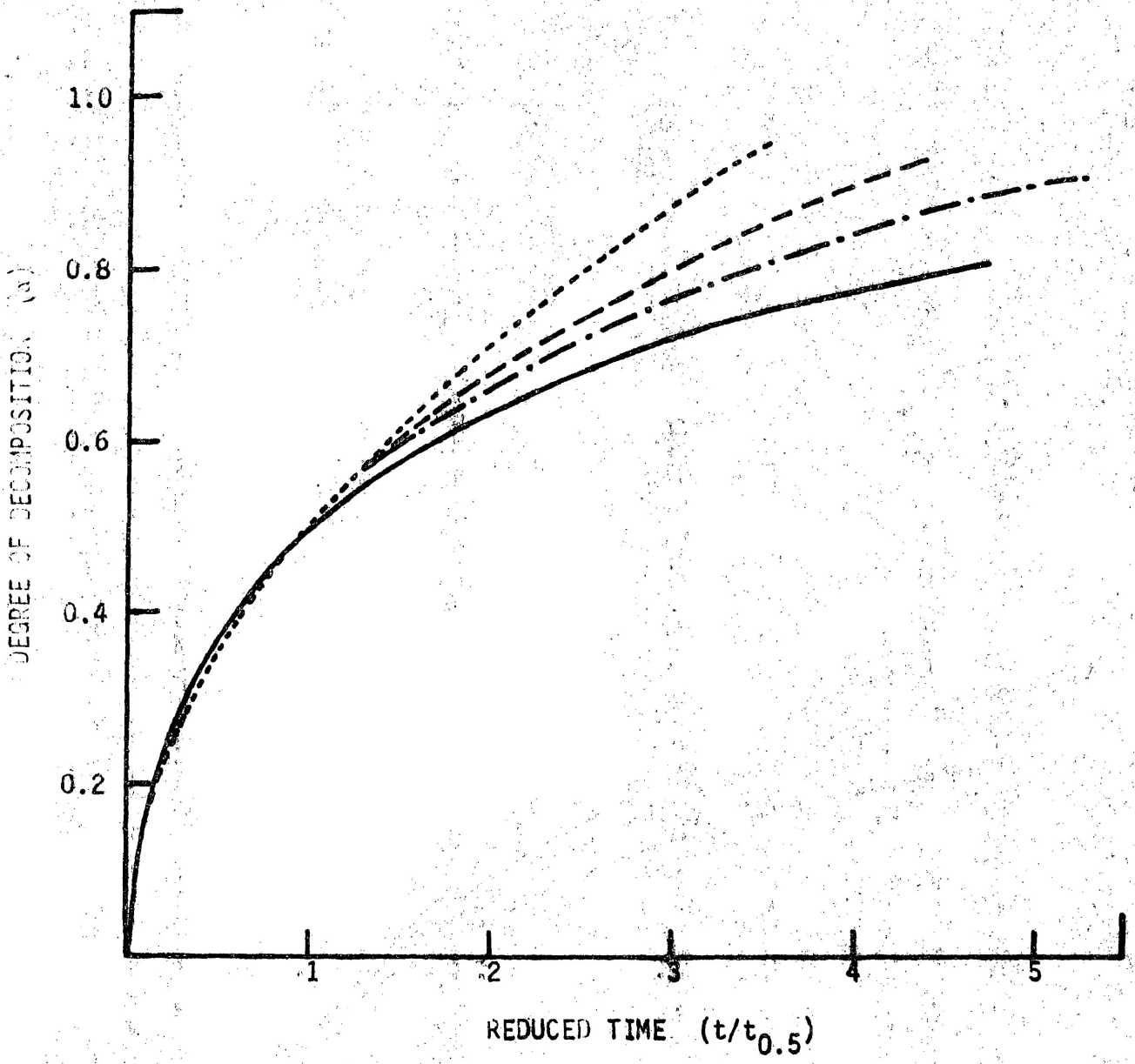

Figure 34 Reduced time plots for white birch sawdust samples and for diffusion-controlled reactions. —— = white birch sawdust; ------ = 1-dimensional diffusion-controlled reaction; - - - - = 2-dimensional diffusion-controlled reaction; —·—·— = 3-dimensional diffusion-controlled reaction.

two- and three-dimensions could possibly occur [69].

The apparent activation energy of 57.4 ± 9.1 kJ mol^{-1} for jack pine bark with 5% potassium carbonate is higher than the value of 43.0 ± 4.7 kJ mol^{-1} reported previously by Fairbridge [26] for plain jack pine bark. However, the rate constants for samples with 5% potassium carbonate are higher than that for plain jack pine bark, Table 7. This indicates that potassium carbonate influenced the Arrhenius reaction parameters by increasing the number of gasification sites rather than by lowering the activation energy.

In contrast, 5% potassium carbonate lowered the activation energy for cellulose from 207.5 to 107.6 kJ mol^{-1}. Perhaps anatomical differences between bark and cellulose can account for these observations. Thus potassium carbonate may catalyze some reactions, for instance, dehydration of cellulose, while it may not be as effective in bark which has a comparatively complex matrix. [A more detailed discussion of potassium carbonate catalysis is given in Section 4.5].

4.4 Gaseous products analysis

4.4.1 Structure and composition differences

The yields of carbon monoxide, carbon dioxide, hydrogen and methane were measured and expressed in terms of mol ℓ^{-1} g^{-1} for both cellulose and jack pine chars pyrolysed in helium at 101.3 kPa from 350 to 650°C. The gas yields from cellulose appear to be much higher than those obtained from jack pine chars at first sight, Figures 12, 27 and 28. However, the results are not strictly comparable since two different generation systems were employed. For cellulose samples, a 'static' system was used. The sample was heated for 30 min. at a selected temperature before gas analysis which gave an 'integral' result. Whereas for jack pine chars, a flow system was used and the concentration of the gases recorded when the required sample temperature was attained in every 5 min. Thus, the gas yields may be considered in terms

of 'differential' analysis. Hence, no conclusions can be drawn regarding direct comparisons of the product yields.

At elevated pressures, the gas yields were expressed in terms of product ratios H_2/CO, CH_4/CO and CO_2/CO. Table 10 gives the maximum values of the product ratios obtained from the pyrolysis of cellulose, white birch sawdust and jack pine chars in helium. It shows that the product ratios for cellulose are significantly higher than the others.

These data may be explained also by differences in composition and anatomy of the materials. It was found [78] that a high carbon monoxide yield was characteristic of the pyrolysis of lignin. For example, the pyrolysis of spruce lignin gave about 51% v/v carbon monoxide. On the other hand, the carbon dioxide content was only 9.6% of total gas yields and that from pyrolysis of cellulose was 62.9% [78]. This accords with the product ratio values for the decomposition of jack pine chars which are the lowest by comparison since bark is composed of a larger proportion of lignin which yields a high carbon monoxide content on pyrolysis. Accordingly, cellulose which is free of lignin, gives the highest product ratios.

4.4.2 The effect of additives

At relatively low temperatures (300 to 500°C), volatile matter, including the primary gases, can be considered to be the principal product of pyrolysis. At around 600°C, volatile tars can undergo secondary reactions, for example, with steam, to produce more gaseous products. Carbon gasification reactions (2) to (4) and the shift reaction (6) would all be expected to exert some effects on the final composition of the products.

	ΔG°_{900} (kJ mol^{-1})	
$C(s) + CO_2(g) \rightleftharpoons 2CO(g)$	+ 13.4	(2)
$C(s) + H_2O(g) \rightleftharpoons CO(g) + H_2(g)$	+ 7.1	(3)

Table 10 Peak product ratios obtained from the pyrolysis of wood waste material in helium

Samples	Pressure (kPa)	Maximum values					
		H_2/CO	Temp. (^oC)	CH_4/CO	Temp. (^oC)	CO_2/CO	Temp. (^oC)
Cellulose	101.3	7.3	570	1.6	540	7.4	550
white birch sawdust	607.8	0.5	>650	0.7	500	1.3	<400
jack pine bark	101.3	1.8	>650	0.4	550	0.5	<400

$$C(s) + 2H_2(g) \rightleftharpoons CH_4(g) \qquad + 8.5 \qquad (4)$$

$$CO(g) + H_2O(g) \rightleftharpoons CO_2(g) + H_2(g) \qquad - 6.3 \qquad (6)$$

The presence of the additives may influence any of the above processes and reactions which would be observed in the nature of the gas yields.

The gaseous products of cellulose samples pyrolyzed in helium at 101.3 kPa are shown in Figures 12 and 13. With the exception of zinc (II) chromite, in general, additives decreased the amount of carbon monoxide formed at a given temperature when compared with plain cellulose. Moreover, the yields of the gases were increased about two fold at 650°C by chromite addition. Thus the additive appears to intervene in the mechanism by promotion of gas-forming reactions while decreasing the quantity of pyrolygeneous tar.

Iron (III) oxide additions increased the yields of hydrogen and carbon monoxide. Hydrogen production was relatively insensitive to temperature from 450 to 600°C which may indicate that the yield of this gas is simply affected by reaction (6) and dependent on the amount of water formed and consumed through equilibrium shifts with temperature. The yield of hydrogen increased above 600°C when the carbon-steam reaction (3) may be expected to intervene.

In general, additions of potassium carbonate decreased the yields of carbon monoxide, carbon dioxide and methane but increased the yields of hydrogen. The total gas yields were lower than that obtained from plain cellulose below 600°C. The increased total gas yields above 600°C may be related to the increased hydrogen production in tune with the likely catalytic effect of potassium carbonate on the carbon-steam reaction (3).

Although all cellulose samples containing potassium carbonate gave increased yields of hydrogen, the effect was maximized at the highest

concentration of this additive. The results show also that the yields of methane were lowered in step with increased potassium carbonate concentration which accords with higher hydrogen yields as signified by step (4) in the reaction scheme.

When gas yields are related to the method of introducing the additives, it may be noted that the yields from samples impregnated with potassium carbonate from aqueous solution were higher than those recorded for cellulose samples when the additive was present as a simple admixture.

White birch sawdust was pyrolyzed at 607.8 kPa and gaseous product ratios were obtained rather than the actual yields of the individual gases. Thus, the results did not give the effect of additives on the absolute gas yields, nevertheless, the product ratios signify, at least, some important trends in the reaction pattern. The data show that iron (III) oxide and zinc (II) chromite did not alter the product ratios which indicates that the gasification reactions were not affected by the additives.

Figures 27 and 28 show the effect of additives on the pyrolysis of jack pine chars. Potassium carbonate addition gave similar effects as in cellulose. Yields of hydrogen were increased at the expense of carbon monoxide and methane. Regarding the effect of concentration of potassium carbonate, hydrogen production increased, while carbon monoxide and methane yields decreased with increasing potassium carbonate concentrations. Carbon monoxide yields generally maximized at 550 to 575^{o}C and dropped at higher temperatures for jack pine chars with other additives. In contrast, for chars containing 2.5% and 5.0% w/w potassium carbonate, the yields of carbon monoxide increased above 600^{o}C. This observation illustrates the likely catalytic effect on carbon-steam reaction (3) suggested earlier for the cellulose samples.

Since potassium carbonate has been observed to be effective in

enhancing hydrogen yields, the effect of potassium sulphate and lithium sulphate on the pattern of gasification has been studied. Gaseous product yields were lowered with these additions. The fact that no observable catalytic gasification effects from either lithium or potassium sulphate differed from those of potassium carbonate indicates that any catalytic activity is most likely related to the cation. In addition, the effect of barium carbonate, an alkaline earth compound, has also been examined and it gave similar results as those for potassium and lithium sulphates.

4.4.3 The effect of water vapour

Figures 27 and 28 show the effect of water vapour (34.5 kPa) on the gasification of jack pine chars. In general, the yields of carbon dioxide and hydrogen increased while those of carbon monoxide and methane remained the same. This suggests that there may have been some effect on the water-gas shift reaction (6), although no significant change of the yields of carbon monoxide was observed. Apparently, water vapour had no effect on the yields of methane.

Samples containing potassium carbonate showed an unusual increase of carbon monoxide yields above 600°C. Furthermore, the enhancement of hydrogen production was also much higher than that given by the other additives. These results may be related to the promotion of the carbon-steam reaction (3) by potassium carbonate. A competitive water-gas reaction (6) may also occur since carbon dioxide yields were increased.

Pyrolysis of cellulose samples in the presence of water vapour, with the exception of those containing 5% potassium carbonate, increased the gaseous product ratios significantly in comparison to those measured in pure helium, Tables 4 and 5. This effect is consistent with the proposal regarding the influence of the water-gas shift reaction. Thus a net increase of carbon monoxide yields would elevate the values of the product ratios.

Zinc (II) chromite may be regarded as a 'negative' catalyst with respect to the forward rate of the water-gas shift reaction since the product yields were less in its presence.

The decrease of CH_4/CO and H_2/CO ratios for the samples with 5% potassium carbonate could be expected since enhancement of the carbon-steam reaction would increase carbon monoxide yields. Increased product ratios for all samples containing 0.7% potassium carbonate reveals the relationship between the carbon-steam reaction and the concentration of potassium carbonate. Thus, at low catalyst concentration, the water-gas shift reaction may make a higher contribution than the carbon-steam reaction to the overall process.

White birch sawdust samples gave similar results to those of cellulose in agreement with the proposals regarding the contribution of the water-gas shift reaction in the presence of water vapour. Iron (III) oxide behaved as 'positive' catalyst and zinc (II) chromite as a 'negative' catalyst in this reaction.

4.4.4 The effect of pressure

Increasing pressure would be expected to shift reaction (4) to the right, thus increasing methane yields. However, the CH_4/CO ratio was found to decrease with increasing pressure which implies that the increase in carbon monoxide concentration was greater than that for methane. Reactions (2), (3) and (6) would not favour the production of carbon monoxide with increasing pressure. Thus it may be that the increase results from secondary reactions involving the pyrolygeneous tars. Tars do not leave the heating reaction zone so readily as pressure increases and hence may undergo secondary reactions to form gaseous products and char [38]. It is not surprising that a trend was not observed for the H_2/CO and CO_2/CO ratios since secondary reactions of tar may increase carbon monoxide yields. On the other hand,

reactions (2) and (3) have a tendency to decrease the carbon monoxide yields with increasing pressure.

4.4.5 The effect of carbon monoxide

Figures 29 and 30 show that in the gasification of jack pine chars in both helium and helium/water vapour, carbon dioxide yields increased in step with the concentration of carbon monoxide added. A relatively slight increase in hydrogen yields was observed. Reactions (2), (3) and (6) would be expected to be influenced by the addition of carbon monoxide. In pure helium, reactions (3) and (6) would be limited. Thus the increase of carbon dioxide yields can be attributed to reaction (2). In helium/water vapour atmospheres, hydrogen yields did not improve significantly which indicates that reaction (6) was not affected to any large extent. A low water vapour concentration could account for the slight effect on reaction (6) with increasing pressure of carbon monoxide. In the end, reaction (2) remains the most affected.

It has been mentioned that reaction (3) is believed to be catalyzed by potassium carbonate and hydrogen yields remained relatively constant regardless of the carbon monoxide addition. Thus, it appears that the carbon monoxide added had little effect on the reaction which may imply that equilibrium had not been attained, and hence carbon monoxide concentration would exert little influence on the reaction.

4.5 The role of potassium carbonate

Potassium carbonate showed the most pronounced effect on gasification of all the additives.

Alkali metal and alkaline-earth metal compounds have been shown to catalyze the gasification of carbon and graphite [55,57,62,63]. Mechanisms proposed to account for the catalytic gasification may be classified into two

categories which differ in the way that interactions are believed to occur on the catalyst. If the catalyst interacts with a gas molecule, it may act as a dissociation centre for the molecule and the well-known oxygen-transfer mechanism, involving an oxidation-reduction cycle [79,80], is an example of this category. An alternative proposition is that gas molecules dissociate on the catalyst surface and then migrate to the active site on the carbon surface to react [53,81]. The second category involves the interaction of the catalyst with carbon as opposed to gas molecules. Long and Sykes theory [58] is based on electron transfer from carbon matrix to metal catalyst. Consequently, carbon-carbon bonds are weakened which facilitates the release of product gases.

The present study showed that potassium carbonate was a very effective gasification catalyst and that potassium sulphate had no catalytic effect. The major influence of the carbonate may be to enhance the carbon-steam reaction. A similar observation was made previously in studies of the steam gasification of coal char [57] when it was noted that potassium hydroxide and potassium carbonate had the same catalytic activity. The identical behaviour of these additives was explained by noting that the hydroxide would be converted to the carbonate in the presence of CO_2, reaction (25):

$$2KOH(\ell) + CO_2(g) \rightleftharpoons K_2CO_3(s) + H_2O(g) \qquad (25)$$

The following mechanism was proposed to account for catalysis:

$$K_2CO_3(s) + 2C(s) \rightleftharpoons 2K(g) + 3CO(g) \qquad (26)$$

$$2K(g) + 2H_2O(g) \rightleftharpoons 2KOH(\ell) + H_2(g) \qquad (27)$$

$$H_2O(g) + CO(g) \rightleftharpoons CO_2(g) + H_2(g) \qquad (6)$$

$$2KOH(\ell) + CO_2(g) \rightleftharpoons K_2CO_3(s) + H_2O(g) \qquad (25)$$

$$2C(s) + 2H_2O(g) \rightleftharpoons 2CO(g) + 2H_2(g) \qquad (3)$$

The standard free energies of the above reactions from 700 to 1200 K are given in Table 11. The free energy of reaction (26) is strongly positive, but it is strongly negative for reaction (27). It has been shown [57] that reaction (26) in sequence with (27) would be favoured thermodynamically above 800°C. A maximum temperature of 650°C was employed in this study. Thus reactions which include the formation of metallic potassium as shown in the above scheme are unlikely to occur.

A modified oxygen-transfer mechanism has been proposed [82] to explain the catalytic behaviour of alkali metal carbonates and oxides in graphite oxidation reactions. The catalytic effects were interpreted on the basis of distinct oxidation-reduction cycles, involving the intermediate formation of peroxides. In helium the catalyzed reaction did not occur until 897°C, the melting point of K_2CO_3. In oxygen, the catalyzed reaction became detectable at the melting point, 490°C, of dipotassium dioxide (K_2O_2). A mechanism was proposed as follows:

$$K_2CO_3(s) + C(s) + O_2(g) \rightleftharpoons K_2O(s) + 2CO_2(g) \qquad (28)$$

$$(n/2)\ O_2(g) + K_2O(s) \rightleftharpoons K_2O_{1+n}(\ell) \qquad (29)$$

$$K_2O_{1+n}(\ell) + nC(s) \rightleftharpoons K_2O(s) + nCO(g) \qquad (30)$$

The free energy of the reactions, Table 11, showed that reaction (28), the carbon-induced decomposition of potassium carbonate to dipotassium monoxide (K_2O), was thermodynamically feasible at 500°C. The reaction was then followed by oxidation of monoxide to higher oxides (29), for example K_2O_2, and subsequent reduction of the oxide formed by carbon to complete the cycle (30). This mechanism was used to explain the oxidation reactions of carbon, but any carbon monoxide formed could partake in secondary reactions, for instance, with water vapour, to form hydrogen.

It was also observed by hot-stage microscopy [82] that the additive

Table 11 Free energies of reaction (based upon data taken from [91])

Reaction	ΔG^{o} (kJ mol^{-1})					
	700 K	800 K	900 K	1000 K	1100 K	1200 K
$2KOH(\ell) + CO_2(g) \rightleftharpoons K_2CO_3(s) + H_2O(g)$ (25)	-120.2	-110.1	-99.7	-85.8	-79.6	-69.9
$K_2CO_3(s) + 2C(s) \rightleftharpoons 2K(g) + 3CO$ (26)	425.8	370.5	315.3	257.5	198.5	131.0
$2K(g) + 2H_2O(g) \rightleftharpoons 2KOH(\ell) + H_2(g)$ (27)	-138.2	-208.5	-195.5	-183.8	-163.7	-137.3
$H_2O(g) + CO(g) \rightleftharpoons CO_2(g) + H_2(g)$ (6)	-13.0	-9.6	-6.3	-2.9	0.4	3.35
$K_2CO_3(s) \rightleftharpoons K_2O(g) + CO_2(g)$ (31)	282.8	267.4	252.3	236.8	221.3	205.9
$C(s) + O_2(g) \rightleftharpoons CO_2(g)$ (1)	-395.4	-395.8	-395.8	-395.8	-396.2	-396.2
$K_2CO_3(s) + C(s) + O_2(g) \rightleftharpoons K_2O(s) + 2CO_2(g)$ (28)	-112.6	-128.4	-143.5	-159.0	-174.9	-190.3
$K_2O(s) + 1/2\ O_2(g) \rightleftharpoons K_2O_2(\ell)$ (29a)	-74.5	-66.5	-59.0	-51.0	-43.9	-36.4
$K_2O_2(\ell) + C(s) \rightleftharpoons K_2O(s) + CO(g)$ (30a)	-99.2	-115.9	-132.2	-149.4	-165.3	-181.2

appeared liquid-like at 500°C, which might indicate the formation of a peroxide. A similar observation on the mobility of potassium carbonate catalyst has been reported in the steam-gasification of coal chars [63]. Potassium carbonate was deposited on non-catalytic beads which were then embedded in a bed of char. After reaction, large cavities or void volumes were created around the beads. Electron microprobe analysis showed high concentrations of potassium in these cavities and indicated that the carbonate was mobile during reaction. It was postulated that the transport of the catalyst may be ascribed to the thermal-steam decomposition of alkali carbonate and formation of the hydroxide, reaction (25). The transport could be in both liquid and gaseous forms since potassium hydroxide could exist in both phases at 650°C. However, thermochemical data, Table 11, shows that the extent of potassium hydroxide formation would be limited unless the carbon dioxide concentration is very low.

Figure 19 shows that after pyrolysis of cellulose at 650°C, the potassium carbonate additive appeared to change from irregular to a globular shape and an incoherent surface film was observed. This suggests some mobility of potassium carbonate during pyrolysis. The X-ray diffraction pattern of the film was quite similar to that of potassium bicarbonate which, although it decomposes above 200°C, may have formed during the sample cooling period from the action of moisture on the carbonate. However, the actual nature of this film-forming phenomena could be complex and the chemical composition may consist of potassium carbonate, potassium bicarbonate, potassium hydroxide and some forms of potassium oxides.

In this study, pyrolysis was conducted in helium and helium/water vapour atmospheres, thus reactions (28) and (29) would not be expected. However, the samples of cellulose and wood waste have a high oxygen content and this may be available as a source of oxygen in similar steps which

could explain the behaviour of the additive.

It is also possible that some direct interaction between carbon and the carbonate takes place which may weaken C - C bonds and enhance the gaseous yields.

The above proposals provide some tentative explanation for the observed behaviour of K_2CO_3. However, there is no evidence in favour of a unified mechanism capable of interpreting all of the data. Many other possibilities may exist and much work remains to be done before a detailed mechanism is established.

An optimum concentration of alkali carbonate for the ignition temperature of carbon in oxygen has been observed [83]. Similar optimum catalyst loading effects for nickel and potassium carbonates have been reported in studies of the hydro- and steam-gasification of carbon and coal [84] and for the catalytic gasification of coal by calcium, potassium and sodium salts [85,86,87]. Presumably, the catalyst saturation concentration is related to the surface area. It is expected that catalyst efficiency would decrease as coverage approaches a monolayer or exceeds this value [81]. Moreover, transport or mobility of the catalyst may also increase the possibility of the deactivation as catalyst concentration increases [88]. Figures 18 and 31 show that surface coverage of cellulose and bark by the catalyst is very low thus, in this regard, an optimum catalyst concentration was not achieved.

Cellulose containing 0.7% impregnated K_2CO_3 showed higher activity than the dry-mix counterpart. Generally, catalysts introduced by impregnation were more efficient than those incorporated by a dry-mix process, in agreement with previous workers [89,90]. Simply, impregnation may enhance a more even catalyst distribution over the surface and also a more uniform penetration throughout the bulk of the solid. Such distribution would serve

to increase the amount of catalyst/solid contact, thus increasing the extent of reaction.

4.6 Calorific values

The gross calorific value of a fuel can be considered as the number of heat units evolved when unit weight (or unit volume in the case of a gas) of a fuel is completely burned and the combustion products cooled to 288 K. A calculated calorific value of a gas mixture which is usually accurate to within 2% of the experimental value can be obtained by multiplying the percentage of each component in the fuel by the known calorific value of the component and summing the results [92].

Samples of jack pine chars were pyrolysed at 650^{o}C for 40 min. The total gas yields and the calorific values of the gas mixtures were calculated, Table 12. The calorific values of the gaseous products from gasifications in the presence of solid additives and water vapour were lowered. However, it must be noted that the total heating value of the gases depends also on the extent to which carbon was gasified - thus influencing the total yields. Since the gas yields were increased by addition of water vapour and potassium carbonate, higher values for the factor 'F' = (calorific value) x (gas yield) were obtained, Table 12. In other words, the gases produced have a higher total heat content.

The 'F' values for all samples are small when compared with the calorific value of the carbonaceous solids, Appendix 1. However, gases evolved below 650^{o}C were not included in this calculation and also the solid samples were not completely gasified at 650^{o}C. An important indicator of the latter is the small values of the percentage of carbon 'gasified' which were calculated from the ratio (carbon content of gaseous products/carbon content of the solid sample). The carbon content of the solid sample can be obtained from

Table 12 Calorific values and yields of gaseous products from the pyrolysis of jack pine chars at 650°C and 101.3 kPa for 40 min.

	helium atmosphere		helium/water vapour (34.5 kPa) atmosphere		
	jack pine char	jack pine char + 5.0% K_2CO_3	jack pine char	jack pine char + 2.5% K_2CO_3	jack pine char + 5.0% K_2CO_3
Composition of gas (% v/v) H_2	69.4	80.6	68.0	69.0	67.3
CO	23.0	17.6	11.3	12.0	13.5
CH_4	4.9	1.1	3.7	1.0	0.5
CO_2	2.7	0.7	17.0	18.0	18.7
Total gas yield (mol of gas/g of char) x 10^{-6}	2,430	2,470	5,090	9,300	13,380
*Calorific value of gas mixture (kJ m^{-3})	12,800	12,110	10,820	10,130	9,810
% of carbon 'gasified'	1.3	0.9	2.9	5.0	7.6
'F' = [Calorific value] x [Total gas yields] (kJ kg^{-1})	696	671	1,230	2,110	2,930

* Calorific values of component gases [92]

CO = 11,850 kJ m^{-3}

H_2 = 11,920 kJ m^{-3}

CH_4 = 37,070 kJ m^{-3}

the CHN analysis. Again, the amount of carbon present in the tars was not determined. A final point is that heat was supplied to vaporize water and although a higher total heating value of gases was obtained in the helium/water vapour atmosphere, the overall thermal efficiency of the steam-gasification process has yet to be established.

The calorific values of the gases obtained from the cellulose samples are summarized in Table 13 and are lower than those found with jack pine chars, in accordance with the higher content of carbon dioxide in the gas mixture.

A notable feature with cellulose is that the total gas yields increased in the presence of potassium carbonate in helium in contrast to the results with jack pine char. It is probable that much more water, which is essential for the carbon-steam reaction catalyzed by potassium carbonate, was produced in the pyrolysis of cellulose.

The gases produced at 650^{o}C have calorific values ranging from 8,660 to 12,756 kJ m^{-3} and may be considered as medium energy sources, similar to water gas in heat content, which could be used in various ways in industry including steam raising. Alternatively, the calorific value of the gas could be upgraded by an add-on process such as reforming to methane, CV = 37,070 kJ m^{-3}, or by scrubbing to remove carbon dioxide. Of course, such additional steps would require the evaluation of the overall thermal efficiency and cost of the process.

Table 13 Calorific values and yields of gaseous products from the pyrolysis of cellulose in helium at 650°C and 101.3 kPa for 30 min.

		cellulose	cellulose + 10.2% iron (III) oxide	cellulose + 14.2% zinc (II) chromite	cellulose + 5.0% potassium carbonate
Composition of gas (% v/v)	H_2	55.8	53.2	53.5	65.2
	CO	9.1	8.3	13.9	12.8
	CH_4	4.9	3.5	5.6	0.2
	CO_2	30.2	35.0	27.0	21.8
Total gas yields (mol of gas/g of cellulose) x 10^{-6}		1,180	1,620	2,600	4,040
*Calorific value of gas mixture (kJ m^{-3})		9,550	8,660	10,080	9,360
% of carbon 'gasified'		1.4	2.3	3.9	4.1
'F' = [Calorific value] x [Total gas yields] (kJ kg^{-1})		250	310	590	850

* See Table 12.

5. Conclusions

The kinetics of decomposition of jack pine bark and white birch sawdust in nitrogen have been described by equations consistent with diffusion controlled reactions. Particle size distribution effects may account for some slight deviations in the experimental rate results. The value of apparent activation energy was not altered by the addition of iron (III) oxide and zinc (II) chromite to white birch sawdust samples, nor by adding potassium carbonate to jack pine bark at 101 kPa from 220 to 340°C.

Cellulose pyrolysis in nitrogen was interpreted by a model established for a phase-boundary reaction. The apparent activation energy was lowered from 207.5 to 187.0 and 107.6 kJ mol^{-1} for the addition of iron (III) oxide and potassium carbonate, respectively, from 240 to 340°C. This indicates that cellulose is more susceptible to the influence of additives than wood because of composition and anatomical differences of a major kind. Potassium carbonate addition to cellulose shifted the kinetics to a diffusion-controlled region which can be related to the possible mobility of the additive with regard to the formation of an incoherent surface film which was somewhat evidenced in scanning electron microscopy.

Gasification studies indicate that iron (III) oxide may catalyze the water-gas reaction, while zinc (II) chromite appeared to behave as a 'negative' catalyst in this process. Potassium carbonate was believed to exert a major influence through catalysing the carbon-steam reaction.

Gasification with increasing pressure up to 2533 kPa appeared to enhance the secondary reactions of tar to form more gaseous products and char.

The addition of both water vapour and solid additives decreased the calorific value of the gaseous products formed from the gasification of cellulose and jack pine chars at 101 kPa and 650°C. However, the total gas yields increased in the presence of water vapour, potassium carbonate, zinc (II)

chromite and iron (III) oxide and hence higher total energy contents were obtained from the gas mixtures drived from the solid wastes than in their absence.

6. Suggestions for further work

In conclusion there is clearly a substantial need for additional research in general areas related to the use of catalysts in the gasification of wood wastes and allied materials.

Although potassium carbonate enhances steam gasification, there is a preferential formation of oxides of carbon relative to methane. Other catalysts, such as nickel, a methanation catalyst, coupled with potassium carbonate should be evaluated in an attempt to produce gases of higher calorific values such as methane, ethane, propane, etc., in an integral process.

Investigation of other potential catalysts which may convert the pyrolysis gas mixture to other synthetic fuels such as methanol and aromatic hydrocarbons should also be carried out.

A more detailed study of the effect of pressure on the rate of gasification and the nature of the products should be undertaken. It is well-known that many synthetic processes, for example, the production of methanol from CO/H_2 mixtures, are possible only at high pressure. Thus in certain instances, gasification at high pressure could be economical and hence further investigations linked to catalytic and pressure effects on the primary gases produced could be worthwhile.

Finally, additional experimental work with a chemical engineering emphasis should be conducted with a view to establishing mass and energy balances, and the overall thermal efficiency of the gasification process.

References

1. Reed, T. B., 'Biomass energy refineries for production of fuel and fertilizer', Appl. Polym. Symp., 28, John Wiley and Sons, New York, 1-9 (1975).

2. Brink, D. L., Charley, J. A., Faltico, G. W. and Thomas, J. F., 'The pyrolysis-gasification-combustion process, energy considerations and overall processing', Thermal Uses and Properties of Carbohydrates and Lignins, Academic Press, New York, San Francisco and London, 97-125 (1976).

3. United Nations, 'World energy supplies, 1979-72', St./Stat/Ser. J/7, New York, N. Y. (1974).

4. Ellwood, E. L., 'The potential of lignocellulosic materials for the production of chemicals, fuels and energy', National Research Council, Washington, D. C. (1976).

5. Reed, T. B., 'Potential impact of widespread use of wood and alcohol: questions and issues', symposium paper, Alcohol as alternative fuels for Ontario, Toronto, Ontario, The Canadian Soc. for Chem. Eng. and The Canadian Soc. for Mech. Eng. (1976).

6. Neill, R. D., 'Options for the use and disposal of bark', Pulp and Paper Canada, 76(3), Montreal, March (1976).

7. Mills, G. A., 'Catalytic aspects of synthetic fuels from coal', Catal. Rev. - Sci. Eng., 14(1), 69-82 (1976).

8. Perry, H., 'The gasification of coal' Scientific American, 230(3), 19-26 (1974).

9. Klass, D. L. and Ghosh, S., 'Fuel gas from organic wastes', Chemtech., Nov., 689-698 (1973).

10. Ghosh, S. and Klass, D. L., 'SMG from refuse and sewage sludge by the biogas process', symposium paper, clean fuels from biomass, sewage, urban refuse, and agricultural wastes, 123-182, sponsored by IGT, Orlando, Fla., January (1976).

11. Jarvis, C. E. and Swartzbaugh, J. T., 'A biogasification mixing study: conversion of municipal solid waste to methane', symposium paper, Energy from biomass and wastes, Washington, D. C., Aug., 677-696, IGT (1978).

12. Azarniouch, M. K. and Thompson, K. M., 'Alcohol from cellulose - production technology', symposium paper, Alcohol as alternative fuels for Ontario, Toronto, Ontario, The Canadian Soc. for Chem. Eng. and The Chem. Soc. for Mech. Eng. (1976).

13. Wenzl, F. J., 'The Chemical Technology of Wood', Academic Press, New York and London, (1970).

14. Andren, R. K., Mandels, M. H. and Medeiros, J. E., 'Production of sugars from waste cellulose by enzymatic hydrolysis. 1..Primary evaluation

of substrates', Appl. Polym. Symp., 28, John Wiley and Sons, New York, 205-220 (1975).

15. Ghose, T. K. and Kostick, J. A., 'Enzymatic saccharification of cellulose in semi - and continuously agitated systems', Adv. in Chem. Ser., 95, Amer. Chem. Soc., Washington, D. C., 415-446 (1969).

16. Reese, E. T., Gilligun W. and Norkrans, B., 'Effect of cellobiose on the enzymic hydrolysis of cellulose and its derivatives', Physiol. Plantarum, 5, 379-90 (1952).

17. Tarkow, H. and Feist, W. C., 'A mechanism for improving the digestibility of lignocellulosic materials with dilute alkali and liquid ammonia', Adv. in Chem. Ser., 95, Amer. Chem. Soc., Washington, D. C., 197-218 (1969).

18. Klass, D. L., 'Energy from biomass and waste: 1978 update', symposium paper, Energy from biomass and wastes, Washington, D. C., Aug., 1-28, IGT (1978).

19. Feldmann, H. F., 'Conversion of forest residues to a methane-rich gas', symposium paper, Energy from biomass and wastes, Washington, D. C., Aug., 537-556, IGT (1978).

20. Walker, P. L., Resinko, F. and Austin, L. G., 'Gas reactions of carbon', Adv. in Cat., 11, 133-221 (1959).

21. Wan, E. I. and Cheng, M., 'A comparison of thermochemical gasification technologies for biomass', symposium paper, Energy from biomass and wastes, Washington, D. C., Aug., 537-556, IGT (1978).

22. Anderson, J. E., 'Solid refuse disposal', U. S. patent 3,729,298 (1973).

23. Mudge, L. K., Sealock, L. J., Robertus, R. T. and Mitchell, D. H., 'Investigation of gasification of biomass in the presence of catalysts', Battelle Pacific Northwest Lab., April (1978).

24. Wright-Malta Corp., 'A technical proposal to fuels from biomass system: catalyzed water/steam gasification of biomass', June (1977).

25. Cameron, G. G. and Kerr, G. P., 'Activation energies of the decomposition of poly (methyl phenylacrylate) from static and dynamic TGA', J. Polym. Sci. Part A-1, 7(11), 3067-74 (1969).

26. Fairbridge, C., 'Low temperature pyrolysis of wood waste materials', M. Sc. thesis, Lakehead University, Thunder Bay, Ontario (1976).

27. Freeman, E. S. and Carroll, B., 'The application of thermoanalytic techniques to reaction kinetics. The thermogravimetric evaluation of the kinetics of the decomposition of calcium oxalate monohydrate', J. Phys. Chem., 62, 394-397 (1958).

28. Coats, A. W. and Redfern, J. P., 'Kinetic parameters from thermogravimetric data', Nature, 201, 68-69 (1964).

29. Sharp, J. H. and Wentworth, S. A., 'Kinetic analysis of thermogravimetric data', Anal. Chem., 41, 2060-2062 (1969).

30. Ozawa, T., 'Critical investigation of methods for kinetic analysis of thermoanalytical data', J. Thermal Anal., 7, 601-617 (1975).

31. Tran, D. Q. and Rai, C., 'A kinetic model for pyrolysis of Douglas fir bark', Fuel, 57, 293-8 (1978).

32. Browne, F. L. and Tang, W. K., 'Thermogravimetric and differential thermal analysis of wood and wood treated with inorganic salts during pyrolysis', Fire Res. Abs. Rev., 4, 76-91 (1962).

33. Brown, L., 'An experimental and analytic study of wood pyrolysis', Ph. D. thesis, Chem. Engineering, University of Oklahoma (1972).

34. Chatterjee, P. K. and Conrad, C. M., 'Kinetics of the pyrolysis of cotton cellulose', Textile Res. J. 36, (6), 487-93 (1966).

35. Lipska, A. E. and Parke, W. J., 'Kinetics of the pyrolysis of cellulose in the temperature range 250-300°C', J. of Appl. Polym. Sci., 10, 1439-53 (1966).

36. Stamm, A. J., 'Thermal degradation of wood and cellulose', Ind. Eng. Chem., 48(3), 413-7 (1956).

37. Martin, S., 'The mechanisms of ignition of cellulosic materials by intense radiation', Research and Development Technical Report, USNR DL-TR-102-NS081-001 (1956).

38. Shafizadeh, F., Cochran, T. G. and Sakai, Y., 'Application of pyrolytic methods for the saccharification of cellulose', AIChE Symp. Ser. 75 (184), 24-34 (1979).

39. Van Krevelen, D. W. and Van Heerden, C., 'Physiochemical aspects of the pyrolysis of coal and related organic compounds', Fuel, 30, 253-9 (1951).

40. Roberts, A. F. and Clough, C., 'Thermal decomposition of wood in an inert atmosphere', Ninth Symp. on Combustion, Cornell Univ., Ithaca, New York, 1962, 158-66 (1963).

41. Akita, K. and Kase, M., 'Determination of kinetic parameters for pyrolysis of cellulose and cellulose treated with ammonium phosphate by differential thermal analysis and thermal gravimetric analysis', J. Polym. Sci., Part A-1, 5, 833-48 (1967).

42. Barooah, J. N. and Long, V. D., 'Rates of thermal decomposition of some carbonaceous materials in a fluidized bed', Fuel, 55(2), 116-20 (1976).

43. Broido, A., 'Kinetics of solid-phase cellulose pyrolysis', Thermal Uses and Properties of Carbohydrates and Lignins, Academic Press, New York, San Francisco and London, 19-36 (1976).

44. Shafizadeh, F. and Bradbury, A. G. W., 'Thermal degradation of cellulose in air and nitrogen at low temperatures', J. Appl. Polym. Sci., 23(5), 1431-42 (1979).

45. Fairbridge, C. and Ross, R. A., 'The thermal reactivity of wood waste systems', Wood Sci. Technol., 12, 169-85 (1978).

46. Fairbridge, C., Ross, R. A. and Sood, S. P., 'A kinetic and surface study of the thermal decomposition of cellulose powder in inert and oxidizing atmospheres', J. of Appl. Polym. Sci., 22(2), 497-510 (1978).

47. Fairbridge, C., Ross, R. A. and Spooner, P., 'A thermogravimetric study of pyrolysis of the bark and chemically-modified bark of jack pine, Pinus banksiana, Lamb', Wood Sci. and Technol., 9, 257-274 (1975).

48. Prakash, C. B. and Murray, F. E., 'Wood waste burning', Pulp Pap. Mag. Can., 73(7), T170-T172 (1972).

49. Bolton, K., Cullingworth, J. E., Ghosh, B. P. and Cobb, J. W., 'The primary gaseous product of carbonization', J. Chem. Soc. (London), 252-63 (1942).

50. Goos, A. W., Trepanier, M. A. and Johnston, M. K., 'Some experiments in sawdust carbonization', Proceedings Forest Products Research Society, 2, 55-9 (1948).

51. Shafizadeh, F., 'Pyrolysis and combustion of cellulosic materials', Adv. in Carbohydrate Chem., 23, 419 (1968).

52. Martin, S., 'Diffusion-controlled ignition of cellulosic materials by intensive radiant energy', NASA Accession No. N64-32518. Rept. No. AD 449236 (1964).

53. Rewick, R. T., Wentrcek, P. R. and Wise, H., 'Carbon gasification in the presence of metal catalysts', Fuel, 53, 274-9 (1974).

54. Otto, K. and Shelef, M., 'Catalytic steam gasification of carbons: effects of Ni and K on specific rates', Proceedings 6th International Congress on Catalysis, Paper B47, London (1976).

55. Haynes, W. P., Gasior, S. J. and Forney, A. J., 'Catalysis of coal gasification at elevated pressure', Adv. in Chem. Ser. 131, 179-202 (1974).

56. Appell, H. R. and Pantages, P., 'Catalytic conversion of carbohydrates to synthesis gas', Thermal Uses and Properties of Carbohydrates and Lignins, Academic Press, New York, San Francisco and London, 127-40 (1976).

57. Veraa, M. and Bell, A. T., 'Effect of alkali metal catalysts on gasification of coal char', Fuel, 57, 194-200 (1978).

58. Long, E. J. and Sykes, K. W., 'The effect of specific catalysts on the reactions of the steam-carbon system', Proceedings of the Royal Society of London, A215, 100-10 (1952).

59. Cover, A. E., Schreiner, W. C. and Skaperdas, G. T., 'Kellogg's coal gasification process', Chem. Eng. Progr., 69(3), 31 (1973).

60. Rai, C. and Tran, D. Q., 'Recovery of medium to high Btu gas from bark and black liquor concentrates', AIChE Symp. Ser., 72(157), 100-115 (1976).

61. Lewis, W. K., Gilliland, E. R. and Howard, H., 'Carbon-steam reaction at low temperature', Ind. Eng. Chem., 45, 1697-703 (1953).

62. Otto, K., Bartosiewicz, L. and Shelef, M., 'Catalytic steam gasification of graphite: effects of calcium, strontium, and barium with and without sulphur', Carbon, 17, 351-57 (1979).

63. Starkovich, J. A., Pinkerton, J. D. and Motley, E., 'Catalytic conversion of coal energy to hydrogen', Report FE-2206-14, 154 p. (1977).

64. Thomas, C. L., Catalytic Processes and Proven Catalysts, Academic Press, New York and London (1970).

65. Lovelock, J. E., 'Ionization methods for the analysis of gases and vapours', Anal. Chem., 33, 162-78 (1961).

66. American Society for Testing Materials Index (1972).

67. Brunauer, S., Emmett, P. H. and Teller, E., 'Adsorption of gases in multimolecular layers', J. Amer. Chem. Soc., 60, 309-19 (1938).

68. Gregg, S. J. and Sing, K. S., Adsorption, Surface Area and Porosity', Academic Press, London and New York (1967).

69. Sharp, J. H., Brindley, G. W. and Achar, B. N., 'Numerical data for some commonly used state reaction equations', J. Amer. Ceram. Soc., 49, 379 (1966).

70. Holt, J. B., Cutler, I. B. and Wadsworth, M. E., 'Rate of thermal dehydration of Kaolinite in vacuum', J. Amer. Cerm. Soc., 45, 133 (1962).

71. Avrami, M., 'Granulation, phase change and microstructure kinetics of phase change', J. Chem. Phy., 9, 177-84 (1941).

72. Erofeev, B. V., 'A generalized equation of chemical kinetics and its application in reactions involving solids', Compt. Rend. (Doklady) Acad. Sci., 52(6), 511-14 (1946).

73. Shafizadeh, F., 'Industrial pyrolysis of cellulosic materials', Appl. Polym. Sym., 28, John Wiley and Sons, New York, 153-74 (1975).

74. Chang, Y., 'Anatomy of common North American pulpwood bark', Tappi Monograph Series, 14 (1954).

75. Tang, W. K. and Eickner, H. W., 'Effect of inorganic salts on pyrolysis of wood, cellulose and lignin determined by DTA', US Forest Serv. Res. Pap., FPL82 (1968).

76. Erins, P., Cinite, V., Jakobsons, M. and Gravitis, J., 'Wood as a multicomponent, crosslinked polymer system', Appl. Polym. Sym., 28, John Wiley and Sons, New York, 1117-38 (1975).

77. Gallagher, K. J., 'The effects of particle size distribution on the kinetics of diffusion reactions in powders in reactivity of solids', G. M. Schwab (ed), Elsevier, Amsterdam, London, New York, 192-203 (1965).

78. Freudenberg, K. and Adam, K., 'Lignin (LXIII) distn. of lignin in a current of H', Chem. Ber. 74B, 387-97 (1941).

79. McKee, D. W., 'Copper-catalyzed oxidation of graphite', Carbon, 8(2), 131-9 (1970).

80. Patrick, J. W. and Walker, A., 'Copper catalyzed combustion of carbon', Carbon, 12(5), 507-15 (1974).

81. Walker, P. L., Jr., Shelef, M. and Anderson, R. A., Chemistry and Physics of Carbon (Edited by Walker, P. L., Jr.), Vol. 4, Marcel Dekker, New York, 287-383 (1968).

82. McKee, D. W. and Chatterji, D., 'The catalytic behavior of alkali metal carbonates and oxides in graphite oxidation reactions', Carbon, 13, 381-90 (1975).

83. Harber, H., 'Catalysis by alkali-metals salts in carbon gasification reactions', Proceedings of the Fourth Conference on Carbon, Buffalo, New York, 125-39 (1960).

84. Guzman,R. and Guillermo, L., 'Catalytic effect of Ni and K_2CO_3 in the gasification of carbon and coal', Ph. D. Diss., University of Notre Dame (1979).

85. Hippo, E. J., 'The effect of cation exchange on the subsequent reactivity of lignite chars to steam', Ph. D. Thesis, The Pennsylvania State University (1977).

86. Johnson, J. L., 'Relationship between the gasification reactivities of coal char and the physical and chemical properties of coal and char', Proceedings of the Nat. Meetg. of the Amer. Chem. Soc., Div. of Fuel Chemistry, 20(4), 85-101 (1975).

87. Mahajan, O. P. and Walker, P. L., Jr., 'Reactivity of heat treated chars', Research and Development Technical Report, U.S. Dept. of Energy, FE-2030-TR8 (1978).

88. Thomas, W. J., 'Microscopic studies of graphite oxidation', Chemistry and Physics of Carbon, Marcel Dekker Inc., New York, 121-202 (1965).

89. Johnson, J. L., 'The use of catalysts in coal gasification', Catal. Rev. - Sci. Eng., 14(1), 131-52 (1976).

90. Otto, K. and Shelef, M., 'Catalytic steam gasification of graphite: effects of intercalated and externally added Ru, Rh, Pd and Pt', Carbon, 15, 317-25 (1977).

91. JANAF Thermochemical Tables (1965).

92. Harker, J. H. and Allen, D. A., Fuel Science, Oliver & Boyd, Edinburgh (1972).

93. Ross, R. A. and Fikis, D. V., 'Gasification reactions of chars and modified chars from jack pine bark', Can. J. Chem. Eng., (in press) (1980).

Appendix 1 Measured calorific values of wood materials and chars (Adiabatic bomb calorimeter)

Sample	Calorific value (kJ kg^{-1})
cellulose	17,000
jack pine sawdust	19,400
jack pine sawdust char	30,500
jack pine bark	21,300
jack pine bark char	26,400

Based on data from [93]